

Theory of first-order phase transitions

This article has been downloaded from IOPscience. Please scroll down to see the full text article.

1987 Rep. Prog. Phys. 50 783

(<http://iopscience.iop.org/0034-4885/50/7/001>)

[View the table of contents for this issue](#), or go to the [journal homepage](#) for more

Download details:

IP Address: 128.151.244.46

The article was downloaded on 14/04/2013 at 09:46

Please note that [terms and conditions apply](#).

Theory of first-order phase transitions

Kurt Binder

Institut für Physik, Johannes-Gutenberg-Universität Mainz, Postfach 3980, D-6500 Mainz, West Germany

Abstract

An introductory review of various concepts about first-order phase transitions is given. Rules for classification of phase transitions as second or first order are discussed, as well as exceptions to these rules. Attention is drawn to the rounding of first-order transitions due to finite-size or quenched impurities. Computational methods to calculate phase diagrams for simple model Hamiltonians are also described.

Particular emphasis is laid on metastable states near first-order phase transitions, on the 'stability limits' of such states (e.g. the 'spinodal curve' of the gas-liquid transition) and on the dynamic mechanisms by which metastable states decay (nucleation and growth of droplets of a new phase, etc).

This review was received in July 1986.

Contents

	Page
1. Introduction	785
2. Phenomenological concepts	786
2.1. Order parameters and the Landau symmetry classification	786
2.2. Second- against first-order transitions in renormalisation group theory	793
2.3. Beyond Landau theory: fluctuation-induced first-order transitions	796
2.4. Finite-size effects and finite-size scaling at first-order phase transitions	801
2.5. Impurity effects on first-order transitions	804
3. Some computational techniques	805
3.1. Models	805
3.2. Molecular field theory and its generalisation (cluster variation method, etc)	808
3.3. Position space renormalisation group methods for phase diagrams exhibiting first-order transitions	809
3.4. Computer simulation methods	811
4. Metastable states near first-order phase transitions	815
4.1. How metastable states in statistical mechanics can be defined and their properties computed	815
4.2. Droplets of the other phase and droplet models	822
4.3. 'Essential' singularity at a first-order phase transition	826
4.4. On the significance of the 'spinodal curve' and related limits of metastability	829
5. Dynamics of first-order phase transitions	832
5.1. Decay of metastable states via nucleation	832
5.2. Later stages of droplet growth: coagulation, the Lifshitz-Slyozov mechanism and phenomenological structure factor scaling	839
5.3. Decay of unstable mixtures via spinodal decomposition	841
5.4. The spinodal curve revisited	847
5.5. The completion time	849
6. Concluding remarks	851
References	853

1. Introduction

Phase transitions—such as the condensation of water, the melting of ice, etc—are very familiar phenomena; nevertheless, some of their basic physical aspects are still incompletely understood. From the viewpoint of statistical mechanics, a connection is drawn between the macroscopic phases of the system and the microscopic properties (such as the forces between the atoms, etc). On a quantitative level, this is still largely impossible: even if the effective atomic interactions are known (e.g. van der Waals type, similar to Lennard-Jones potentials, in rare gases such as Ar), it is hardly possible to predict theoretically under which thermodynamic conditions (temperature T , pressure p , etc) phase transitions occur. Analytical methods for predicting phase diagrams are mainly useful for lattice problems: for example, order-disorder phase transitions in the face-centred cubic (FCC) alloy Cu₃Au, where in the ordered phase the Au atoms populate mainly one of the four simple cubic sublattices, while in the disordered phase the Au atoms are equally distributed over all four sublattices. For off-lattice problems, such as the solid-liquid and liquid-gas transitions of Ar, one has to rely entirely on numerical computer simulation approaches ('Monte Carlo' and 'molecular dynamics' techniques).

In this review we shall deal with this problem of phase diagram calculations only rather briefly in § 3; instead we shall emphasise qualitative aspects, applying to a large class of transitions and not only to a particular material. First we are concerned with understanding the 'order' of a transition: this basic thermodynamic classification considers the thermodynamic potential (e.g. the Helmholtz free energy F) and its derivatives at the transition. If first derivatives of F exhibit jump singularities there, the transition is called 'first order'; if first derivatives are continuous but second derivatives are singular (at least one of them then is divergent), we have a 'second-order' transition, i.e. a critical point in the phase diagram. Critical points are much more special than first-order transitions: for example, at the gas-liquid transition of a one-component system the Gibbs free energies $G_{\text{gas}}(T, p)$ and $G_{\text{liquid}}(T, p)$ of the two phases must be equal, which means that in the temperature-pressure plane the gas-liquid transition shows up as a transition line $T_{\text{cond}}(p)$. The additional condition that the compressibility diverges is satisfied only in a single point, the critical point $T_c = T_{\text{cond}}(p_c)$ where the gas-liquid transition line terminates. In more complicated systems (e.g. mixtures of two fluids), the space of thermodynamic variables is larger: the first-order transitions occur at surfaces of a three-dimensional parameter space and critical phenomena occur along lines where such surfaces terminate. One then also may find multicritical phenomena, at 'multicritical points' where several distinct critical lines meet.

Although critical and multicritical phenomena are more special than first-order transitions, they are theoretically much better understood. This is because critical phenomena arise due to a diverging correlation length of the fluctuations of the 'order parameter', a thermodynamic variable distinguishing the phases. Close to the critical point, this length is very large, and only the structure of the configurations of the system on this large length scale is important, while the behaviour on the much smaller scale given by the range of direct interactions becomes irrelevant. As is well known,

this fact is responsible for the scaling behaviour of thermodynamic functions near a critical point; it also forms the basis for the renormalisation group approach. At a first-order transition, however, there is no diverging correlation length, and in general one cannot restrict attention to long-wavelength phenomena; thus no such universality as in critical phenomena is to be expected.

Nevertheless, the renormalisation group theory has also contributed to a better understanding of first-order transitions, namely the prediction of whether a particular transition should be first order or second order. While in the above example of a simple liquid-gas transition this is not a problem, this is not so for order-disorder transitions in metallic alloys: for example, the body-centred cubic (bcc) β -brass (CuZn) has a second-order transition, while the fcc CuAu has a first-order transition. Similar problems occur in order-disorder transitions of monolayers adsorbed on surfaces, in structural phase transitions of various crystals, etc. This problem will be mentioned in § 2, together with other problems which are closely related to the theory of critical phenomena: for example, there is a finite-size scaling behaviour for first-order transitions similar to finite-size scaling at second-order transitions. As we shall see in § 2, first-order transitions show up in the framework of renormalisation group theory via ‘discontinuity fixed points’. Therefore the renormalisation group helps us to understand them although there is no diverging length.

A problem familiar already from the gas-liquid condensation is the phenomenon of metastability: one may undercool the transition and obtain metastable supersaturated gas. This leads us in § 4 to several challenging problems of statistical mechanics. How does one define a metastable state thermodynamically? Is there a significance to the concept of a ‘limit of metastability’? Is there a precursor effect due to droplets of the other phase heralding a first-order transition? The droplet model in fact is a reasonable starting point also for a description of the dynamics of first-order transitions (§ 5), namely the theory of nucleation, droplet growth and coarsening, etc.

2. Phenomenological concepts

In this section we present first an elementary thermodynamic discussion of phase transitions on the basis of Landau’s theory (Landau and Lifshitz 1958, Aizu 1970, Khachaturyan 1973, Michel 1980, Toledano 1981, Schick 1981). This serves to introduce the concept of an order parameter; the expansion of the free energy in powers of the order parameter, together with symmetry arguments, gives a first criterion on the order of the transition (§ 2.1). In § 2.2 we discuss instances where renormalisation group treatments lead to different conclusions. Note that we aim neither at a complete exposition of the Landau classification of various transitions nor at an exhaustive review of the renormalisation group results—either of these topics would fill a review of its own. We wish rather to describe the spirit of the approach and to give the flavour of the type of results that one can obtain. In addition, Landau theory is a convenient starting point also for a discussion of finite-size effects at first-order phase transitions (§ 2.3) and of effects due to quenched impurities (§ 2.4).

2.1. Order parameters and the Landau symmetry classification

Table 1 lists some condensed matter systems which can exist in several phases, and identifies an extensive variable (denoted symbolically by ϕ) which distinguishes them—

Table 1. Order parameters for phase transitions in various systems.

System	Transition	Order parameter
Liquid-gas	Condensation/evaporation	Density difference $\Delta\rho = \rho_{\text{liquid}} - \rho_{\text{gas}}$
Binary liquid mixture	Unmixing	Composition difference $\Delta c = c_{\text{coex}}^{(2)} - c_{\text{coex}}^{(1)}$
Nematic liquid	Orientational ordering	$\frac{1}{2}(3 \cos^2 \theta - 1)$
Quantum liquid	Normal fluid \leftrightarrow superfluid	$\langle \psi \rangle, \psi = \text{wavefunction}$
Liquid-solid	Melting/crystallisation	$\rho_G, G = \text{reciprocal lattice vector}$
Magnetic solid	Ferromagnetic (T_c)	Spontaneous magnetisation \mathbf{M}
	Antiferromagnetic (T_N)	Sublattice magnetisation \mathbf{M}_s
Solid binary mixture	Unmixing	$\Delta c = c_{\text{coex}}^{(2)} - c_{\text{coex}}^{(1)}$
AB	Sublattice ordering	$\psi = (\Delta c^{(1)} - \Delta c^{(2)})/2$
Dielectric solid	Ferroelectric (T_c)	Polarisation \mathbf{P}
	Antiferroelectric (T_N)	Sublattice polarisation \mathbf{P}_s
Molecular crystal	Orientational ordering	$Y_{lm}(\theta, \phi)$

the ‘order parameter’. It is identically zero in the disordered phase and non-zero in the ordered one. We then use the thermodynamic potential F which has the ‘field’ H conjugate to the order parameter ϕ as a ‘natural variable’ (in addition to temperature T):

$$\phi = -(\partial F / \partial H)_T \quad (\text{e.g. ferroelectric: polarisation } \mathbf{P} = -(\partial F / \partial \mathbf{E})_T). \quad (2.1)$$

The other derivative of F is the entropy $S = -(\partial F / \partial T)_H$. Studying the change of ϕ when an independent variable is varied (e.g. T), ϕ may disappear at the transition continuously ($\phi \propto (1 - T/T_c)^\beta$, ‘second-order transition’, figure 1(a)) or discontinuously (‘first-order transition’, figure 1(b)). At a second-order transition, the ‘susceptibility’ χ_T and the specific heat C_H typically have power law singularities:

$$\begin{aligned} \chi_T &\equiv -(\partial^2 F / \partial H^2)_T \propto |1 - T/T_c|^{-\gamma} \\ C_H &\equiv -T(\partial^2 F / \partial T^2)_H \propto |1 - T/T_c|^{-\alpha}. \end{aligned} \quad (2.2)$$

Here $\alpha, \beta, \gamma, \dots$ are the well known ‘critical exponents’ (e.g. Stanley 1971). At the first-order transition, typically a jump discontinuity ΔS of entropy occurs, and hence a latent heat $\Delta Q = T_c \Delta S$; second derivatives of F often are finite at T_c and rather seem to diverge at the ‘stability limits’ T_0 and T_1 of the disordered and ordered phases respectively.

It is now natural to classify the transitions according to whether ϕ is a scalar quantity or has vector or tensor character: for fluids or mixtures the density or concentration differences are obviously scalar; for the λ transition of ${}^4\text{He}$ the complex wavefunction has two components (real and imaginary part) and hence ϕ is a vector, as in magnetic or dielectric systems; for orientational order, both in liquid crystals and in molecular crystals, ϕ is a tensor of second rank.

First we formulate Landau theory for a scalar order parameter density $\phi(\mathbf{x})$. The free energy functional $\mathcal{F}\{\phi(\mathbf{x})\}$ is then expanded as ($d\mathbf{x}$ is a d -dimensional volume element)

$$\frac{1}{k_B T} \mathcal{F}\{\phi(\mathbf{x})\} = \frac{F_0}{k_B T} + \int d\mathbf{x} \left(\frac{1}{2} r \phi^2(\mathbf{x}) + \frac{1}{4} u \phi^4(\mathbf{x}) - \frac{H}{k_B T} \phi(\mathbf{x}) + \frac{1}{2d} (R \nabla \phi(\mathbf{x}))^2 \right). \quad (2.3)$$

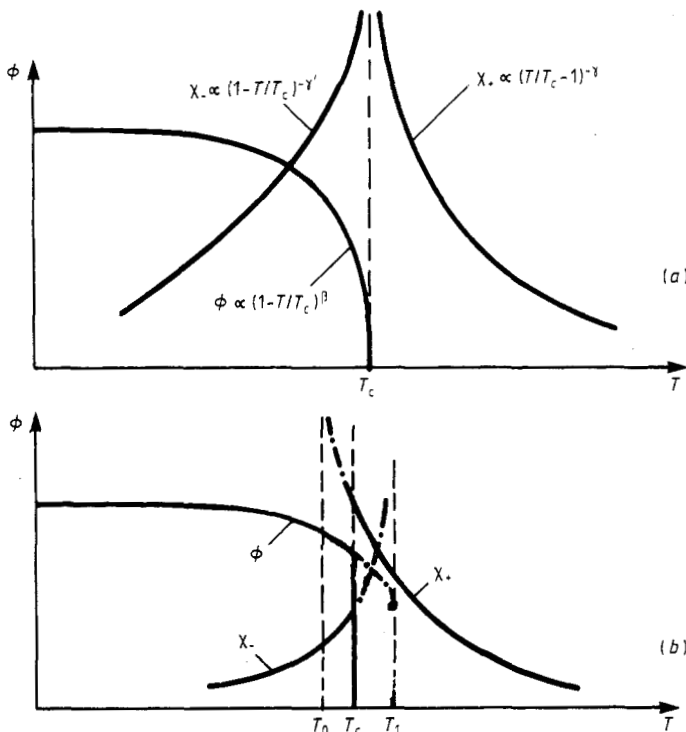


Figure 1. Order parameter ϕ and associated order parameter susceptibilities above (χ_+) and below the transition (χ_-) plotted schematically against temperature (a) at a second-order transition and (b) at a first-order transition.

Here $\phi(x)$ is assumed small (no terms ϕ^6 , etc), slowly varying in space (no terms $(\nabla^2\phi(x))^2$, etc), and the coefficients $u > 0$ and $R > 0$; in addition, for $H = 0$ a symmetry against the change of sign of ϕ is required (no term $\phi^3(x)$).

Now \mathcal{F} is minimal for the homogeneous case, $\nabla\phi(x) \equiv 0$, and implying further that $r = r'(T - T_c)$ with another coefficient $r' > 0$, we find for $H = 0$ (V being the volume of the system)

$$\frac{1}{k_B TV} \frac{\partial \mathcal{F}}{\partial \phi} = r\phi_0 + u\phi_0^3 = 0$$

$$\Rightarrow \begin{cases} \phi_0 = 0 & (T \geq T_c) \\ \phi_0 = \pm(-r/u)^{1/2} = \pm(r'/u)^{1/2}(T_c - T)^{1/2} & (T < T_c). \end{cases} \quad (2.4)$$

Thus (2.3) yields a second-order transition when T is varied (figure 1(a)). For $T < T_c$ a first-order transition occurs as a function of H , however, since ϕ jumps from $(-r/u)^{1/2}$ to $-(-r/u)^{1/2}$ as H changes sign. Thus we also consider the response to fields: we introduce a wavevector-dependent field $\Delta H(\mathbf{x}) = H_k \exp(i\mathbf{k} \cdot \mathbf{x})$ and consider the response $\Delta\phi(\mathbf{x})$, putting $\phi(\mathbf{x}) = \bar{\phi} + \Delta\phi(\mathbf{x})$ and linearising the functional derivative

$$\frac{\delta(\mathcal{F}/k_B T)}{\delta\phi(\mathbf{x})} = r(\bar{\phi} + \Delta\phi(\mathbf{x})) + u(\bar{\phi}^3 + 3\bar{\phi}^2\Delta\phi(\mathbf{x})) - \frac{\Delta H_k}{k_B T} \exp(i\mathbf{k} \cdot \mathbf{x}) - \frac{1}{d} R^2 \nabla^2(\Delta\phi(\mathbf{x})) = 0. \quad (2.5)$$

With $\Delta\phi(x) = \Delta\phi_k \exp(ik \cdot x)$ the solution of (2.5) is

$$\frac{\Delta\phi_k}{\Delta H_k} \equiv \chi(k) = \frac{1}{k_B T} \left(r + 3u\bar{\phi}^2 + \frac{1}{d} R^2 k^2 \right)^{-1} = \frac{\chi_T}{1 + k^2 \xi^2} \quad (2.6)$$

where the susceptibility χ_T and the correlation length ξ of the order parameter fluctuations are

$$\begin{aligned} k_B T \chi_T &= [r'(T - T_c) + 3u\bar{\phi}^2]^{-1} \\ \xi &= (R/\sqrt{d})[r'(T - T_c) + 3u\bar{\phi}^2]^{-1/2}. \end{aligned} \quad (2.7)$$

Now there are several ways a first-order transition driven by temperature can arise in this Landau theory with a scalar order parameter.

(i) If $u < 0$ in (2.3), one must not stop the expansion at fourth order but rather must include a term $\frac{1}{6}v\phi^6(x)$, with $v > 0$. While in the second-order case $\mathcal{F}(\phi)$ has two minima for $T < T_c$ which merge at T_c (figure 2(a)), $\mathcal{F}(\phi)$ now has three minima for $T_0 < T < T_1$ (figure 1(b)) and T_c is reached when these minima are equally deep (figure 2(b)). One finds from $r = r'(T - T_0)$ that

$$T_c = T_0 + 3u^2/32r'v \quad T_1 = T_0 + u^2/8r'v \quad (2.8)$$

and the order parameter jumps at T_c from $\phi_0 = \pm(3u/4v)^{1/2}$ discontinuously to zero. Note that when external parameters p (other than T, H) are varied, it may happen that u changes sign at a value p_t , and hence a line $T_c(p)$ of second-order transitions ends there, at a so-called tricritical point $T_t \equiv T_c(p_t)$, and continues as a line of first-order transitions.

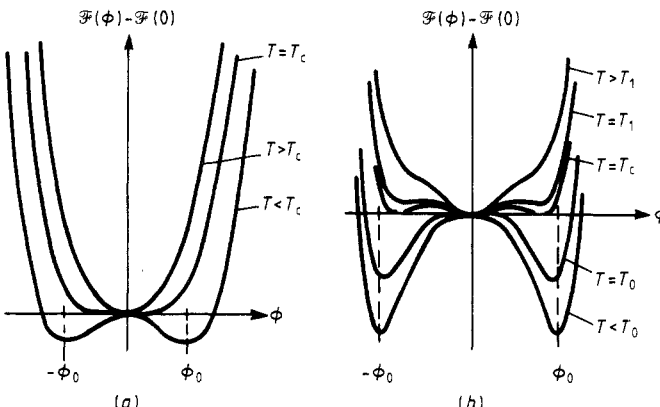


Figure 2. Variation of the Landau free energy at transitions of (a) second order and (b) first order as a function of the (scalar) order parameter ϕ , assuming a symmetry around $\phi = 0$.

(ii) If there is no symmetry of \mathcal{F} between ϕ and $-\phi$, a term $\frac{1}{3}w\phi^3$ will exist in (2.3). For $u > 0$, $\mathcal{F}(\phi)$ may have two minima (figure 3(a)); again the transition occurs when they are equally deep. For $r = r'(T - T_0)$ this happens for T_c given by

$$T_c = T_0 + 8w^2/81ur' \quad T_1 = T_0 + w^2/4ur' \quad (2.9)$$

and the order parameter jumps at T_c from $\phi_0 = -9r/w$ to zero. Again T_0 and T_1 have the significance shown in figure 1(b)—stability limits of the disordered and ordered phases respectively.

The simplest first-order transition occurs when we consider for (2.3) the variation of ϕ with the field H at $T < T_c$ (figure 3(b)). From (2.7) one finds the stability limit

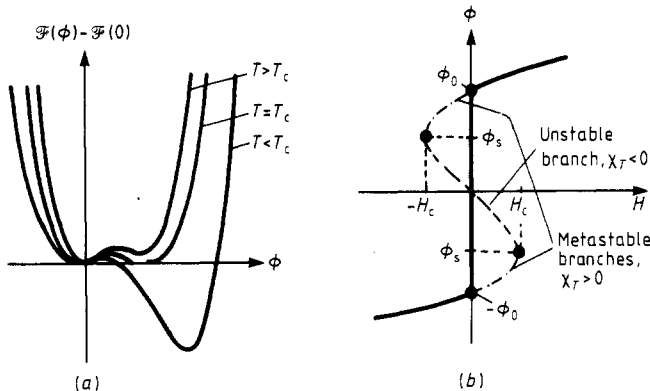


Figure 3. (a) Variation of the free energy with ϕ in the presence of a cubic term. (b) First-order transition due to variation of the field H at a temperature less than the critical temperature of a second-order transition ($\pm H_c$ are the corresponding limits of metastability).

(spinodal) ϕ_s as

$$\phi_s = \pm(-r/3u)^{1/2} = \phi_0/\sqrt{3} \quad H_c = \pm(-2r/3)^{3/2}/\sqrt{u}. \quad (2.10)$$

At this point, an important caveat must be added: free energy functions as drawn in figures 2 and 3(a) are so commonly used that many researchers believe these concepts to be essentially exact. However, general thermodynamic principles tell us that in thermal equilibrium the thermodynamic potentials are convex functions of their variables. As a matter of fact, $\mathcal{F}(\phi)$ should then be convex as a function of ϕ , which excludes multiple minima! For figure 2 this means that for states with $-\phi_0 < \phi < \phi_0$ the *thermal equilibrium state* is not a pure phase: the minimum free energy state is given by the *double-tangent construction* to $\mathcal{F}(\phi)$ and this corresponds to a *mixed-phase state*. Now it is standard *folklore*, dating back to van der Waals, to interpret the part of $\mathcal{F}(\phi)$ in figures 2 and 3(a) lying above this double-tangent free energy as ‘non-equilibrium free energies’: states with $\chi_T > 0$, i.e. $(\partial^2 F / \partial \phi^2)_T > 0$, are interpreted as *metastable states* (chain curves in figure 3(b)), while states with $\chi_T < 0$ (broken curves in figure 3(b)) are interpreted as *unstable states*. As we shall see in § 4, this notion is intrinsically a concept valid only in mean-field theory, but lacks any fundamental justification in statistical mechanics. Pictures such as figures 2 and 3(a) make sense for a sort of *local ‘coarse-grained free energy functional’* only, but not for the global free energy.

We now return to the Landau expansion and consider the case where the order parameter has vector character: how do we find the appropriate structure of the expansion of F in terms of ϕ ? The answer to this question is, of course, that F must be invariant against all symmetry operations of the symmetry group \mathbf{G}_0 describing the disordered phase. In the ordered phase, some symmetry elements of \mathbf{G}_0 fall away (spontaneously broken symmetry); the remaining elements form a subgroup \mathbf{G} of \mathbf{G}_0 . Now the invariance of F must hold for terms ϕ^k of any order k separately. As an example we consider a cubic crystal exhibiting a transition from a paraelectric phase to a ferroelectric one, where a spontaneous polarisation \mathbf{P} appears. Then F is given by ($\mathbf{P} = (P_1, \dots, P_n)$, $n = 3$)

$$\mathcal{F}/k_B T = F_0/k_B T + \int d\mathbf{x} \left[\frac{1}{2} \chi_{\text{el}}^{-1} \mathbf{P}^2 + \frac{1}{4} \left(u \sum_{i=1}^n P_i^4 + V \sum_{i < j=1}^n P_i^2 P_j^2 \right) + (R/2d) \sum_{i=1}^n (\nabla P_i)^2 \right]. \quad (2.11)$$

While the quadratic term of a general dielectric medium would involve the inverse of the dielectric tensor $\Sigma_{ij}(\chi_{\text{el}}^{-1})_{ij}P_iP_j$, this term is completely isotropic for cubic crystals. Inversion symmetry requires invariance against $\mathbf{P} \rightarrow -\mathbf{P}$ and hence no third-order term occurs. The fourth-order term now contains the two ‘cubic invariants’ $\Sigma_i P_i^4$ and $(\Sigma_i P_i^2)^2$. One here invokes the principle that all terms allowed by symmetry will actually occur. Now (2.11) leads, in the framework of Landau theory, to a second-order transition if both

$$u > 0 \quad \text{and} \quad u + v > 0 \quad (2.12)$$

while otherwise one has a first-order transition (then terms of sixth order are needed in (2.11) to ensure stability).

Another approach to construct the Landau expansion, which is useful if one considers a particular model Hamiltonian \mathcal{H} , is the formulation of the molecular field approximation (MFA) where one then expands the molecular field free energy directly. For example, consider the model introduced by Potts (1952), where each site of a given lattice may be in one of Q equivalent states and an energy J is won only if two neighbouring sites are in the same state:

$$\mathcal{H}_{\text{Potts}} = -\sum_{\langle ij \rangle} J\delta_{ij}. \quad (2.13)$$

The symbol $\langle ij \rangle$ denotes a summation over all pairs of lattice sites. In the MFA, the free energy is found by adding the entropy of mixing to the enthalpy term (n_α is the fraction of sites in state α):

$$\frac{\mathcal{F}}{V k_B T} = -\frac{zJ}{2k_B T} \sum_{\alpha=1}^Q n_\alpha^2 + \sum_{\alpha=1}^Q n_\alpha \ln n_\alpha. \quad (2.14)$$

Here z is the coordination number of the lattice and $\sum_{\alpha=1}^Q n_\alpha = 1$. In the disordered phase, $n_\alpha = 1/Q$, so we expand \mathcal{F} in terms of the Q variables $\phi_i = n_i - 1/Q$, $i = 1, \dots, Q-1$ (Kihara *et al* 1954, Straley and Fisher 1973). Assuming $\phi_1 = (Q-1)m/Q$ and $\phi_{i>1} = m/Q$, where m is an order parameter with $0 \leq m \leq 1$, we find

$$\frac{\mathcal{F}(m) - \mathcal{F}(0)}{V k_B T} = \frac{Q-1}{2Q} \left(Q - \frac{zJ}{k_B T} \right) m^2 - \frac{1}{6}(Q-1)(Q-2)m^3 + \dots \quad (2.15)$$

Thus for $Q > 2$ the Landau expansion of the Potts model contains a third-order invariant, as expected, since there is no symmetry against $\phi_i \rightarrow -\phi_i$. So Landau theory would imply a first-order transition for $Q > 2$ and a second-order transition for $Q = 2$ (where (2.13) reduces to the Ising model).

As a third example, consider rare gas monolayers adsorbed on graphite: at low temperatures and pressures the adatoms form a ‘ $\sqrt{3}$ structure’ commensurate with the graphite lattice. This $\sqrt{3}$ structure can be viewed as a triangular lattice decomposed into three sublattices, such that the adatoms occupy one sublattice preferentially. As an order parameter, one takes mass density waves (Bak *et al* 1979, Schick 1981)

$$\rho(\mathbf{x}) = \sum_{\alpha=1}^3 [\psi_\alpha \exp(i\mathbf{q}_\alpha \cdot \mathbf{x}) + \psi_{-\alpha} \exp(-i\mathbf{q}_\alpha \cdot \mathbf{x})]. \quad (2.16)$$

Here the \mathbf{q}_α are the three primitive vectors associated with the *reciprocal lattice of the rare gas monolayer* (a being the lattice spacing of the triangular lattice)

$$\mathbf{q}_1 = \frac{2\pi}{a} \left(0, \frac{1}{\sqrt{3}} \right) \quad \mathbf{q}_2 = \frac{2\pi}{a} \left(-\frac{1}{2}, -\frac{1}{2\sqrt{3}} \right) \quad \mathbf{q}_3 = \frac{2\pi}{a} \left(\frac{1}{2}, -\frac{1}{2\sqrt{3}} \right) \quad (2.17)$$

and ψ_α and $\psi_{-\alpha}$ are (complex) order parameter amplitudes. In constructing the free energy expansion with the help of (2.16), one must note that the periodicity of the

underlying graphite lattice allows invariant ‘umklapp’ terms (the phase factors of third-order terms add up to a *reciprocal lattice vector of the graphite lattice*). Keeping only those terms in the Landau expansion which are non-zero in the $\sqrt{3}$ structure, one obtains with the real order parameter components

$$\begin{aligned}\phi_1 &= \sum_{\alpha=1}^3 (\psi_\alpha + \psi_{-\alpha}) / 2\sqrt{3} & \phi_2 &= \sum_{\alpha=1}^3 (\psi_\alpha - \psi_{-\alpha}) / 2i\sqrt{3} \\ \frac{\mathcal{F}}{V k_B T} &= \frac{1}{2}r(\phi_1^2 + \phi_2^2) + \frac{1}{3}W(\phi_1^3 - 3\phi_1\phi_2^2) + \frac{1}{4}u(\phi_1^2 + \phi_2^2)^2\end{aligned}\quad (2.18)$$

which is identical to the three-state Potts model (Alexander 1975). A three-dimensional analogue of this order (where the planes exhibiting $\sqrt{3}$ structure are stacked together to form a hexagonal lattice) occurs in the intercalation compound C_6Li (Guerard and Herold 1975, Bak and Domany 1979).

Finally we state the general symmetry conditions for which Landau theory allows second-order transitions (Lifshitz 1942) in group theoretical language.

- (i) The order parameter ϕ transforms as a basis of a *single irreducible representation X of \mathbf{G}_0* .
- (ii) The symmetric part of the representation X^3 should not contain the unit representation.
- (iii) If the antisymmetric part of X^2 has a representation in common with the vector representation, the wavevector \mathbf{q} associated with X is *not* determined by symmetry. In this case one expects \mathbf{q} to vary continuously in the ordered phase.

If these conditions are met, a transition can nevertheless be first order, because a fourth-order term may be negative. If they are not met, the transition must be first order according to the Landau rules. However, in $d = 2$ dimensions the Potts models with $Q = 3$ and 4 are well known counter-examples to these rules (violating rule (ii), see (2.15) and (2.18)), as shown exactly by Baxter (1973). One now expects that in a generalised Potts model with continuous Q there would be a line $Q_c(d)$ such that the transition is second order for $Q \leq Q_c(d)$ and first order for $Q > Q_c(d)$. Landau theory is correct only for d exceeding the upper critical dimension d_u ($d_u = 6$ for the Potts model; see, e.g., Wu (1982)). So $Q_c(d \geq 6) = 2$, but $Q_c(d)$ exceeds 2 for $d < 6$ and reaches $Q_c(d = 2) = 4$. It is believed, however, that $Q_c(d = 3) < 3$, so in $d = 3$ for integer Q the Landau rule would not be violated (Blöte and Swendsen 1979). However, an experimental example where there is a third-order invariant (Bak and Mukamel 1979) but the transition seems nevertheless to be second order is the transition to a charge density wave state in $2H-TaSe_2$ (Moncton *et al* 1977). It is of course possible that the transition is very weakly first order so that experimentally it could not be distinguished from second order. Other systems where the Landau rules are apparently violated are discussed by Toledano and Pascoli (1980) and Toledano (1981).

Before we discuss the effect of fluctuations beyond Landau theory (§ 2.2), we mention briefly transitions where no group-subgroup relation between the two groups \mathbf{G}_1 and \mathbf{G}_2 exist: they must be first order. Examples for this case are well known for structural phase transitions: for example, the tetragonal-orthorhombic transition of $BaTiO_3$ or the ‘reconstructive’ transition from calcite to aragonite (Guymont 1981). For the so-called ‘non-disruptive transitions’ (Guymont 1981), where *the new structure can be described (i.e. its symmetry elements, Wyckoff positions of atoms, etc, can be located) in the frame of reference of the old structure*, Landau-type symmetry arguments still yield information on the *domain structures arising in such phase transitions*.

(Guymont 1978, 1981). The tetragonal-orthorhombic transition of BaTiO₃ is considered as an example of such a non-disruptive transition, while reconstructive transitions and martensitic transitions (e.g. the FCC-BCC transition in Fe) are disruptive.

It is sometimes useful to incorporate such a situation into Landau theory by considering the more general situation involving a third structure \mathbf{G}_0 , of which both \mathbf{G}_1 and \mathbf{G}_2 are subgroups. As an example, we mention the weakly anisotropic Heisenberg antiferromagnet in a magnetic field H_{\parallel} :

$$\mathcal{H} = - \sum_{\langle ij \rangle} \{J(1-\Delta)[S_i^x S_j^x + S_i^y S_j^y] + JS_i^z S_j^z\} - H_{\parallel} \sum_i S_i^z \quad (2.19)$$

where we assume $J < 0$ (antiferromagnetism) and for $\Delta > 0$ the easy axis is the z axis. For small H_{\parallel} we have a uniaxial antiferromagnetic structure and the order parameter is the z component of the staggered magnetisation M_s^z . For stronger fields H_{\parallel} , however, we have a transition to a spin flop structure (two-component order parameter, due to the perpendicular components M_s^x and M_s^y of the staggered magnetisation). Clearly there is no group-subgroup relation in this transition. However, one may formulate a Landau theory by including also the magnetically disordered phase (\mathbf{G}_0) and using all three components of M_s as order parameters. In terms of M_s^z and M_s^{\perp} ($(M_s^{\perp})^2 = (M_s^x)^2 + (M_s^y)^2$) one finds

$$\frac{\mathcal{F}}{k_B T} = \frac{F_0}{k_B T} + \int d\mathbf{x} \{ \frac{1}{2} r_{\parallel} (M_s^z)^2 + \frac{1}{2} r_{\perp} (M_s^{\perp})^2 + \frac{1}{4} u_{\parallel} (M_s^z)^4 + \frac{1}{4} u_{\perp} (M_s^{\perp})^4 + \frac{1}{4} v (M_s^z)^2 (M_s^{\perp})^2 \\ + \dots + \text{gradient terms} \}. \quad (2.20)$$

In this example, to which we shall return in § 3.3 below, there are second-order transitions to the disordered phase at $T_N^{\parallel}(H_{\parallel})$ (where M_s^z vanishes) and at $T_N^{\perp}(H_{\parallel})$ (where M_s^{\perp} vanishes). Both lines $T_N^{\parallel}(H_{\parallel})$ and $T_N^{\perp}(H_{\parallel})$ as well as the first-order line between the two antiferromagnetic structures join in a *bicritical point*.

Finally we draw attention to phase transitions between commensurate and incommensurate superstructures (e.g. Ishibashi 1978, 1981, Aslanyan and Levanyuk 1977, 1978, Hornreich 1979, Guilluy and Toledano 1981) discussed in the framework of Landau theory, a topic which is outside of consideration here.

2.2. Second- against first-order transitions in renormalisation group theory

It has been emphasised above that double-well or multiple-well free energies as drawn in figure 2 and 3(a) respectively are not permissible as bulk free energies of a macroscopic system. However, expressions such as (2.3), (2.11), (2.20), etc, do make sense as the result of coarse graining. Let us assume that we start from a microscopic Hamiltonian such as (2.13) or (2.19) and we wish to eliminate short-wavelength fluctuations (which are not important if the transition is second order or very weakly first order). We can do this by dividing the system into cells of linear dimensions L and introducing an order parameter field $\Phi(\mathbf{x})$ as (\mathbf{S}_i being the n -component spin at lattice site i , in (2.19), for instance)

$$\Phi(\mathbf{x}) = \frac{1}{L^d} \sum_{i \in L^d} \mathbf{S}_i \quad (2.21)$$

such that \mathbf{x} is the centre of gravity of the cell L^d (d is the dimensionality). We then define a coarse-grained Hamiltonian $\mathcal{H}_{cg}\{\Phi(\mathbf{x})\}$ by

$$\exp(-\mathcal{H}_{cg}\{\Phi(\mathbf{x})\}/k_B T) = \text{Tr}_{\langle \mathbf{S}_i \rangle} P(\{\Phi(\mathbf{x})\}, \{\mathbf{S}_i\}) \exp(-\mathcal{H}\{\mathbf{S}_i\}/k_B T) \quad (2.22)$$

where the projection operator $P(\{\phi(x)\}, \{S_i\})$ means that we perform a restricted trace only, keeping a particular configuration $\{\phi(x)\}$ (which is then related to the spin configuration $\{S_i\}$ via (2.21)) fixed. Although the procedure (2.22) can hardly ever be carried out in practice, the common belief is that the coarse-grained Hamiltonian $\mathcal{H}_{cg}\{\phi(x)\}$ will have the Landau form if one is close to a second-order transition and $L \ll \xi$. If $L \approx \xi$ or $L > \xi$, $\mathcal{H}_{cg}(\phi)$ no longer needs to have an analytic expansion in ϕ ; at least the expansion coefficients must then have a singular temperature dependence (Kawasaki *et al* 1981). For Ising models, an approximate construction of $\mathcal{H}_{cg}(\phi)$, in the form (2.3), has been attempted via Monte Carlo methods (Kaski *et al* 1984, Milchev *et al* 1986). We shall return to this problem in § 4 and assume for the moment that $\mathcal{H}_{cg}\{\phi(x)\} = \mathcal{F}$, as given by (2.3) for instance. Then the free energy F is obtained as

$$F = -k_B T \ln Z = -k_B T \ln \int d\{\phi\} \exp(-\mathcal{F}\{\phi(x)\}/k_B T). \quad (2.23)$$

If the distribution $\exp(-\mathcal{F}\{\phi(x)\}/k_B T)$ is very sharply peaked at the minimum of $\mathcal{F}\{\phi(x)\}$, we may replace the actual distribution by a delta function, instead of dealing with the fluctuations around the minimum still included in the functional integral (2.23), and then it is simply $\mathcal{F}\{\phi(x)\}$ which has to be minimised in order to describe thermal equilibrium. Thus the Landau theory of § 2.1 is simply an approximation to (2.23) where statistical fluctuations are neglected.

Next we describe a simple argument to check whether this neglect of fluctuations is legitimate—the ‘Ginzburg criterion’ (Ginzburg 1960, Ma 1976, Patashinskii and Pokrovskii 1979). Below T_c , fluctuations $\delta\phi \equiv \phi(x) - \phi_0$ will make a small contribution to (2.23) only as long as they are small in comparison with the order parameter ϕ_0 itself:

$$\langle(\delta\phi(x))^2\rangle_{T,L} \ll \phi_0^2. \quad (2.24)$$

Here we have explicitly indicated that the mean-square fluctuation has to be averaged over the coarse-graining volume (of linear dimension L) considered in (2.21). Now this fluctuation can be rewritten as

$$\langle(\delta\phi(x))^2\rangle_{T,L} = \frac{1}{L^{2d}} \sum_{i,j \in L^d} \langle(S_i S_j)_T - \phi_0^2\rangle \approx L^{-d} \int dx \langle(\phi(0)\phi(x))_T - \phi_0^2\rangle \quad (2.25)$$

where the integration is extended over a sphere of volume L^d . Since the correlation function in (2.25) is related to the wavevector-dependent susceptibility $\chi(k)$ through the static limit of the fluctuation-dissipation relation

$$k_B T \chi(k) = S(k) = \int dx \exp(ik \cdot x) \langle(\phi(0)\phi(x))_T - \phi_0^2\rangle \quad (2.26)$$

we find from (2.25) and (2.6) for $x \leq \xi$

$$\langle(\phi(0)\phi(x))_T - \phi_0^2\rangle \propto R^{-2} x^{-(d-2)} \quad (2.27)$$

while for $x \gg \xi$ the correlation function decays exponentially, proportional to $\exp(-x/\xi)$. From (2.25) and (2.27) we obtain $\langle(\delta\phi(x))^2\rangle_{T,L} \propto R^{-2} L^{2-d}$. Choosing now the maximum permissible value for L , $L = \xi$, (2.24) yields (using (2.7) with $\bar{\phi} = \phi_0$)

$$1 \ll R^2 \xi^{d-2} \phi_0^2 \propto R^d (1 - T/T_c)^{(4-d)/2}. \quad (2.28)$$

This condition is fulfilled if either the interaction range R is very large or the dimensionality d exceeds the upper critical dimension, $d_u = 4$. For $d < 4$ and finite R , however, (2.8) always breaks down close to T_c , fluctuations becoming important, and the Landau mean-field theory becomes very inaccurate.

A correct description of critical phenomena then is achieved by the renormalisation group approach (Wilson and Kogut 1974, Fisher 1974, Ma 1976). Rather than attempting to solve the functional integral (2.23) in a single step, one constructs an iteration scheme where short-wavelength fluctuations are integrated out step by step. Formally the renormalisation group transformation can be written as (we now interpret \mathcal{F} as a Hamiltonian \mathcal{H})

$$\mathcal{H}'\{\phi'\} = \mathbf{R}[\mathcal{H}\{\phi\}] \quad \mathcal{H}''\{\phi''\} = \mathbf{R}[\mathcal{H}'\{\phi'\}] \dots \mathcal{H}^{(k)}\{\phi^{(k)}\} = \mathbf{R}^k[\mathcal{H}\{\phi\}] \quad (2.29)$$

where the operator \mathbf{R} reduces the degrees of freedom by a factor b^d ($b > 1$ being the scale factor) and the spin field ϕ' is a rescaled version of ϕ (this rescaling is necessary since we require (2.29) to keep the partition function Z invariant). Thus, while initially we keep all fluctuations with wavelengths exceeding L , after one renormalisation we keep fluctuations with wavelengths exceeding bL , after two steps b^2L , etc. If we work above T_c , after a sufficient number k of iterations the length b^kL must exceed ξ , and then the ‘block spin’ $\phi^{(k)}$ describing the spin field averaged over a block of size b^kL will be essentially decoupled from neighbouring blocks. The $\mathcal{H}^{(k \rightarrow \infty)}$ converges towards a trivial limit, the ‘infinite temperature’ fixed-point Hamiltonian, describing a simple Gaussian distribution of the spin field. On the other hand, exactly at criticality, repeated iterations will lead to $\mathcal{H}^{(k \rightarrow \infty)} \rightarrow \mathcal{H}^*$, a non-trivial fixed-point Hamiltonian. We now linearise \mathbf{R} near \mathcal{H}^* , and this linearised renormalisation group operator \mathbf{L} is represented by eigenoperators Q_j and eigenvalues Λ_j as usual, $\mathbf{L}Q_j = \Lambda_j Q_j$. Then near \mathcal{H}^* the renormalisation group relation can be written as (the h_j are called ‘scaling fields’)

$$\begin{aligned} \mathcal{H} &= \mathcal{H}^* + \sum_j h_j Q_j \\ \mathcal{H}' &= \mathbf{L}\mathcal{H} = \mathcal{H}^* + \sum_j h'_j Q_j = \mathcal{H}^* + \sum_j h_j \Lambda_j Q_j. \end{aligned} \quad (2.30)$$

Thus one obtains diagonalised recursion relations

$$h'_j = \Lambda_j h_j = b^{\lambda_j} h_j \quad (2.31)$$

where the λ_j are independent of the choice of the scale factor b . Since the free energy density $f\{\mathcal{H}\}$ has to be rescaled as $f\{\mathcal{H}'\} = b^d f\{\mathcal{H}\}$ —remember that Z and hence F are kept invariant and the number of degrees of freedom decreases by a factor b^d in a renormalisation step—we find from (2.30) and (2.31) that

$$f(h_1, h_2, h_3, \dots) = b^{-d} f(b^{\lambda_1} h_1, b^{\lambda_2} h_2, b^{\lambda_3} h_3, \dots). \quad (2.32)$$

This relation is basically the asymptotic homogeneity relation implying scaling properties of the free energy density. Relating h_1 to the temperature, $h_1 = k_1(1 - T/T_c)$, h_2 to the ordering field, $h_2 = k_2 H$, k_1 and k_2 being constants, and choosing $b^{\lambda_1}(1 - T/T_c) = 1$ yields

$$f(1 - T/T_c, H, h_3, \dots)$$

$$= (1 - T/T_c)^{d/\lambda_1} f(k_1, k_2 H / (1 - T/T_c)^{\lambda_2/\lambda_1}, h_3 / (1 - T/T_c)^{\lambda_3/\lambda_1}, \dots). \quad (2.33)$$

From this λ_1 is identified as the ‘thermal eigenvalue’ $1/\nu$ and λ_2 the ‘magnetic eigenvalue’ $\beta\delta/\nu$, where β , δ and ν are standard critical exponents (Ma 1976); at an ordinary critical point, there are only two relevant scaling fields (having positive

eigenvalues), h_3 being ‘irrelevant’ (i.e. $\lambda_3 < 0$; this yields a ‘correction to scaling’ (Fisher 1974)).

If we work at $T < T_c$, however, the renormalisation group flow takes the system to another trivial limit, the zero-temperature strong-coupling limit: in this case we still have a fixed-point behaviour as described in (2.30)–(2.32), but with only one relevant eigenvalue, $\lambda_2 = d$. This behaviour reflects the discontinuity of the magnetisation at zero conjugate field (figure 3(b)), and hence a fixed point with an eigenvalue $\lambda = d$ is called a ‘discontinuity fixed point’ (Nienhuis and Nauenberg 1975, Niemeijer and van Leeuwen 1976). The description of a first-order transition in a renormalisation group framework hence occurs via such a discontinuity fixed point.

Formally, the description of first-order transitions in terms of scaling (equation (2.32)) and renormalisation group can also be obtained as a limiting case of second-order transitions (Fisher and Berker 1982). Consider a transition driven by a field H occurring at H_t in an Ising-type model. Then the magnetisation should vary as $M - \bar{M}_t \approx \pm D|H - H_t|^{1/\delta}$ where $\bar{M}_t = \frac{1}{2}[M(H_t+) + M(H_t-)]$ is the mean magnetisation on the phase boundary (for the standard Ising model, of course, $H_t = 0$ and $\bar{M}_t = 0$, by symmetry). A first-order transition is described simply by $\delta \rightarrow \infty$ which leads to a discontinuity in $M(H)$. Now, if this transition is represented by a renormalisation group fixed point, we have a recursion relation $H' = b^\lambda H$ (taking $H_t = 0$ for simplicity) and $f(H) = b^{-d}f(H')$. Thus, choosing $b = |H|^{-1/\lambda}$, we obtain $f(H) \approx D_\pm |H|^{d/\lambda}$ with $D_\pm \approx f(\pm 1)$. Since $M \propto (\partial f / \partial H)_T$, this leads to $d/\lambda = 1 - 1/\delta$. In the limit $\delta \rightarrow \infty$ this in turn reduces to $\lambda = d$.

At this point we mention that in the isotropic n -vector model ((2.19) for $\Delta = 0$ is an example for $n = 3$) below T_c at $H \rightarrow 0$ additional singularities occur (Wegner 1967, Vaks *et al* 1967, Halperin and Hohenberg 1969):

$$\chi(H) \propto \begin{cases} H^{-(4-d)/2} & (2 < d < 4) \\ |\ln H| & (d = 4). \end{cases} \quad (2.34)$$

These *singularities (due to spin waves) superimposed at the first-order transition at $H = 0$* have been confirmed by the renormalisation group approach (Brézin and Wallace 1973, Nelson 1976, Schäfer and Horner 1978).

A similar behaviour has also been shown to occur at the first-order transition of (2.19) at the critical field H_c^c from the uniaxial antiferromagnetic structure to the spin flop phase (Feder and Pytte 1968): the uniform susceptibility χ diverges as $\chi \propto |H - H_c^c|^{-1/2}$ on both sides of the transition.

2.3. Beyond Landau theory: fluctuation-induced first-order transitions

There are many transitions which the above three Landau symmetry criteria would permit to be second order but which are actually observed to be first order. Notable examples are type I or type II antiferromagnetic structures, consisting of ferromagnetic (100) or (111) sheets respectively with alternating magnetic moment direction between adjacent sheets. Choosing Ising spins, these structures can also be translated into models of alloy ordering (figure 4). Experimentally first-order transitions are known for FeO (Roth 1958), TbP (Bucher *et al* 1976, Kötzler *et al* 1979), TbAs (Levy 1969) (these systems have order parameter dimensionality $n = 4$), UO₂ (Frazer *et al* 1965) ($n = 6$), MnO (Bloch and Mauri 1973), NiO (Kleemann *et al* 1980) and ErSb (Knorr *et al* 1983) ($n = 8$) for instance. (Further systems are listed in Grazhdankina (1969).)

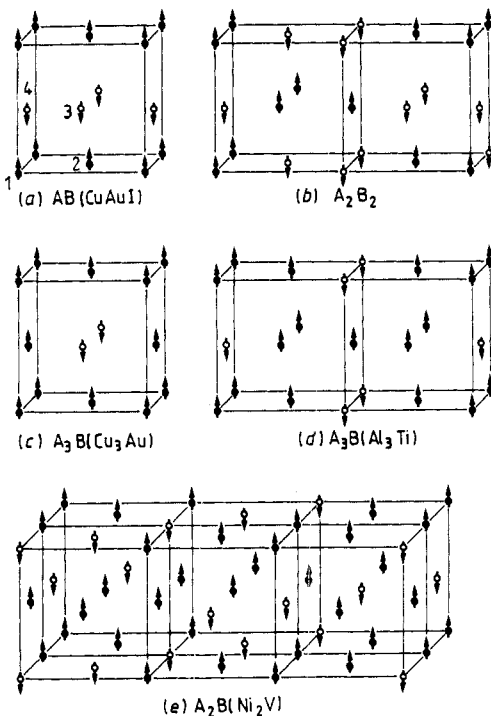


Figure 4. Some examples of structures for FCC Ising antiferromagnets and the corresponding binary alloy systems (AB) when A is associated with 'spin up' and B with 'spin down' (from Binder *et al* 1981).

The standard phenomenological understanding of the first-order transitions in these materials invoked magnetostrictive couplings (Bean and Rodbell 1962, Lines and Jones 1965) or crystal field effects (in the case of UO_2 ; see Blume 1966), which make the coefficient u in (2.3) negative and thus produce a free energy of the type shown in figure 2(b).

Now it has been suggested that the first-order character of the phase transition in these materials is a fundamental property due already to the large number n of order parameter components and the symmetry of the Hamiltonian (while u and v in (2.11) may still be positive, strong magnetoelastic couplings not being involved): in a renormalisation group expansion in $\epsilon = d_u - d$ near $d_u = 4$, one finds for cubic systems with $n \geq 4$ order parameter components that there is no stable fixed point (Mukamel *et al* 1976, Mukamel and Krinsky 1976a, b, Bak *et al* 1976, Brazovskii and Dzyaloshinskii 1975, Allesandrini *et al* 1976). Since upon renormalisation one encounters a 'runaway' into a region where u is negative, this is interpreted as a first-order transition induced by fluctuations. In fact, this already occurs for the cubic model with $n = 3$, (2.11), if (2.12) is satisfied (so Landau theory yields a second-order transition) but either $v < 0$ or $v - 3u > 0$ (Aharony 1976). A closely related mechanism would be that, though a stable fixed point exists, it is inaccessible (Nattermann and Trimper 1975, Nattermann 1976, Rudnick 1978).

Other classes of models argued to have fluctuation-induced first-order transitions are systems in which the order parameter couples to a fluctuating gauge field, examples being the superconducting and the nematic-smectic-A phase transitions (Halperin *et*

al 1974). However, since the Ginzburg criterion (2.28) shows that the non-mean-field region of superconductors is extremely narrow, the first-order character is not observable in practice. It is disturbing, however, that liquid crystals are found (Als-Nielsen *et al* 1977) in which the nematic-smectic-A transition is second-order; this discrepancy between theory and experiment is not yet understood.

The third class of systems with fluctuation-induced first-order transitions are ϕ^4 models with an $O(n)$ symmetric vector field ϕ for which the quadratic terms in the Landau-Ginzburg-Wilson Hamiltonian attain their minimum value not at wavevector $q=0$ but on a surface of $m-1$ dimensions in q space (Brazovskii 1975, Swift 1976, Swift and Hohenberg 1977, Mukamel and Hornreich 1980, Ling *et al* 1981). This situation occurs for the nematic-smectic-C transition, which is hence argued to be of first order (Swift 1976). This conclusion must be taken with caution, however, since $d=3$ is the lower critical dimension for smectic-C phases, so strictly speaking there is no positional long-range order (Als-Nielsen *et al* 1977). For the convective Rayleigh-Bénard instability studied by Swift and Hohenberg (1977), on the other hand, the region where thermal fluctuations are important, and hence the transition is turned first-order again, is extremely narrow and hardly observable in practice. (Of course, at this point the additional assumption is invoked that one can construct some analogue to the free energy functional also for the Bénard problem, a system far from thermal equilibrium.)

So antiferromagnets with $n \geq 4$ order parameter components seem practically to be the most important cases of fluctuation-induced first-order transitions. Unfortunately, also for this renormalisation group prediction there exist many counter-examples, i.e. cubic $n \geq 4$ antiferromagnets with second-order transitions: CeS, CeSe, CeTe (Hulliger *et al* 1978, Ott *et al* 1979), GdS, GdSe, GdTb (Hulliger and Siegrist 1979) (all these systems have $n=4$), GdSb and GdBi (McGuire *et al* 1969) ($n=8$; for additional examples see Kötzler (1984)). Now this discrepancy between theory and experiment can have two reasons (Mukamel and Wallace 1979).

(i) The critical number $n^*(d)$ of order parameter components separating the regime where second-order transitions occur ($n < n^*(d)$) from the first-order regime ($n > n^*(d)$) increases from $n^*(d=4)=4$ with decreasing d , sufficiently so that for $d=3$ second-order transitions are again possible for $n=4-8$. This possibility is unlikely, since one rather expects $n^*(d=3) \approx 3.1$ (Aharony 1976, Mukamel and Wallace 1979).

(ii) The phase transition in all the above compounds is in fact first order, albeit so weakly that they are erroneously identified as second order in all the experiments. If this interpretation of Mukamel and Wallace (1979) is correct, an explanation is needed why in some systems the order parameter discontinuity is unobservably small, while in other systems it is very large, such as in TbP, which is frequently quoted as an example of a fluctuation-induced first-order transition (Mukamel and Krinsky 1976a, Brazovskii *et al* 1976, Kerszberg and Mukamel 1981a, b, Blankschtein and Aharony 1981). In fact, this interpretation has been questioned by Kötzler (1984), who points out that, using data on the magnetostrictive coupling (taken from the softening of the elastic constant when approaching the magnetic transition in TbP), standard mean-field theory along the lines of Lines and Jones (1965) does account for the temperature dependence of spontaneous sublattice magnetisation, susceptibility and specific heat quantitatively (figure 5; see also Kötzler and Raffius (1980) and Morin and Schmitt (1983)). Moreover, the same approach accounts very well for the data on TbBi and TbSb, which have second-order transitions (to within experimental accuracy). Clearly not every first-order transition in an $n \geq 4$ antiferromagnet needs to be fluctuation-induced!

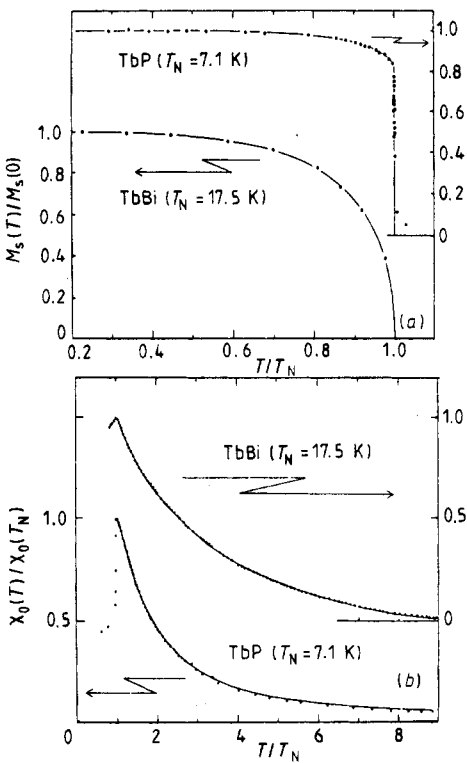


Figure 5. (a) Spontaneous sublattice magnetisation and (b) zero-field susceptibility for TbP (Kötzler *et al.* 1979) and TbBi (Neresson and Arnold 1971). Points show experimental data, while full curves are due to a mean-field calculation which includes crystal field effects and magnetostrictive couplings taken from other measurements (from Kötzler 1984).

Another mechanism for first-order transitions in cases where a low-order Landau expansion predicts a second-order transition is the ‘renormalisation’ of the low-order coefficients due to high-order terms (Galam and Birman 1982). For a range of values of the coupling constant of the anisotropic eighth-order term, the sign of the effective coefficient of the fourth-order term is reversed. Galam and Birman (1982) suggest that this mechanism might explain the first-order transitions in Cr, Eu, UO₂ and MnO, instead of the fluctuation-induced mechanism.

When a fluctuation-induced first-order transition occurs, application of a symmetry-breaking field may effectively reduce the order parameter dimensionality and hence restore a second-order transition in the renormalisation group framework (Bak *et al.* 1976, Domany *et al.* 1977, Kerszberg and Mukamel 1979, 1981a, b, Blankschtein and Mukamel 1981). The crossover from first order to continuous transition observed in MnO under a [111] uniaxial stress (Bloch *et al.* 1980) and in RbCaF₃ under a [100] uniaxial stress (Buzaré *et al.* 1979) is interpreted along such lines (Aharony and Bruce 1979). Blankschtein and Aharony (1981, 1983) show that near tricritical points one finds a regime where the transition is second order although Landau theory would predict it to be first order: fluctuations simply shift the tricritical point into the region where u is negative. However, such a ‘fluctuation-driven continuous transition’ may be turned back to first order by suitable symmetry-breaking fields, and hence very complicated phase diagrams may result, where several tricritical points occur.

Blankschtein and Aharony (1983) predict that application of pressure to a metamagnet at a fixed temperature above the tricritical point may turn the continuous transition into first order, and thus interpret experiments on FeCl_2 and FeBr_2 (Vettier *et al* 1973).

Perhaps the most convincing demonstration of fluctuation-induced first-order transitions could be given by applying the Monte Carlo computer simulation method (Binder 1979, 1984a) to suitable model Hamiltonians, for which the MFA is easily worked out. In fact Mouritsen *et al* (1977) and Knak-Jensen *et al* (1979) found a rather weak first-order transition in a classical Heisenberg antiferromagnet with suitable interactions stabilising an $n = 6$ AF type II structure. Phani *et al* (1980) study the Ising Hamiltonian

$$\mathcal{H}_{\text{Ising}} = - \sum_{i \neq j} J_{ij} S_i S_j - H \sum_i S_i \quad (S_i = \pm 1) \quad (2.35)$$

with exchange interactions $J_{nn} < 0$ between nearest neighbours and $J_{n\bar{n}n} < 0$ between next-nearest neighbours in zero field at the FCC lattice. This model provides an example for an $n = 4$ AF type II structure. Phani *et al* (1980) find a first-order transition for $J_{nnn}/J_{nn} \leq 1$, while for $J_{nnn}/J_{nn} \geq 1$ the data are consistent with a second-order transition. Unfortunately, due to finite-size effects, the distinction of the order of transitions in computer simulations may be very difficult (see § 2.4). So more work is needed to clarify the questions about fluctuation-induced first-order transitions.

As a final point of the section, we draw attention to elastic phase transitions where the order parameter is the strain tensor ϵ_{ik} (Cowley 1976, Folk *et al* 1976) and hence the Landau expansion is (applying the summation convention)

$$\begin{aligned} \mathcal{F} = F_0 + \int d\mathbf{x} (& \tfrac{1}{2} C_{iklm} \epsilon_{ik} \epsilon_{lm} + \tfrac{1}{3} C_{iklmrs}^{(3)} \epsilon_{ik} \epsilon_{lm} \epsilon_{rs} \\ & + \tfrac{1}{4} C_{iklmrsuv}^{(4)} \epsilon_{ik} \epsilon_{lm} \epsilon_{rs} \epsilon_{uv} + \dots + \text{gradient terms}). \end{aligned} \quad (2.36)$$

Here the C_{iklm} are elastic constants and $C_{iklmrs}^{(3)}$ and $C_{iklmrsuv}^{(4)}$ analogous coefficients of anharmonic terms. For most elastic transitions, symmetry permits some non-zero $C_{iklmrs}^{(3)}$ and hence leads to first-order transitions. The elastic distortions at these transitions may be very large: for example, for transitions where no group-subgroup relation exists, such as the martensitic transformations in Fe-C and Fe-Ni, ϵ_{ik} at the transition is of order 10^{-1} ; in other systems, however, they are extremely small ($\epsilon_{ik} \approx 10^{-4}$ in Nb_3Sn and V_3Si). (In fact Toledano (1981) mentions V_3Si as a second-order transition violating the Landau rules.) Unlike magnetic first-order transitions, where microscopic molecular field theories can sometimes account for experimentally observed jumps (figure 5), the microscopic molecular field theory for elastic transitions is much more difficult, and even for well investigated transitions like that of KCN it still remains at a rather qualitative level (De Raedt *et al* 1981).

Unlike the magnetic and structural transitions discussed above, one expects that fluctuation effects are much less important for elastic phase transitions. This is seen for the cases where the symmetry of (2.36) admits second-order transitions (Folk *et al* 1976): the upper critical dimension below which Landau theory breaks down close to the second-order transitions is lowered to $d_u = 3$ or even $d_u = 2.5$ in several cases of experimental interest. Nevertheless a fluctuation-induced first-order transition might occur for the transition from cubic to rhombohedral symmetry (which has $d_u = 3$), where the softening of acoustic modes (elastic constant $C_{44} \rightarrow 0$) implies a divergence of the mean-square displacements of the atoms at the transition (Folk *et al* 1976). A transition belonging to this class has recently been discovered in $(\text{KBr})_{0.27}$ ($\text{KCN})_{0.73}$ but the transition in fact is continuous (Knorr *et al* 1985).

2.4. Finite-size effects and finite-size scaling at first-order phase transitions

In a first-order transition driven by temperature (figure 1(b)) a δ function singularity occurs in the specific heat at the transition temperature T_c due to the latent heat; similarly, in a first-order transition driven by the ordering field (figure 3(b)) a δ function singularity occurs in the ordering susceptibility at the transition, due to the jump in the order parameter. However, such singularities can occur only in the thermodynamic limit where the volume L^d of the system tends to infinity: *for finite linear dimension L we expect the transition to be both rounded and shifted.* (Only the cube geometry with all linear dimensions equal is considered here—for a discussion of other geometries see, e.g., Privman and Fisher (1983), Cardy and Nightingale (1983) and Fisher and Privman (1985).)

While such finite-size effects on second-order transitions (where the power law singularities are rounded and shifted) have had a lot of attention (Fisher 1971, Barber and Fisher 1972) (for recent reviews see Barber (1983) and Binder (1987)), finite-size effects on first-order transitions were only discussed rather recently (Imry 1980, Fisher and Berker 1982, Privman and Fisher 1983, Binder and Landau 1984, Challa *et al* 1986). At a second-order transition, the correlation length ξ diverges ($\xi \propto |T - T_c|^{-\nu}$) and it is then the ‘thermal eigenvalue’ $1/\nu$ of the renormalisation group, which controls rounding and shifting, both being of the order of $L^{-1/\nu}$. For a first-order transition, the only eigenvalue of the discontinuity fixed point is the dimensionality d , and hence one predicts a rounding and shifting of the order of L^{-d} .

We now describe a more quantitative theory of finite-size scaling at first-order transitions, which also yields explicit expressions for the scaling functions involved (Binder and Landau 1984, Challa *et al* 1986). We start from (2.23) and integrate out spatial fluctuations to obtain the probability distribution of finding an order parameter ϕ in the system

$$P_L(\phi) \propto \exp(-L^d f(\phi)/k_B T) \quad (L \rightarrow \infty) \quad (2.37)$$

where $f(\phi)$ is the free energy density of the system. At the first-order transition, $f(\phi)$ for the various phases coexisting there is precisely the same; consequently $P_L(\phi)$ there consists of several sharp peaks of exactly the same height, representing the various phases.

At a transition driven by temperature, we consider the energy distribution $P_L(E)$ to discuss the smearing of the latent heat. Suppose the transition at T_c occurs from one disordered state (energy E_+) to a q -fold degenerate ordered state (energy E_-). Since all q peaks of (2.37) representing ordered states superimpose in the energy distribution, we must have $P_L(E_-) = q P_L(E_+)$ at $T = T_c$. Now standard thermodynamic fluctuation theory states that the probability distribution $P_L(E)$ for a single phase is Gaussian (Landau and Lifshitz 1958), $P_L(E) \propto \exp[-L^d (E - E_0)^2 / 2k_B T^2 C]$, C being the specific heat and E_0 the average energy. This result is straightforwardly generalised to the present situation where several phases compete, for $\Delta T = T - T_c$,

$$\begin{aligned} P_L(E) &\propto \exp\left(-\frac{-L^d \Delta F}{2k_B T}\right) \exp\left(-\frac{[E - (E_+ + C_+ \Delta T)]^2 L^d}{2k_B T^2 C_+}\right) \\ &\quad + q \exp\left(\frac{L^d \Delta F}{2k_B T}\right) \exp\left(-\frac{[E - (E_- + C_- \Delta T)]^2 L^d}{2k_B T^2 C_-}\right) \end{aligned} \quad (2.38)$$

C_+ and C_- being the specific heats in the disordered and ordered states respectively, and the two peaks are weighted according to the free energy difference $\Delta F = F_+ - F_-$

of the two phases. Using $F_+(T_c) = F_-(T_c)$, one finds $\Delta F = -(E_+ - E_-)\Delta T/T_c$. From (2.38) it is easy to obtain the energy $\langle E \rangle_L \equiv \int_{-\infty}^{\infty} EP_L(E) dE$ and specific heat $C_L = L^d(\langle E^2 \rangle_L - \langle E \rangle_L^2)/k_B T^2$ of the finite system. One finds (Challa *et al* 1986) that the maximum of C_L occurs at T_c^L given by

$$(T_c^L - T_c)/T_c = \frac{k_B T_c}{E_+ - E_-} \ln \left[q \left(\frac{C_-}{C_+} \right)^{1/2} \right] L^{-d} \quad (2.39)$$

and has the height

$$C_L^{\max} = \frac{(E_+ - E_-)^2}{4k_B T^2} L^d. \quad (2.40)$$

The area underneath $C_L(T)$ is just given by the latent heat $E_+ - E_-$, since the width over which the δ function is smeared is just given by $[(E_+ - E_-)L^d]^{-1}$.

As an example, figure 6 shows Monte Carlo results for the specific heat of the two-dimensional ten-state Potts model obtained by Monte Carlo methods (Challa *et al* 1986). Figure 7 shows the same data in rescaled form, compared to the scaling function which follows from (2.38),

$$\frac{C_L/k_B}{L^2} = [(E_+ - E_-)/k_B T_c]^2 q (C_-/C_+)^{1/2} [e^x + e^{-x} q (C_-/C_+)^{1/2}]^{-2} \quad (2.41)$$

where $x = L^d(E_+ - E_-)\Delta T/2k_B T_c^2$.

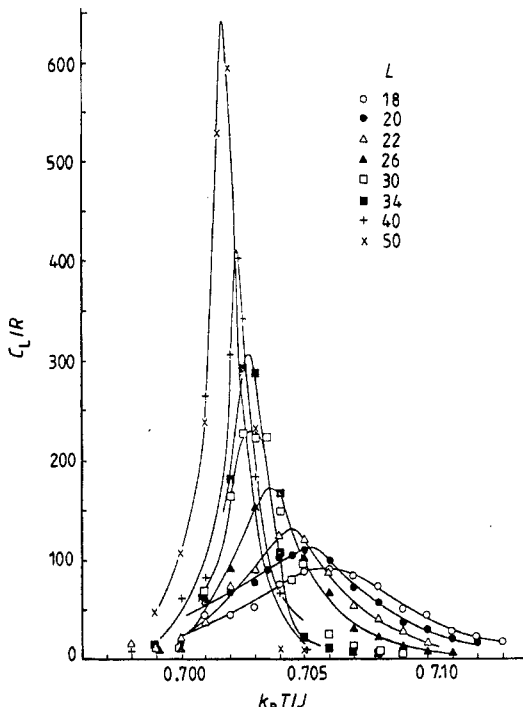


Figure 6. Specific heat of the ten-state Potts model plotted against temperature, as obtained from Monte Carlo simulation of various $L \times L$ lattices with periodic boundary conditions. The transition for $L \rightarrow \infty$ occurs at $k_B T_c/J = 0.701\ 232$ (Baxter 1973) (from Challa *et al* 1986).

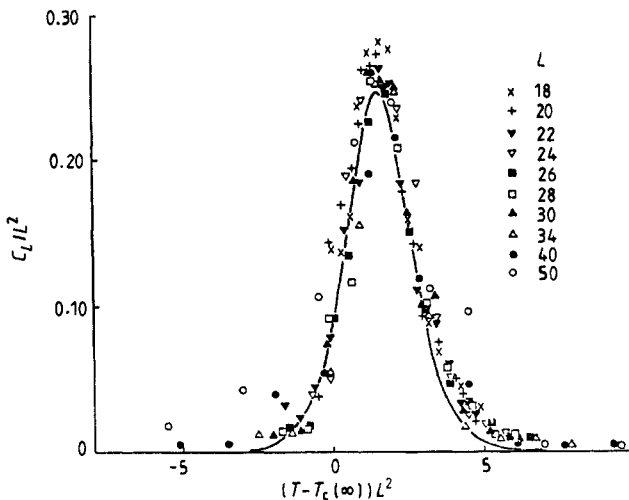


Figure 7. Scaling of the specific heat results for the ten-state Potts model. The full curve represents (2.41) (from Challa *et al* 1986).

Similar results are readily derived for the case of a first-order transition driven by the ordering field (figure 3(b)). As an example, figure 8 shows the susceptibility χ_L of finite square Ising lattices, and the same Monte Carlo data replotted in scaled form, together with the scaling function (Binder and Landau 1984)

$$\chi_L/L^d = \phi_0^2/k_B T \cosh^2(H\phi_0 L^d/k_B T). \quad (2.42)$$

In this case there is no shift of the transition, due to the symmetry $H \leftrightarrow -H$.

The result (2.42) only holds for anisotropic magnets (Heisenberg spins). For isotropic magnets (Heisenberg spins), the susceptibility peak $\chi_L \propto L^d$ as given by (2.42) is superimposed on another peak of width proportional to L^{-2} and height L^{4-d} due to spin waves (Fisher and Privman 1985).

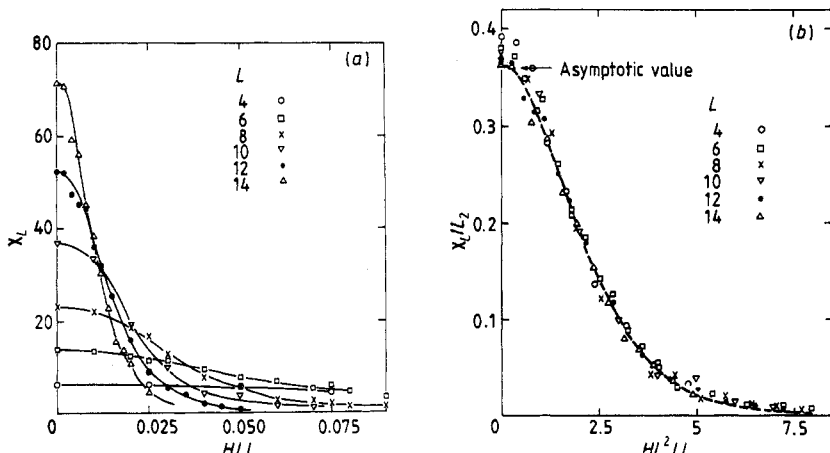


Figure 8. (a) Susceptibility χ_L of finite square Ising lattices with nearest-neighbour coupling J plotted against field at $k_B T/J = 2.1$ (note $k_B T_c/J = 2.269$), for various L . (b) Scaling of the susceptibility data: the broken curve is the scaling function (2.42) (from Binder and Landau 1984).

While qualitative evidence for finite-size rounding of first-order transitions has been obtained from specific heat measurements of phase transitions in monolayers adsorbed on surfaces (Marx 1985), a quantitative analysis of such phenomena for real systems still remains to be done.

2.5. Impurity effects on first-order transitions

This section presents a brief phenomenological discussion of phenomena due to *quenched* (immobile, frozen) randomly distributed impurities (point defects), following a discussion of Imry and Wortis (1979). There is no need to discuss the case of *annealed* (mobile) impurities—they act just like an additional component and thus simply enlarge the space of thermodynamic variables.

We consider a lattice model where each site has a probability p of being occupied by an impurity species: the system is assumed to have a transition at a temperature $T_c(p)$. When $p = 0$, the system is pure, and we suppose the transition to be weakly first order: the correlation length ξ (measured in units of the lattice spacing) at the transition is large but finite. We now assume that the average number of impurities in a correlation volume, $p\xi^d > 1$ —then probability theory shows that the *typical fluctuation* of this impurity number is $\overline{\Delta p} \sim [p(1-p)]^{1/2} \xi^{-d/2}$. Correspondingly one has a spread in ‘local intrinsic transition temperatures’ $\Delta T_c = |dT_c(p)/dp| \overline{\Delta p}$. Of course, it would be wrong to think that each correlation volume undergoes a transition at its own $T_c(p + \Delta p)$, thus leaving the sample in an inhomogeneously mixed phase between $T_c(p) - \Delta T_c$ and $T_c(p) + \Delta T_c$: thereby one would create a lot of interfaces, which is unfavourable. If the average impurity concentration p at a temperature $T_c(p) - \Delta T$ corresponds to a state in phase 2, a correlation volume can be in phase 1 only if the cost in interface energy is not too great:

$$\xi^d [f_2(p + \Delta p, T_c(p) - \Delta T) - f_1(p + \Delta p, T_c(p) + \Delta T)] > C f_{\text{int}} \xi^{d-1} \quad (2.43)$$

where C is a geometrical factor, f_{int} is the interfacial tension and f_1 and f_2 are the bulk free energy densities of the two phases. Since $T_c(p)$ is defined from $f_1(p, T_c(p)) = f_2(p, T_c(p))$, and since the variation of f_1 and f_2 with Δp and ΔT is linear for $\Delta p, \Delta T \rightarrow 0$, one concludes that

$$\left| \frac{dT_c(p)}{dp} \right| = \left| \frac{\partial}{\partial p} (f_2 - f_1) \left(\frac{\partial}{\partial T} (f_2 - f_1) \right)^{-1} \right|$$

and hence (2.43) yields

$$\left| \frac{dT_c(p)}{dp} \right| \Delta p > \frac{C f_{\text{int}} T_c(p)}{L(p) \xi} + \Delta T \quad (2.44)$$

where the latent heat at the transition, $L(p) \equiv T \partial / \partial T (f_2 - f_1)_{p, T_c(p)}$ is introduced.

If for some interval ΔT close to $T_c(p)$ (2.44) holds for the typical fluctuation $\overline{\Delta p} \sim [p(1-p)]^{1/2} \xi^{-d/2}$, one expects a rounding of the transition: the discontinuity is either removed completely or at least reduced by a fraction of order unity. If for the typical fluctuation (2.44) does not hold, it may still be satisfied in the rare cases where Δp in some correlation volumes is much larger than its typical value $\overline{\Delta p}$: then close to $T_c(p)$ the system will already contain some impurity-induced small ‘precursor domains’ of the other phase. These precursor effects, however, are exponentially small.

In this discussion we have tacitly assumed that the interactions in the system driving the transition are in a sense ‘simple’, and then the impurities can either produce a

rounding of the transition or at least produce precursor effects, but cannot change its character. In systems with competing interactions, however, the addition of quenched impurities may in fact stabilise an ordered phase which does not occur in the pure system, or it may even lead to a glass-like structure. An example where both of these effects occur has recently been provided by the molecular crystal NaCN diluted with NaCl (Elschner *et al* 1985) (see figure 9).

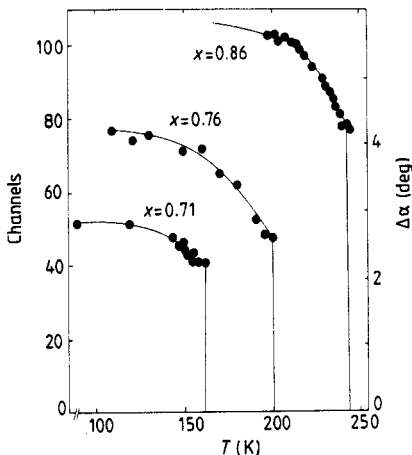


Figure 9. Order parameter $\Delta\alpha = 90 - \alpha_r$, α_r being the rhombohedral cell angle, plotted against temperature for the $(\text{NaCl})_{1-x}(\text{NaCN})_x$ system for three values of x . For $x = 0.71$ the transition is to a mixed phase, rhombohedral order and quadrupolar glass phase, while for $x \leq 0.68$ only the glass phase occurs (from Elschner *et al* 1985).

3. Some computational techniques

3.1. Models

While the phenomenological theories of § 2 yield qualitative insights about phase transitions, they cannot describe any real material quantitatively; also model Hamiltonians such as (2.13), (2.19) and (2.35) need a more detailed analysis.

The phenomenological theory hence needs to be complemented by a more microscopic approach. In a first step, the essential degrees of freedom for a particular transition are identified and an appropriate model is constructed. In a second step, the statistical mechanics of the model is treated by suitable approximate or numerical methods. (We disregard here the rare cases where the transition temperature of a first-order transition can be located exactly from duality, such as the two-dimensional Potts model with $Q > 4$ states (Baxter 1973) or the FCC lattice with purely four-spin interaction (Pearce and Baxter 1981, Liebmann 1981).)

We have already mentioned the modelling of magnetic systems in terms of Ising and Heisenberg models—indeed it is believed that a large class of systems exists for which such models are appropriate (De Jongh and Miedema 1974). Thus we discuss here the modelling of the order-disorder phase transitions in solids (figure 10). There occur transitions where the basic degree of freedom is the (thermally activated) diffusion process of atoms between various lattice sites. This happens for unmixing alloys such

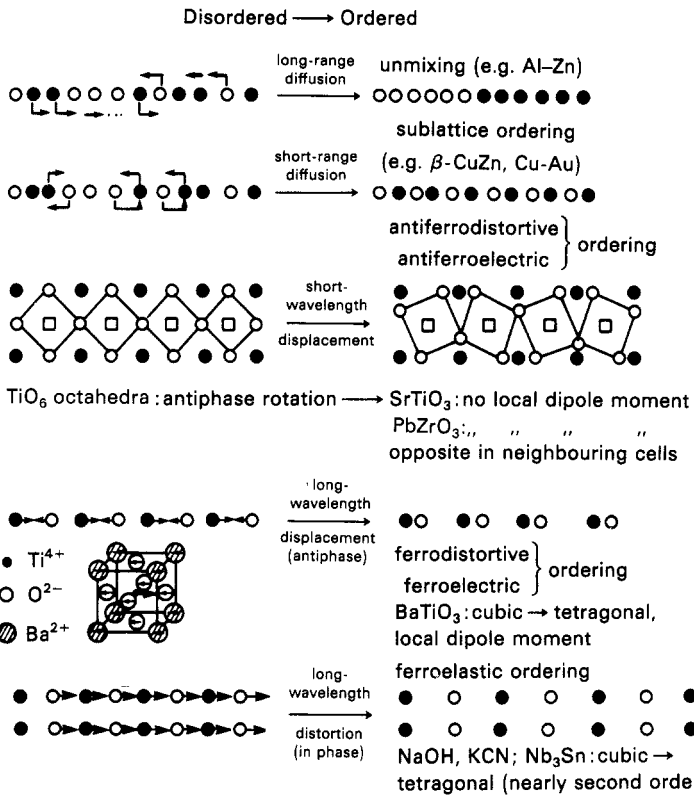


Figure 10. Degrees of freedom essential for the description of various order-disorder transitions in solids.

as Al-Zn or for ordering alloys such as β -CuZn or the Cu-Au system for instance. Since this diffusive motion is so much slower than other degrees of freedom (such as lattice vibrations), we may describe the configurational statistics of a substitutional binary alloy by local occupation variables $\{c_i\}$ ($c_i = 1$ if lattice site i is taken by an atom of species B, $c_i = 0$ if it is taken by A) and neglect the coupling between these variables and other degrees of freedom. The Hamiltonian then is

$$\mathcal{H} = \mathcal{H}_0 + \sum_{i \neq j} [c_i c_j v_{\text{BB}}(\mathbf{x}_i - \mathbf{x}_j) + 2c_i(1 - c_j)v_{\text{AB}}(\mathbf{x}_i - \mathbf{x}_j) + (1 - c_i)(1 - c_j)v_{\text{AA}}(\mathbf{x}_i - \mathbf{x}_j)] + \dots \quad (3.1)$$

where v_{AA} , v_{AB} and v_{BB} are pairwise interactions between pairs of AA, AB and BB atoms. In fact, terms involving three- and four-body interactions may also occur, but are not written down here.

As is well known, (3.1) can be reduced to the Ising model (2.35) by the transformation $S_i \equiv 1 - 2c_i = \pm 1$, apart from a constant term which is of no interest to us here. The 'exchange interaction' J_{ij} and magnetic field H in (2.35) are related to the interaction parameters of (3.1) by

$$H = \frac{1}{2} \left(\sum_{j(j \neq i)} [v_{AA}(x_i - x_j) - v_{BB}(x_i - x_j)] - \Delta\mu \right) \quad (3.2)$$

where $\Delta\mu$ is the chemical potential difference between the two species. The same mapping applies for the lattice gas model of interstitial alloys or adsorbed layers on surfaces, where A corresponds to a vacant site and B to an occupied site.

We emphasise here these Ising-type models just for their simplicity. They serve as a testing ground for various approximate methods of statistical mechanics and for numerical methods, as will be discussed further in §§ 3.2–3.4.

On the other hand, many structural transitions in solids are of a rather different kind (figure 10): we encounter periodic lattice distortions where atomic displacements are comparable with those of lattice vibrations. Short-wavelength distortions may give rise to ‘antiferrodistortive’ and ‘antiferroelectric’ orderings, as exemplified by the perovskites SrTiO_3 , PbZrO_3 , etc. Long-wavelength distortions corresponding to optic phonons give rise to ‘ferroelectric’ orderings, while those corresponding to acoustic phonons give rise to ‘ferroelastic’ or ‘martensitic’ ordering.

A further distinction concerns the effective single-particle potential felt by the atoms undergoing the distortion. Suppose the ordered structure is doubly degenerate: then the atoms can sit in the right or the left minimum of a double-minimum potential below T_c . If the potential above T_c is essentially the same, and only the distribution of the atoms over the minima is more or less random, the transition is called of ‘order-disorder-type’. This occurs, for example, for hydrogen-bonded ferroelectrics and is analogous to the sublattice ordering case mentioned above. On the other hand, if the single-particle potential changes above T_c to a single-well form, the transition is called ‘displacive’. We may consider (2.3) as a model Hamiltonian of such a system, $\phi(\mathbf{x})$ being the displacement at lattice site \mathbf{x} . A more microscopic description of structural transitions is of course based on the phonon concept: displacements $\mathbf{u}_i(\mathbf{x})$ can be related to phonon normal coordinates $Q_{k,\lambda}$ via

$$\mathbf{u}_i(\mathbf{x}) = (NM_i)^{-1/2} \sum_{k\lambda} \exp(i\mathbf{k} \cdot \mathbf{x}) \mathbf{e}_i(\mathbf{k}, \lambda) Q_{k,\lambda} \quad (3.3)$$

where $\mathbf{e}_i(\mathbf{k}, \lambda)$ is a phonon polarisation vector, M_i is the mass of the atom at site \mathbf{R}_i^I in the i th unit cell, λ labels the phonon branch and \mathbf{k} its wavevector. Now $\langle Q_{k_0, \lambda_0} \rangle_T$ plays the role of an order parameter component for the transition: in mean-field theory, the associate eigenfrequency vanishes at a temperature T_0 (‘soft phonon’). If this happens for a phonon with wavevector \mathbf{k}_0 at the Brillouin zone edge, we have an antiferroelectric order (if the phonon is polar, i.e. producing a local dipole moment) or antiferrodistortive order (for non-polar phonons). Soft optic phonons at the Brillouin zone centre give rise to ferroelectric (or ferrodistortive) orderings and soft acoustic phonons to ferroelastic ordering.

Note that the $Q_{k,\lambda}$ are defined such that the Hamiltonian of the crystal in the quasi-harmonic approximation is diagonalised (Born and Huang 1954):

$$\mathcal{H} = U_0 + \frac{1}{2} \sum_{\substack{i,j \\ I,I'}} [\partial^2 U / (\partial \mathbf{R}_i^I)_\alpha (\partial \mathbf{R}_j^{I'})_\beta] u_i^\alpha(\mathbf{R}_i) u_j^\beta(\mathbf{R}_j) = U_0 + \frac{1}{2} \sum_{k\lambda} \omega^2(\mathbf{k}, \lambda) Q_{-k,\lambda} Q_{k,\lambda}. \quad (3.4)$$

Thus, in the spirit of the Landau expansion, the coefficient $\omega^2(\mathbf{k}_0, \lambda_0)$ in front of the square of the order parameter corresponds to the term $r = r'(T - T_c)$ in (2.3). Of course, as in the Landau theory, higher-order terms in the expansion (2.3) are crucial for the description of the ordered phase: one needs to include anharmonic terms here which then couple the Q_{k_0, λ_0} also to the non-critical $Q_{k,\lambda}$. This is quite analogous to the couplings produced in (2.3) by $\phi^4(\mathbf{x})$ if one diagonalises the quadratic part of $\mathcal{F}\{\phi(\mathbf{x})\}$ by introducing the Fourier transform $\Delta\phi_k$ (cf (2.6)).

It is rather clear from this description that realistic microscopic models for most structural phase transitions are rather complicated. Thus we shall not discuss them further and rather refer to the recent literature (Bruce and Cowley 1981).

If one restricts the analysis entirely to the framework of the quasi-harmonic approximation, one can write the free energy at temperature T and volume V as

$$F(T, V) = U_0(V) + \frac{1}{2} \sum_{\mathbf{k}, \lambda} \hbar \omega_V(\mathbf{k}, \lambda) + k_B T \sum_{\mathbf{k}, \lambda} \ln[1 - \exp(-\hbar \omega_V(\mathbf{k}, \lambda)/k_B T)]. \quad (3.5)$$

Thus, if effective potentials specifying the dynamical matrix $\partial^2 U / (\partial \mathbf{R}_i^\dagger)_\alpha (\partial \mathbf{R}_j^\dagger)_\beta$ in (3.4) are known, one can obtain the phonon frequencies $\omega_V(\mathbf{k}, \lambda)$ for a given volume and obtain $F(T, V)$. Of course, in this approach, knowledge of the structure of the material is supposed. First-order transitions between different structures can be handled by performing this calculation for both phases and identifying the temperature T_c where the free energy branches of the two phases cross. Since the quasi-harmonic theory is a calculation of the mean-field type, as pointed out above, first-order transitions also show up via stability limits of the phases, where the soft modes vanish (thereby one is not locating T_c but rather temperatures T_0 or T_1 , cf figure 1(b), which are often not very far from the actual transition temperature, however). This quasi-harmonic approach to structural phase transitions has been tried for many materials: recent examples include RbCaF_3 (Boyer and Hardy 1981) and the systems CaF_2 and SrF_2 (Boyer 1980, 1981a, b) which show phase transitions to a superionic conducting state.

3.2. Molecular field theory and its generalisation (cluster variation method, etc)

The molecular field approximation (MFA) is the simplest theory for the description of phase transitions in condensed matter systems; it still finds widespread application and has been described in great detail in various textbooks (Brout 1965, Smart 1966). For first-order transitions it is still a rather popular approach, as it is thought that the statistical fluctuations neglected in this approach are less important than for second-order transitions. We shall see, however, that this statement has to be taken with a pinch of salt.

Here we do not wish to expose the MFA in full, but rather give only the spirit of the approach. For simplicity, we only deal with the Ising model (2.35). One can find the exact free energy formally as the minimum of the functional (Morita 1972)

$$\mathcal{F} = \sum_{\{S_i = \pm 1\}} \mathcal{H}_{\text{Ising}}(\{S_i\}) P(\{S_i\}) + k_B T \sum_{\{S_i = \pm 1\}} P(\{S_i\}) \ln P(\{S_i\}) \quad (3.6)$$

where the sums extend over all configurations of spins in the system and $P(\{S_i\})$ is the probability that a configuration $\{S_i\}$ occurs: this yields $P_{\text{eq}}(\{S_i\}) \propto \exp[-\mathcal{H}_{\text{Ising}}(\{S_i\})/k_B T]$, as desired. The MFA can now be found by factorising the probability $P(\{S_i\})$ of a configuration of the whole lattice into a product of single-site probabilities p_i which can take two values: $p_\uparrow = (1+m)/2$ that the spin at site i is up and $p_\downarrow = (1-m)/2$ that it is down ($p_\uparrow - p_\downarrow = m$ is the magnetisation). Now the expression $J_{ij} S_i S_j p_i p_j$ summed over the possible values p_\uparrow and p_\downarrow simply yields $J_{ij} m^2$, and hence (3.6) reduces to

$$\frac{1}{N} \mathcal{F}^{\text{MFA}} = \frac{1}{2} J(0) m^2 - Hm + k_B T \left[\frac{1+m}{2} \ln \left(\frac{1+m}{2} \right) + \frac{1-m}{2} \ln \left(\frac{1-m}{2} \right) \right] \quad (3.7)$$

where $J(\mathbf{k}) = \sum_{j(\neq i)} J_{ij} \exp[i\mathbf{k} \cdot (\mathbf{r}_i - \mathbf{r}_j)]$. Minimising now \mathcal{F}^{MFA} with respect to m yields

the standard result

$$m = \tanh \frac{1}{k_B T} (J(0)m + H). \quad (3.8)$$

Now a systematic improvement is obtained if one approximates the probability of configurations not just by single-point probabilities but by using 'cluster probabilities'. We consider probabilities $p_{n,c}(k, i)$ that a configuration k of the n spins in a cluster of geometry c occurs ($k = 1, \dots, 2^n$). These probabilities can be expressed in terms of the multispin correlation functions $g_{nc}(i) = \langle S_i S_{j_1} \dots S_{j_n} \rangle$ where the set of vectors $r_{j_1} - r_i, \dots, r_{j_n} - r_i$ defines the n -point cluster of type c located at lattice site i . Now the free energy functional to be minimised in this cluster variation method (Kikuchi 1951, Sanchez and de Fontaine 1980, 1982) is a more complicated approximation to (3.6) than (3.7) but has the advantage that the energy term in $F = U - TS$ is treated exactly; one now rather approximates the entropy. We find

$$\mathcal{F} = \frac{1}{2} \sum_i \sum_j J_{ij} g_{2,r_j}(i) + k_B T \sum_i \sum_{n,c} \gamma_{nc} \sum_{k=1}^{2^n} p_{n,c}(k, i) \ln p_{n,c}(k, i) \quad (3.9)$$

where the coefficients γ_{nc} are combinatorial factors depending on the lattice geometry and the clusters included in the approximation. Assuming the ordered structure to be known, one can apply the symmetry operations of the associated group to reduce the number of variational parameters in (3.9) to a finite number. While in the MFA one has a single non-linear self-consistent equation, (3.8) (or a set of equations involving the order parameter components, if one considers a problem more complicated than the Ising ferromagnet), one now ends up with a much larger set of coupled non-linear equations involving the short-range order parameters $g_{nc}(i)$ when one minimises (3.9). Thus while the simple MFA is still manageable for a wide variety of systems (Brout 1965, Smart 1966), the cluster variation (cv) method is essentially restricted to Ising-type problems relevant for phase transitions in metallic alloys (de Fontaine 1979, Binder 1986). We shall discuss the merits of the various approaches when we discuss a few examples which have also been studied by Monte Carlo computer simulation (§ 3.4).

3.3. Position space renormalisation group methods for phase diagrams exhibiting first-order transitions

In § 2.2 we have already briefly encountered the renormalisation group approach, where the partition function is calculated step by step, integrating out long-wavelength degrees of freedom in a transformation $\mathcal{H}\{\phi\} = \mathbf{R}[\mathcal{H}\{\phi\}]$ which is iterated. Now we are concerned with the practical realisation of such methods in $d = 2$ and $d = 3$ dimensions to obtain phase diagrams. Again a thorough discussion of these 'real space' or 'position space' renormalisation group methods is beyond the scope of this review and can be found in the literature (Niemeijer and van Leeuwen 1976, Burkhardt and van Leeuwen 1982). We restrict ourselves to brief comments.

To give explicit meaning to (2.29), we consider for simplicity the Ising model (2.35) and assume that spins $\{S_i\}$ in blocks of linear dimension b (e.g. $b = 2$ or 3) are grouped together to form a 'block spin' S'_i . This transformation is made precise by defining a weight function $P(\{S'_i\}, \{S_i\})$ which satisfies $\sum_{\{S'_i\}} P(\{S'_i\}, \{S_i\}) = 1$. An example is the 'majority rule'

$$S'_i = \text{sgn} \left(\sum_{i \in \text{block}} S_i \right).$$

We choose a convention where a factor $-1/k_B T$ is absorbed in the Hamiltonian, $\tilde{\mathcal{H}} \equiv -\mathcal{H}/k_B T$, and we also wish to eliminate additive constants by requiring $\sum_{\{S_i\}} \tilde{\mathcal{H}} = 0$. Then the transformation (2.29), consistent with the requirement that the partition function is left invariant, is

$$\exp(G + \tilde{\mathcal{H}}'(\{S'_i\})) = \sum_{\{S_i\}} P(\{S'_i\}, \{S_i\}) \exp(\tilde{\mathcal{H}}(\{S_i\})). \quad (3.10)$$

Here G is an additive constant independent of the spin configuration. In practice the step (3.10) can only be carried out with uncontrolled approximations. Iterating (3.10), one would generate more and more coupling constants $\{K_\alpha\} \equiv \{J_{ij}/k_B T, \dots\}$: one has then not only pairwise interactions J_{ij} but also multispin interactions. In approximate calculations only a finite subset of these couplings can be kept, which we denote as \mathbf{K} . Then (3.10) yields for the free energy per spin, $f = F/N$ ($g = G/N$),

$$f(\mathbf{K}) = g(\mathbf{K}) + f(\mathbf{K}')/b^d \quad \mathbf{K}' = \mathbf{K}'(\mathbf{K}). \quad (3.11)$$

Iterating (3.11) yields an explicit expression for the free energy

$$f(\mathbf{K}) = \sum_{n=0}^{\infty} b^{-nd} g(\mathbf{K}^{(n)}) + \lim_{m \rightarrow \infty} b^{-md} f(\mathbf{K}^{(m)}) \quad (3.12)$$

where $\mathbf{K}^{(n)}$ is the set of coupling constants after n iterations. The fixed points mentioned in § 2.2 are found from $\mathbf{K}^* = \mathbf{K}'(\mathbf{K}^*)$, and the eigenvalues λ_j (see (2.31)) are found by diagonalising the matrix $T_{\alpha\beta} = (\partial K'_\alpha / \partial K_\beta)_{\mathbf{K}=\mathbf{K}^*}$. A fixed point $\lambda_j = d$ leads to a discontinuity in derivatives of the free energy, as has been shown by the scaling analysis discussed after (2.33) (Fisher and Berker 1982, Nienhuis and Nauenberg 1975), and hence corresponds to a first-order transition.

These concepts were tested for the Potts model (2.13), and at first it was a major puzzle that many variants of these approaches invariably yielded second-order phase transitions irrespective of the number of states Q (Dasgupta 1977, Burkhardt *et al* 1976, den Nijs 1979). This problem was resolved by Nienhuis *et al* (1979), who argued that it is necessary to generalise the model (2.13), including vacancies, to make it a *Potts lattice gas*. The reason for this is that it is essential that one is able to characterise the thermodynamic phases of the system by states of one or a few cell variables, since only the configurations associated with the phases survive under the renormalisation transformation. For the Ising model in a field, the first-order transition takes place between two ordered phases: thus the two states of an Ising spin suffice to characterise the phases. The first-order transition in the Potts model takes place between ordered and disordered phases. In this case, more than a few sites would be needed to represent the disordered phase. This problem is circumvented by generalising the model, since now a vacant site can represent the disordered phase: under renormalisation the Potts model may develop vacancies and the first-order transition happens by a ‘condensation’ of effective vacancies (see also Berker and Andelman 1982). The fact that there exists a critical value Q_c such that the transition is second order for $Q < Q_c$ and first order for $Q > Q_c$ is interpreted by the fact that for $Q < Q_c$ there are two fixed points, a critical and a tricritical one, which merge at Q_c and annihilate each other (Nienhuis *et al* 1979). This approach has been applied also to models for Kr adsorbed onto graphite (Berker *et al* 1978), where one can account qualitatively for the phase diagram of the commensurate solid $\sqrt{3}$ phase and the disordered phase exhibiting a tricritical point and a two-phase coexistence region.

Thus, choosing a weight function to capture the essential physics in a simple approximate transformation appears sometimes to be a rather subtle matter demanding

considerable physical insight. On the other hand, by constructing transformations for the equivalent one-dimensional quantum problem (the ‘Hamiltonian version’ of the Potts model), the correct fixed-point structure emerges straightforwardly (Sólyom and Pfeuty 1981, Iglói and Sólyom 1983a, b), but the accuracy of the determination of Q_c is poor: $Q_c = 6.81$ for $b = 2$ and $Q_c = 5.85$ for $b = 5$, while the Kadanoff (1975) variational method applied to the Potts lattice gas yields $Q_c \approx 4.08$ (Nienhuis *et al.* 1980a, b, Burkhardt 1980), close to the exact value $Q_c = 4$ (Baxter 1973).

An alternative approach to (3.10) is the phenomenological renormalisation using transfer matrix calculations of strips of finite width L (Nightingale 1976, 1982). Under a length rescaling transformation from L to L' , the correlation length ξ scales as

$$\xi_L(\mathbf{K}) = (L/L')\xi_{L'}(\mathbf{K}') \quad (3.13)$$

because all length scales change by the same scale factor $b = L/L'$ and the relation $\mathbf{K}' = \mathbf{K}_b(\mathbf{K})$ is interpreted as a renormalisation group transformation. A critical point is found as a fixed point of this transformation. Rikvold *et al.* (1983) have applied this method to a square lattice gas model with nearest-neighbour repulsion and next-nearest-neighbour attraction. Both the tricritical point and the first-order phase boundary could be located accurately, and also estimates for the discontinuity at the first-order transition were obtained from the transfer matrix calculation. On the other hand, this was no longer possible for a more complicated lattice gas model (Rikvold *et al.* 1984).

While at a second-order transition \mathbf{K}^* the bulk correlation length $\xi = \infty$ and hence this is a fixed point of (3.13) for $L, L' \rightarrow \infty$, at the discontinuity fixed point corresponding to a first-order transition one iterates to $\xi \rightarrow 0$ in the bulk. However, ξ_L as extracted from the transfer matrix for infinitely long strips does not measure this ‘bulk’ correlation length but rather the average distance between walls separating ordered domains along the strip. This behaviour is very reasonable, since the strip is a quasi-one-dimensional object and the free energy cost to create a wall is finite, proportional to L , in the ordered region. The situation is qualitatively similar to the one-dimensional Ising model at non-zero temperature, where the energy cost to introduce ‘walls’ between up spins and down spins is also finite, and the correlation length there also measures the average distance between these ‘walls’. This length increases exponentially with L in the ordered region, while in the disordered region ξ_L is small and, for $L \rightarrow \infty$, independent of L . Thus (3.13) is also suitable for locating a first-order transition.

Iglói and Sólyom (1983b) address the problem of how the latent heat shows up in the transfer matrix renormalisation for the ‘Hamiltonian’ version of the Potts model, and suggest that in the corresponding excitation spectrum the first-order transition shows up as a ‘level crossing’, while there remains a gap in the spectrum—the mode does not become ‘soft’ as at a second-order transition.

Finally we emphasise that these position space renormalisations are practically rather successful for $d = 2$ but not for $d = 3$. Attempts to study the FCC Ising antiferromagnet in a field by such methods have yielded rather unsatisfactory results (Mahan and Claro 1977).

3.4. Computer simulation methods

In a computer simulation, one considers a finite system (e.g. a cubic box of size L^d with periodic boundary conditions) and obtains information on the thermodynamic properties, correlation functions, etc, of the system which is exact, apart from statistical

errors. The principal approaches of this type are the molecular dynamics (MD) technique (Rahman 1964) and the Monte Carlo (MC) technique (Metropolis *et al* 1953). In the former, one numerically integrates Newton's equation of motion which follows from the chosen Hamiltonian; assuming ergodic behaviour, the quantities of interest are obtained as time averages from the simulation. In the MC method, one uses random numbers to construct a random walk through the configuration space of the model system; again averages are obtained as '(pseudo)time' averages along the trajectory of the system in phase space, the only difference from the MD method being that the trajectory now is stochastic rather than deterministic.

Both methods have been extensively reviewed recently (Binder 1979, 1984a, 1985, Heermann 1986, Alder and Hoover 1968, Sangster and Dixon 1976, Hockney and Eastwood 1981, Abraham 1982); hence we shall give only the main points relevant for the investigation of first-order phase transitions, emphasising why this may still be difficult.

One principal difficulty is the finite-size rounding and shifting of the transition. In principle the phenomena are well understood (§ 2.4); in practice this makes it difficult to distinguish between second-order and weakly first-order transitions. For example, rather extensive work was necessary to show (Abraham 1983, 1984, Bakker *et al* 1984) that the melting transition in two-dimensional Lennard-Jones fluids is in fact first order, and the suggested two continuous transitions involving the hexatic phase (Nelson and Halperin 1979) do not occur in these systems.

Another difficulty is that the periodic boundary condition (for a chosen shape of the box) prefers certain structures of a solid and suppresses other ones which do not 'fit': this is a particularly cumbersome problem for off-lattice systems (studies of the fluid-solid transition or phase transitions between different lattice symmetries). The traditional approach has been to repeat the calculation for different box shapes and compare the free energies of the different phases. An interesting alternative method has recently been suggested by Parrinello and Rahman (1980) and Parrinello *et al* (1983), who generalised the MD method by including the linear dimensions of the box as separate additional dynamical variables.

Another problem is the occurrence of metastability and hysteresis: the system may get trapped in a metastable state, the lifetime of which is longer than the observation time of the simulations. The distinction of such long-lived metastable states from equilibrium states is difficult and may require computation of the free energies of the phases in question.

One must be aware of these problems when one studies first-order transitions by computer simulation, choosing suitable box sizes, observation times and preparations of the initial states. Then, employing sufficient effort in computing time—which is not cheap—and performing a careful analysis of all the possible pitfalls mentioned above, one can obtain very reliable and useful results which are superior in most cases to any of the other methods discussed here.

As an example, we mention the problem of binary alloy order-disorder transitions on the FCC lattice, relevant, for example, for CuAu alloys. The simplest model which has been extensively studied (Shockley 1938, Li 1949, Kikuchi 1974, Gahn 1973, 1974, 1982, 1986, Binder 1980a, 1981a, Binder *et al* 1981, Finel and Ducastelle 1986, Sanchez *et al* 1982, Mohri *et al* 1985, Polgreen 1984, Lebowitz *et al* 1985, Diep *et al* 1986) is (3.1), where the interaction $J_{ij} < 0$ is restricted to nearest neighbours. Figure 11 shows that the phase diagram found in the mean-field approximation (Shockley 1938, Gahn 1973, 1974), in the quasi-chemical approximation (Li 1949) (this can be viewed as a

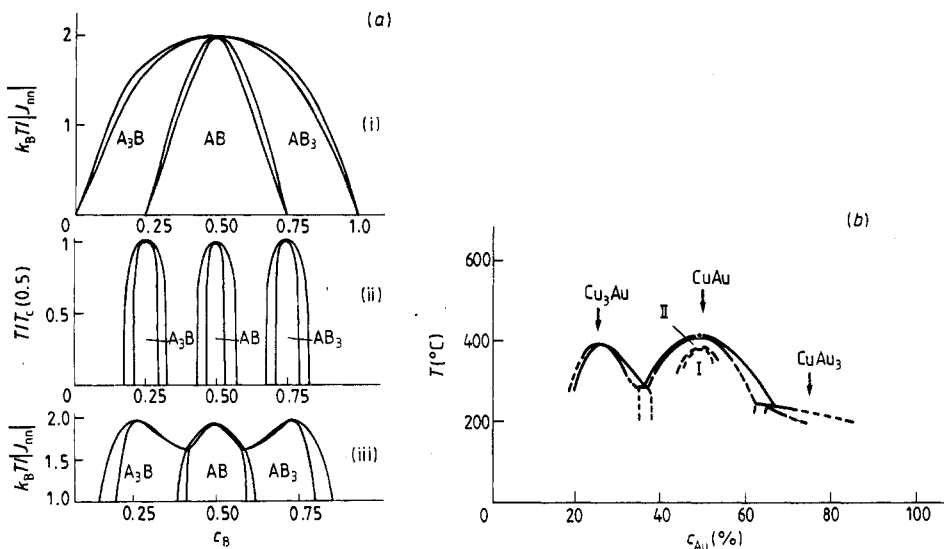


Figure 11. (a) Temperature concentration phase diagram of a binary alloy AB at the FCC lattice with nearest-neighbour interaction J_{nn} , according to three approximations: (i) the Bragg-Williams molecular field approximation (Shockley 1938); (ii) the quasichemical approximation (Li 1949); (iii) the cluster variation calculation in the tetrahedron approximation (Kikuchi 1974). The AB and A_3B structures are displayed in figures 4(a) and 4(c) respectively (from Binder 1980a). (b) Experimental phase diagram of the CuAu system. The CuAu II phase is a long-period superstructure, while CuAu I is the structure shown in figure 4 (from Hansen 1958).

special case of (3.9), the largest cluster being a nearest-neighbour pair) and in the cv method, choosing the tetrahedron as the largest cluster (Kikuchi 1974), differ considerably from each other. Choosing larger clusters in the cv method still changes the phase diagram somewhat (Mohri *et al* 1985, Finel and Ducastelle 1986), although all transitions found are of first order! Thus fluctuation effects at this transition are still important. This conclusion is corroborated by the Monte Carlo work (Binder 1980a, 1981a, Binder *et al* 1981, Polgreen 1984). Figure 12 compares the phase diagram found by Binder *et al* (1981) with that of Kikuchi (1974). Although there is still controversy about one feature of the Monte Carlo predictions, namely whether the triple point between the AB, A_3B and disordered phases appears at zero temperature (Binder 1980a, 1981a) or at a (low!) temperature $k_B T / |J| \leq 1.0$ (Gahn 1986, Diep *et al* 1986), it is well established that no analytical approximation method has so far been found which reproduces this phase diagram with an accuracy of 5% or better. Polgreen (1984) estimates, for $c_B = 0.5$, the correlation length at T_c to be about 2.5 lattice spacings—too large already for the methods of § 3.2 to be accurate, but too small for any renormalisation group approach. In fact, an attempt to study this phase diagram with the position space renormalisation group method failed (Mahan and Claro 1977).

Now one could argue that the nearest-neighbour FCC alloy problem and the equivalent problem (FCC antiferromagnet in a field) are exceptional pathological models due to their high ground-state degeneracy (Danielian 1964). However, similar discrepancies have recently been found between MFA, CV and MC calculations for order-disorder transitions on the BCC lattice (Dünweg and Binder 1987); the BCC lattice has no effects due to ‘frustration’ (Toulouse 1977) and non-degenerate ground states.

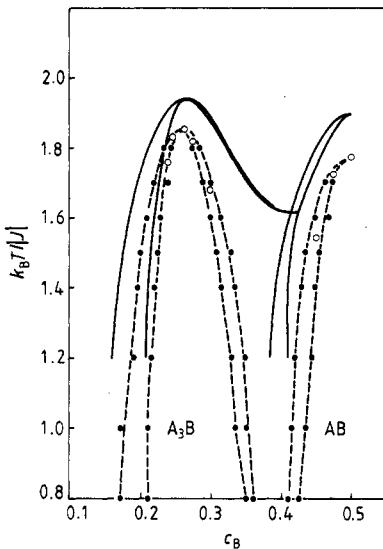


Figure 12. Temperature concentration phase diagram of a binary alloy AB at the FCC lattice with nearest-neighbour interaction J according to Monte Carlo work (full circles and open circles refer to the grand canonical and canonical ensemble respectively; broken curves are only to guide the eye) and the CV method in the tetrahedron approximation (Kikuchi (1974), full curves) (from Binder *et al* 1981).

A study of the FCC lattice with nearest-neighbour interaction $J_{nn} < 0$ and next-nearest-neighbour interaction $J_{nnn} > 0$ (Binder 1981a, Binder *et al* 1983) is also very educative (figure 13). For $R \equiv J_{nnn}/J_{nn} > R_c \approx -\frac{1}{4}$ all phase transitions are first order and the transition from AB to A_3B ends in a triple point, as well as that from AB to AB_3 . For $R < R_c$, however, the two triple points have merged at $c_B = 0.5$ and the transition from the AB phase to the disordered phase is of second order. This behaviour has been discussed by Domany *et al* (1982) from the symmetry classification point of view: the AB phase belongs to the class of the three-state Potts model (2.13) and the A_3B phase to the class of the four-state Potts model. Consequently, the direct transition of either phase to the disordered phase should be first order in $d = 3$, as observed (figure 13). However, if both transitions coincide (figure 13), the transition acquires the symmetry of the Heisenberg model with cubic anisotropy and hence a second-order transition is predicted. In any case, this example of the FCC AB structure at $c_B = 0.5$ shows that, depending on the ratio R of the interactions, the transition may be either second or first order and *symmetry considerations alone do not suffice to predict the order of the transition*, since symmetry does not tell us whether to expect a phase diagram of the type of figure 13(a) or 13(b).

For models with continuous degrees of freedom, such as the anisotropic Heisenberg antiferromagnet in a field (2.19), neither the CV method nor the position space renormalisation group method is convenient: MFA and MC methods are the only techniques for such problems available so far. Figure 14 compares the phase diagrams resulting from these approaches for an anisotropy parameter $\Delta = 0.2$ (Landau and Binder 1978). In this system, the MFA overestimates somewhat the stability of the ordered phases; the location of the first-order line between antiferromagnetic and spin flop phases is predicted rather accurately by the MFA at low temperatures, but the bicritical point where the first-order line ends occurs at a distinctly lower temperature.

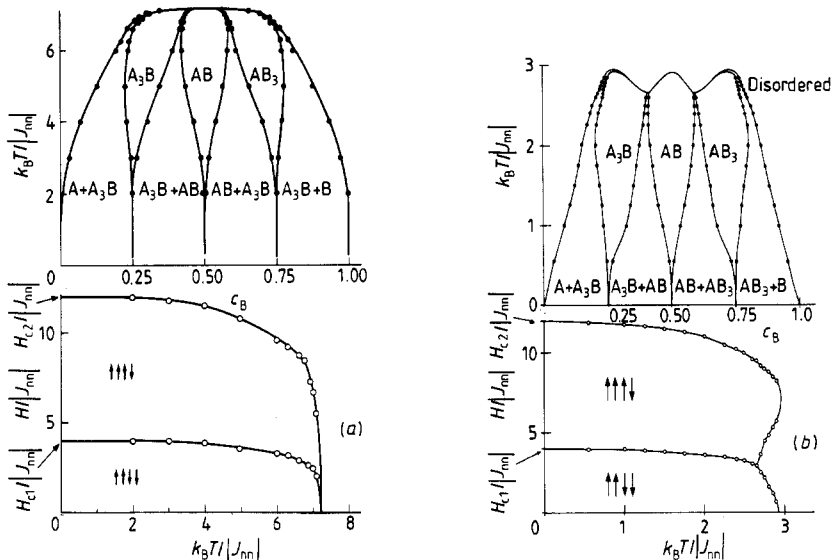


Figure 13. Phase diagram of binary alloys on the FCC lattice with nearest (J_{nn}) and next-nearest interaction ($J_{n\bar{n}n}$), for (a) $R = J_{n\bar{n}n}/J_{nn} = -0.2$ and (b) $R = -1$. The upper parts of the figures show the temperature-composition phase diagram, while the lower parts show the corresponding diagram in the 'magnetic field'-temperature plane. For notation of phases of figures 4(a) and 4(c) respectively ((a) from Binder 1981a, (b) from Binder *et al* 1983).

As discussed in § 3.3, the position space renormalisation group method is most powerful for two-dimensional problems with discrete variables (Ising, Potts spins, etc.). But even for such problems, the computer simulation method may be competitive or even superior, if the model exhibits a larger range of interactions and/or large unit cells in the ordered structure. Figure 15 shows, as an example (Landau and Binder 1985), the phase diagram of an Ising model on the square lattice with nearest-, next-nearest- and third-nearest-neighbour interactions (J_{nn} , $J_{n\bar{n}n}$, J_3). Large unit cells (4×2 and 4×4 structures) do occur in a certain parameter range. As expected from symmetry classification arguments (Schick 1981), these structures have first-order transitions, while the 2×1 and $c(2 \times 2)$ structures have second-order transitions.

4. Metastable states near first-order phase transitions

4.1. How metastable states in statistical mechanics can be defined and their properties computed

Metastable phases are very common in nature, and for many practical purposes not at all distinct from stable ones (for instance, diamond is only a metastable modification of graphite!). Also, approximate theories of first-order phase transitions easily yield free energy branches which do not correspond to the thermal equilibrium states of minimum free energy, and hence are commonly interpreted as metastable or unstable states. We have seen this for the Landau theory of a ferromagnet (cf figure 3(b) and (2.10); the same result follows from the molecular field equation of state, (3.8)), and similar behaviour occurs in many other theories as well: for example, the van der

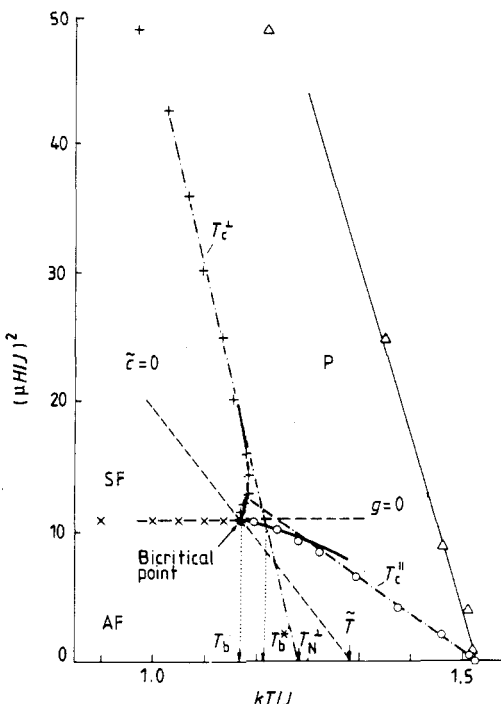


Figure 14. Phase diagram of a uniaxial classical Heisenberg antiferromagnet on the simple cubic lattice, as a function of temperature T and field H_\parallel applied in the direction of the easy axis. The anisotropy parameter Δ in the Hamiltonian (2.19) is chosen as $\Delta = 0.2$. Both Monte Carlo results and mean-field predictions (chain lines) are shown. The broken lines are the theoretical scaling axes. The triangles show the critical field in the $T-H_\perp$ plane (from Landau and Binder 1978).

Waals equation of state describing gas-liquid condensation exhibits an analogous loop of one-phase states in the two-phase coexistence region.

Unfortunately, while the description of metastability in the framework of mean-field approximations (MFA) seems so straightforward, this is not so if one deals with the more rigorous approach of statistical thermodynamics. A heuristic computational approach, discussed in § 3.2, consisted of going beyond MFA by the cluster variation method, taking more and more short-range correlations into account the larger one chooses the cluster. Computing the isotherms for a nearest-neighbour Ising ferromagnet in this way (Kikuchi 1967), one finds that the stable branch is nicely convergent, while the metastable loop becomes flatter and flatter the larger the cluster, i.e. the critical field H_c (2.10) converges towards zero—an exact calculation of the equation of state yields the magnetisation jump from ϕ_0 to $-\phi_0$ as H changes from 0^+ to 0^- in figure 3(b), but does not yield any metastable state! This is not really a surprise, of course: statistical mechanics is constructed to yield thermal equilibrium states, and the partition function is dominated by the system configurations yielding the minimum free energy. In a magnet with $H < 0$, states with negative magnetisation have lower free energy than those with positive magnetisation, and hence the latter do not result from the partition function in the thermodynamic limit.

Similarly, a more rigorous treatment of the gas-fluid system, even with long-range interactions for which the van der Waals equation of state becomes exact in the

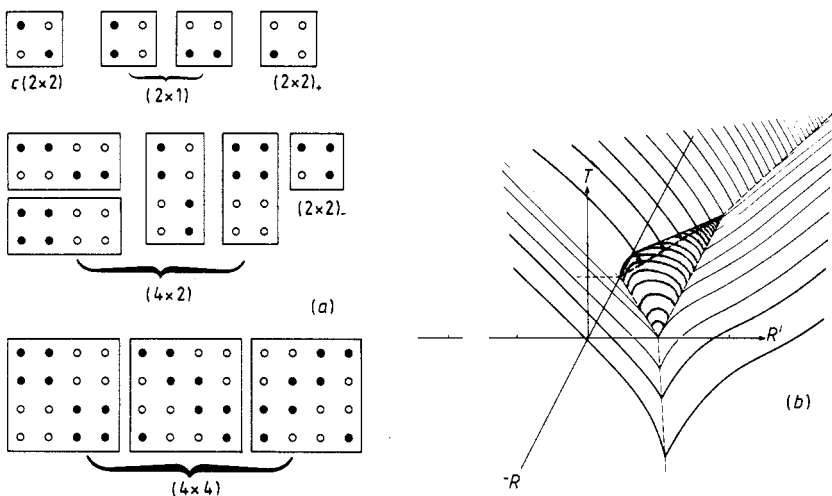


Figure 15. (a) Ordered structures and (b) global phase diagram occurring in a square lattice gas with nearest- (J_{nn}), next-nearest- (J_{nnn}) and third-nearest-neighbour (J_3) repulsive interactions as a function of temperature $T/|J_{nn}|$, $R = J_{nnn}/|J_{nn}|$ and $R' = J_3/|J_{nn}|$. The (4×2) phase occurs in the dark region in the centre of the phase diagram; its transition is of first order, as for the (4×4) phase, which occurs for large R' on the right-hand side of the phase diagram. The $c(2 \times 2)$ phase (left forward part of the figure) and (2×1) phase (left backward part) have second-order transitions to the disordered phase. Different orderings coexist at $T=0$ only (from Landau and Binder 1985).

one-phase region, yields only mixed-phase configurations for densities inside the coexistence curve (Lebowitz and Penrose 1966). This statement holds if one proceeds in the usual manner, taking first the thermodynamic limit (particle number $N \rightarrow \infty$) and afterwards the interaction range $R \rightarrow \infty$. However, if one proceeds differently, taking both limits together in such a way that one suppresses mixed-phase states satisfying the condition (r_0 is the nearest-neighbour distance)

$$N \gg (R/r_0)^d \gg \ln N \quad (4.1)$$

one does recover the standard metastable branches of the van der Waals equation (Penrose and Lebowitz 1971).

Hence the idea originates that for defining a metastable state in the framework of statistical mechanics one has to constrain the phase space suitably: by calculating suitable ‘restricted partition functions’ one forbids two-phase configurations and hence defines metastable states. The question, of course, is how this should be done in practice. Various approaches of this type have been suggested. In an Ising ferromagnet at low temperatures one can, for the state with positive magnetisation in a negative field, forbid all spin configurations containing clusters of overturned spins exceeding some given size (Capocaccia *et al* 1974). Of course, the properties of metastable states defined in this way must depend to some extent on this cut-off cluster size—only for $T \rightarrow 0$, where such excitations no longer contribute, is a unique, but trivial, answer obtained. At finite T , one needs guidance from physical arguments as to how this cut-off size should be optimally chosen. A prescription to do this results from nucleation theory in the framework of the droplet model—we shall return to this point in § 4.2.

Another approach (e.g. Langer 1974), to suppress phase separation into the two phases with order parameters ϕ_1^{coex} and ϕ_2^{coex} coexisting at a first-order phase transition,

consists of constraining the system by dividing it into cells of size L^d and requiring that an order parameter ϕ with $\phi_1^{\text{coex}} < \phi < \phi_2^{\text{coex}}$ is fixed not only globally but inside each cell. (For the example of the Ising magnet, $\phi_1^{\text{coex}} = -\phi_0$ and $\phi_2^{\text{coex}} = \phi_0$, ϕ_0 being given by the spontaneous magnetisation.) If L is small enough, phase separation within a cell cannot occur and hence one obtains a coarse-grained free energy density $f_{\text{cg}}(\phi)$ of states with uniform order parameter ϕ . This is essentially the same procedure encountered in § 2.2, where a coarse-grained Hamiltonian was introduced which is related to $f_{\text{cg}}(\phi)$ by

$$\mathcal{H}_{\text{cg}}\{\phi(\mathbf{x})\} = \int d\mathbf{x} \left(f_{\text{cg}}(\phi) + \frac{1}{2d} R^2 (\nabla \phi(\mathbf{x}))^2 \right). \quad (4.2)$$

Now identifying $f_{\text{cg}}(\phi)$ with the free energy density of metastable and unstable states is not fully satisfactory either, since $f_{\text{cg}}(\phi)$ shows some dependence on the coarse-graining length L (figure 16). This must occur, since any long-wavelength fluctuations with wavelengths exceeding L are suppressed. In the one-phase region, if we let $L \rightarrow \infty$ then $f_{\text{cg}}(\phi)$ tends towards $f(\phi)$, the true free energy density. If we let $L \rightarrow \infty$ in the two-phase region, however, we allow phase separation already within each cell: these phase-separated configurations have a free energy density excess down by a surface-to-volume ratio L^{-1} in comparison with the free energy excess of uniform states (of order unity), and hence dominate completely. As an example, figure 17 shows isotherms calculated for various cell sizes in the lattice gas model (Furukawa and Binder 1982). It is seen that the maximal supersaturation $\mu - \mu_{\text{coex}}$ reached (which corresponds to H_c in the Ising magnet) decreases as L^{-1} for increasing L .

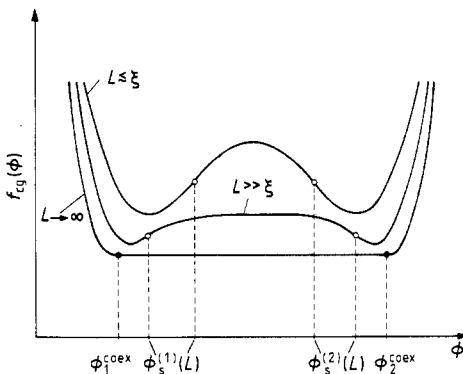


Figure 16. Schematic plot of the coarse-grained free energy density $f_{\text{cg}}(\phi)$ as a function of order parameter ϕ in a first-order transition from ϕ_1^{coex} to ϕ_2^{coex} . Spinodals $\phi_s^{(1,2)}(L)$ defined from inflection points of $f_{\text{cg}}(\phi)$ depend distinctly on the coarse-graining length L .

A completely different approach starts from the fact that experimentally one observes time averages only which are equivalent to ensemble averages in thermal equilibrium if the system is ergodic; but a metastable state is a situation far from equilibrium and hence is much more naturally defined by considering the dynamic relaxation of the system (Binder 1973). If we again consider the Ising model as an example, we can associate dynamics with it by assuming a Markovian master equation

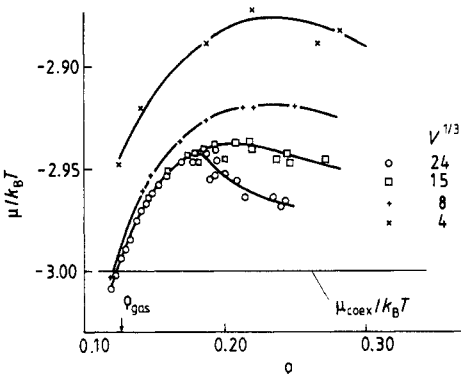


Figure 17. Chemical potential μ of the three-dimensional simple cubic lattice gas model with nearest-neighbour interactions J plotted against density ρ at a temperature $k_B T/J = 4.0$ ($k_B T_c/J = 4.51$). Recall that this model is isomorphic to the Ising ferromagnet at magnetisation $\phi_0(\rho = (1 - \phi_0)/2)$; the magnetic field translates into the chemical potential difference, $H = -(\mu - \mu_{\text{coex}})/2$. Several linear dimensions $L = V^{1/3}$ are shown as indicated (from Furukawa and Binder 1982).

for the probability $P(S_1, \dots, S_N, t)$ that a spin configuration $\{S_1, \dots, S_N\}$ occurs at time t (Glauber 1963, Kawasaki 1972):

$$\begin{aligned} \frac{d}{dt} P(S_1, \dots, S_N, t) &= - \sum_{i=1}^N W(S_i \rightarrow -S_i) P(S_1, \dots, S_i, \dots, S_N, t) \\ &\quad + \sum_{i=1}^N W(-S_i \rightarrow S_i) P(S_1, \dots, -S_i, \dots, S_N, t). \end{aligned} \quad (4.3)$$

The transition probability $W(S_i \rightarrow -S_i)$ is given by

$$W(S_i \rightarrow -S_i) = (2\tau_s)^{-1} [1 - \tanh(\delta\mathcal{H}/2k_B T)] \quad (4.4)$$

where τ_s is a time constant fixing the time unit and $\delta\mathcal{H}$ is the energy change produced by the spin flip.

Now let us consider the relaxation of the system after sudden changes of the field H from a positive value H' to $H = H' + \Delta H < 0$. We define a ‘non-equilibrium relaxation function’

$$\mathcal{S}^{\Delta H}(t) = (\langle \phi(t) \rangle_{T,H'} - \langle \phi(\infty) \rangle_{T,H'}) / (\langle \phi(0) \rangle_{T,H'} - \langle \phi(\infty) \rangle_{T,H'}) \quad (4.5)$$

where $\langle \phi(t) \rangle = \sum_i S_i (S_1, \dots, S_N, t)$ is a time-dependent order parameter. In the function $\mathcal{S}^{\Delta H}(t)$, metastability will show up as a relaxation occurring in two steps. After a short time (which is of the order of the order parameter relaxation time τ_ϕ^{eq} in equilibrium if H' and ΔH are small) the system will settle down at a value $\langle \phi(t) \rangle_{T,H'} \approx \phi_{\text{ms}}$, the order parameter of the metastable state. As a consequence, we expect a plateau in a plot of $\mathcal{S}^{\Delta H}(t)$ against time. Only at a much larger timescale τ_ϕ^{ms} , the ‘lifetime’ of the metastable state, can one see that the metastable ‘equilibrium’ is in fact no stationary state but slowly relaxing. The condition that metastability occurs is then simply that the two timescales are clearly distinct: for example (Binder 1973), $\tau_\phi^{\text{ms}} \geq 10^2 \tau_\phi^{\text{eq}}$ —the equality sign would yield an extreme ‘limit of metastability’ defined in a purely kinetic sense.

Although this approach is conceptually very different from the restricted partition function approach, practical results need not be different: for example, Penrose and

Lebowitz (1971) also consider an 'escape rate' from the metastable state and show that it becomes very small in the limit considered in (4.1). For example, choosing $R/r_0 = 6$, (4.1) is satisfied for macroscopic volumes ($N = 10^{22}$) and the inverse of the escape rate exceeds a time $\tau_0 \exp [\text{constant} \times (R/r_0)^d]$. Even if τ_0 is microscopic, $\tau_0 = 10^{-13}$ s, this bound for the lifetime may exceed the age of the universe! Similar conclusions also apply for the nearest-neighbour Ising model at $T \rightarrow 0$ when one considers the rate at which the 'forbidden' clusters would form (Capocaccia *et al* 1974).

As an example of the kinetic approach to metastability we first consider Ising ferromagnets where the range R of the exchange J_{ii} is very large. Then fluctuations of $\sum_k J_{jk} S_k$ may be neglected and one obtains from (4.3) and (4.4) a time-dependent Ginzburg-Landau equation for $\phi(x, t) = \sum_{\{S_i\}} S_k P(\{S_i\}, t)$ in the continuum limit where the coordinate x corresponds to lattice site k (Binder 1973):

$$-\tau_s \frac{d}{dt} \phi(x, t) = -\left(1 - \frac{T}{T_0}\right) \phi(x, t) + \frac{1}{3} \left(\frac{T_c}{T}\right)^3 \phi^3(x, t) + \frac{H}{k_B T} - \frac{1}{2d} \frac{T_c}{T} R^2 \nabla^2 \phi(x, t). \quad (4.6)$$

Due to the neglect of fluctuations, (4.6) for $H/H_c < 1$ describes the relaxation into the metastable state only: metastable states have infinite lifetimes in molecular field theory. A more interesting behaviour is found if H exceeds H_c slightly (figure 18): then relaxation in two steps is indeed observed, and the flat region of $\mathcal{S}^{\Delta H}(t)$ may be taken to define ϕ_{ms} from a time average over times which are much larger than τ_ϕ^{eq} but much smaller than τ_ϕ^{ms} . This 'flatness' behaviour of $\mathcal{S}^{\Delta H}(t)$ has an interesting interpretation if one continues the metastable and unstable solutions M of (3.8), which merge at $H = H_c$ (figure 3(b)) into the complex plane for $H/H_c > 1$: while the value of ϕ in the flat part of $\mathcal{S}^{\Delta H}(t)$ is approximately given by $\text{Re } M$, the lifetime of the metastable state is proportional to $\text{Im } M$!

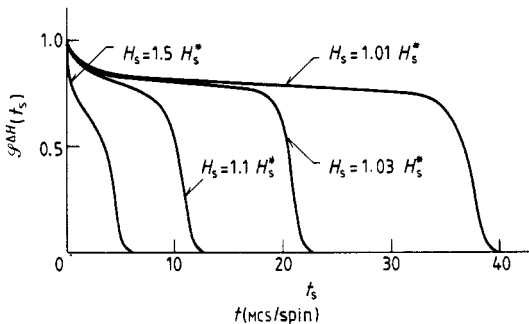


Figure 18. Non-equilibrium relaxation function $\mathcal{S}^{\Delta H}(t)$ plotted against time for different choices of $H_s \equiv H/k_B T$. The results are not dependent on temperature when one chooses a scaled time $t_s = (t/\tau_s)(1 - T/T_c)$ and $H_s^* \equiv H_c/k_B T$ (from Binder 1973).

This observation leads us to discuss the concept of defining metastable states via analytic continuations of the free energy beyond the first-order transition. In mean-field theory this analytic continuation is a real function, but the lifetime of the metastable state in mean-field theory is infinite and there is not really any distinction between equilibrium and metastable states then. Beyond mean field, a real analytic continuation beyond a first-order transition does not exist (see § 4.3, where the 'essential singularity' due to droplet-type fluctuations is discussed). But the concept that a metastable state can be described by a complex analytic continuation of the free energy, the imaginary

part of which is related to the lifetime of the metastable state, remains valid for $H \rightarrow 0$ (Langer 1967).

The kinetic approach to metastability has also been used in the study of nearest-neighbour Ising models by means of Monte Carlo simulations (Binder and Müller-Krumbhaar 1974, Binder 1976). As an example, figure 19 shows that again flat regions in the time evolution of the magnetisation are detected. From such data it is possible, at least within reasonable error margins, to 'measure' the field dependence of magnetisation, susceptibility and relaxation time as one moves deeper and deeper inside the metastable region. In fact the data seem to be compatible with a critical behaviour at a 'pseudospinodal' point, which can be located by extrapolation (Chu *et al.* 1969) but not actually reached because the metastable state is already quickly decaying before then. We discuss further the significance of this 'critical' behaviour in § 4.4.

We conclude this discussion of metastable states by remarking that $\mathcal{S}^{\Delta H}(t)$ can be precisely defined, but the properties of the metastable 'state' itself can only be defined within some intrinsic uncertainty. This uncertainty is extremely small when a metastable state close to the first-order transition is considered, but becomes larger and larger the deeper one gets into the metastable region. This is also true in experiments: in order to prepare a system in a metastable state, one has to change some external control

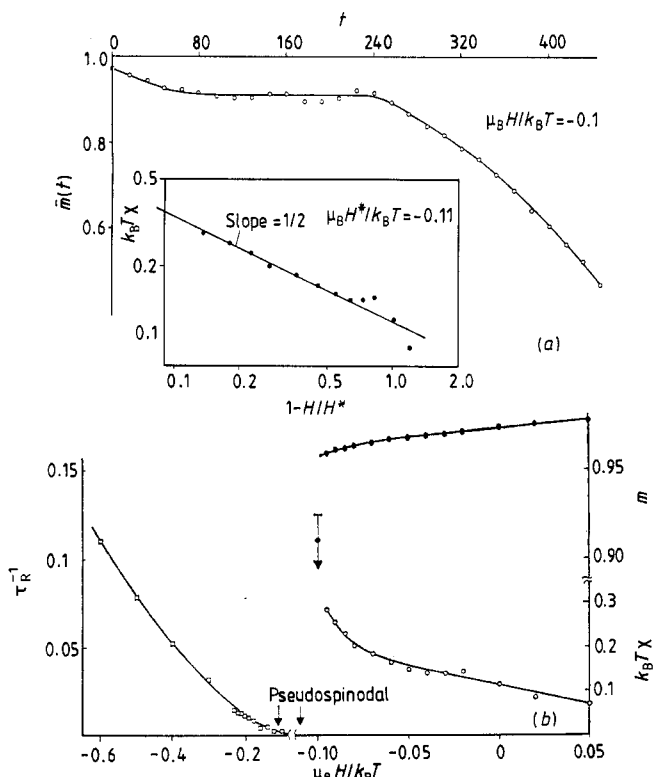


Figure 19. (a) Variation of the magnetisation (coarse-grained over a time interval of 40 Monte Carlo steps (MCS) spin) with time for a field $H/k_B T = -0.1$ at the inverse temperature $J/k_B T = 0.6$ in a two-dimensional square Ising lattice with nearest-neighbour exchange J . The log-log plot indicates the estimation of a 'pseudospinodal' H^* by fitting data on the susceptibility χ to a law $\chi \propto (H - H^*)^{-1/2}$. (b) Inverse relaxation time (left part), magnetisation m and susceptibility χ (right part) of metastable states in the two-dimensional Ising model at $J/k_B T = 0.6$ plotted against magnetic field (from Binder 1976).

parameters (such as T, H). One then has to wait some time until the relaxation process into the metastable state has died out; at the same time the relaxation out of the metastable state towards full equilibrium may already have started. Thus some intrinsic time dependence is inevitable in principle, though often not relevant in practice.

Still another approach to metastability is based on the analysis of the eigenvalues of the transfer matrix in a transfer matrix approach to calculate the partition function (e.g. Newman and Schulman 1980, Privman and Schulman 1982). This approach is beyond the scope of our introductory discussion.

4.2. *Droplets of the other phase and droplet models*

At a first-order transition, creation of a domain of one phase embedded in the other coexisting phase will cost only a contribution due to the interfacial free energy density f_{int} between the two phases, which is proportional to the domain surface area; there is no bulk term (proportional to the domain volume), since the free energies of the two phases are equal. Thus spontaneous formation of such domains ('droplets') due to statistical fluctuations is relatively easy. In a metastable state, formation and growth of sufficiently large droplets ('nucleation') is the basic mechanism of decay towards the stable equilibrium state (§ 5.1), but such 'heterophase' fluctuations occur already in the one-phase region and are thought to be responsible for the 'essential' singularity at the coexistence curve (§ 4.4). Hence we shall briefly review some of the basic ideas about 'droplet models' here.

The standard line of thinking (Becker and Döring 1935, Zettlemoyer 1969) is to consider droplets as macroscopic objects that can be described by bulk and surface terms. In an isotropic system the shape of the minimum free energy at a given volume V will be spherical, and hence the formation free energy of a droplet of radius ρ is

$$\Delta F(\rho) = H(\phi_2^{\text{coex}} - \phi_1^{\text{coex}})\rho^d V_d + S_d \rho^{d-1} f_{\text{int}} \quad (4.7)$$

where S_d and V_d denote surface area and volume of a d -dimensional unit sphere and we consider the phase with $\phi_2^{\text{coex}} = \phi_0$ as the background phase. For f_{int} , the interfacial tension of a flat planar interface between infinitely extended bulk phases is taken ('capillarity approximation').

In a solid f_{int} in general is anisotropic and so the construction of the equilibrium shape of a droplet is a formidable problem (Rottman and Wortis 1984, Wortis 1985), which we shall not consider here. But even in an isotropic system, (4.7) is a crude approximation only, valid at best to leading order for $\rho \rightarrow \infty$.

(i) f_{int} need not be the same quantity for small droplets as for an infinite flat interface. A phenomenological way to account for this is the idea of a curvature-dependent interface tension (Tolman 1949).

(ii) Apart from the droplet shape that yields the minimum droplet free energy, one should also take fluctuations around this shape into account. It has been shown (Langer 1967, Günther *et al* 1980) that capillary wave excitations yield an additive correction to $\Delta F(\rho)$ proportional to $\ln \rho$.

(iii) The macroscopic separation of the droplet free energy into bulk and surface terms becomes meaningless when the droplet radius ρ is of the same order as the correlation length ξ , since the latter length also describes the intrinsic interface thickness. If one describes this smaller-scale fluctuation also by droplets, then ramified or fractal clusters should also be taken into account, not only compact droplets.

Obviously to make progress with these questions one would need a more precise definition of what exactly is meant by a 'droplet'. This lack of a generally accepted precise definition also hampers the work on small droplets of atoms or molecules interacting with realistic potentials (Lee *et al* 1973, Abraham 1974). As an operational definition, a droplet then is often defined in terms of a constraining box with hard walls, which keeps together the atoms that build up the 'droplet'. Unfortunately some residual dependence of the droplet properties on the size of this artificial constraining box is expected, which is negligible only (for gas-liquid coexistence) if the gas pressure is very small (Binder and Kalos 1980). Other definitions for liquid droplets in a gas have also been discussed (e.g. Binder 1975a, Abraham and Barker 1975), but these too suffer from some arbitrariness. In addition, conclusions about the validity of corresponding numerical work are difficult, since neither the gas pressure at gas-liquid coexistence nor the gas-liquid interfacial tension are known exactly, but rather have to be determined by computer simulations as well.

Neither of these two latter difficulties occurs for the two-dimensional Ising ferromagnet: the first-order phase transition occurs precisely at $H = 0$, and the interface tension f_{int} is known exactly (Onsager 1944). In addition, for a lattice model it is no problem to define 'clusters' of reversed spins in terms of closed contours separating them from the surrounding up spins. Consequently the study of such clusters in the Ising model both for $d = 2$ and $d = 3$ has had much attention (Fisher 1967, Stoll *et al* 1972, Müller-Krumbhaar 1974a,b, Müller-Krumbhaar and Stoll 1976, Binder 1976, Coniglio and Klein 1980, Binder *et al* 1975, Stauffer *et al* 1982, Dickman and Schieve 1982, Marro and Toral 1983, Jacucci *et al* 1983, Hu 1984, Heermann *et al* 1984, Binder and Heermann 1985, Heermann and Klein 1983a,b, Nauenberg and Cambier 1986). Despite this large activity, clusters in the Ising model are still incompletely understood, and hence our discussion will focus on a few aspects of this problem only.

We denote the number of reversed spins within a cluster by l and the number of broken bonds at the surface of the cluster by s . Then magnetisation m and internal energy U per spin are expressed in terms of the number $Np(l, s)$ of clusters with coordinates l, s as follows (Binder 1976):

$$m = 1 - 2 \sum_{l,s} lp(l, s) \quad U = -J \left(z - 2 \sum_{l,s} sp(l, s) \right) - Hm \quad (4.8)$$

where z is the coordination number. When one considers the magnetisation only, it suffices to work with a reduced cluster concentration n_l :

$$n_l \equiv \sum_s p(l, s) \quad m = 1 - 2 \sum_{l=1}^{\infty} ln_l. \quad (4.9)$$

The droplet model of Fisher (1967) assumed that $n_l = n_0 \exp(-\Delta F_l / k_B T)$ with a non-classical expression for the droplet free energy ΔF_l (n_0 and a are some coefficients):

$$\Delta F_l = aJ(1 - T/T_c)l^\sigma + 2Hl + k_B T \tau \ln l. \quad (4.10)$$

It was shown that, by choosing the exponents $\sigma = 1/\beta\delta$ and $\tau = 2 + 1/\delta$, with β and δ the critical exponents of the magnetisation of the Ising model ($m(T, H=0) \propto (1 - T/T_c)^\beta$, $m(T=T_c, H) \propto H^{1/\delta}$), (4.9) and (4.10) yield a qualitatively reasonable equation of state in the critical region.

Since $m = -(\partial F / \partial H)_T$, one can write the free energy in this droplet model as

$$F_{\text{droplets}} = -H - k_B T \sum_l n_l. \quad (4.11)$$

Equation (4.11) is just an ideal gas law for a non-interacting assembly of droplets of different sizes l occurring at densities n_l . This is a physically reasonable picture as long as the droplets are very dilute, but not in the critical region where $m \rightarrow 0$. Therefore, while (4.9) is exact, the H dependence of ΔF_l in (4.10) certainly is not. In (4.10), one may interpret $2Hl$ as the analogue of the bulk droplet free energy $H(\phi_2^{\text{coex}} - \phi_1^{\text{coex}})$ $\rho^d V_d$ in (4.7), and $aJ(1 - T/T_c)l^\sigma + k_B T \tau \ln l$ as the analogue of the surface free energy term $S_d \rho^{d-1} f_{\text{int}}$. While the latter has a singular temperature dependence ($f_{\text{int}} \propto (1 - T/T_c)^{(d-1)\nu}$), (4.10) is regular in T as $T \rightarrow T_c$, as expected for a finite cluster of fixed size l which should have only smooth temperature dependences. In any case, the form ΔF_l , and hence n_l , is rather arbitrary; it only should be considered as a special case of a general scaling formula (Binder 1976)

$$n_l = l^{-(2+y/\delta)} \tilde{n}(Hl^y/k_B T, (1 - T/T_c)l^{y/\delta}) \quad (T \rightarrow T_c, H \rightarrow 0) \quad (4.12)$$

which involves an additional, undetermined, exponent y and an unknown scaling function \tilde{n} . In addition, it was suggested (Binder *et al* 1975, Binder 1976) that one should not interpret l as the total number of reversed spins, but rather as the excess number of down spins in a volume region V_l defining the cluster, with $V_l \propto l^{1+1/\delta}$: then it is possible to have $y=1$ in (4.12), and for clusters of the order of a correlation volume ($V_l \approx \xi^d$) one has an order parameter excess

$$l/V_l \propto l^{-1/\delta} \propto V_l^{-1/(\delta+1)} \propto \xi^{-d/(\delta+1)} \propto \epsilon^{d\nu/(\delta+1)} = \epsilon^\beta$$

using the scaling law (Stanley 1971) $d\nu = \beta(\delta+1)$. Therefore a smooth crossover from the term $2Hl$ in (4.10) to the bulk term in (4.7) at $V_l \approx \xi^d$ is possible, as well as of the term $aJ(1 - T/T_c)l^\sigma$ to the surface term in (4.7). Hence it was argued that there is not really a contradiction between (4.8)–(4.12) and the classical droplet model: rather the latter describes only very large droplets, with $V_l \gg \xi^d$, while for droplets describing critical fluctuations ($V_l \approx \xi^d$) a different theory is required.

In any case, clusters in the Ising model must represent groups of spins which are strongly thermally correlated, and this is the main drawback of the ‘geometric’ cluster definition in terms of contours around reversed spins: even when one studies Ising magnets at $T \rightarrow \infty$ as a function of H , one would have large clusters, and a percolation transition (Stauffer 1979) occurs, where a cluster of infinite size occurs, when H/T becomes less than a critical value. But these geometric clusters at $T \rightarrow \infty$ have no physical significance, there are no spatial correlations ($\langle S_i S_j \rangle_\infty = \delta_{ij} + m^2(1 - \delta_{ij})$) and the equation of state is trivial ($m = \tanh(H/k_B T)$). This random percolation transition is the $T \rightarrow \infty$ limit of a line of correlated percolation transitions which exist throughout the paramagnetic region (Coniglio and Klein 1980) and ends for $d=2$ in the critical point $T=T_c$, $m=0$, while for $d=3$ it ends even below T_c at the coexistence curve (Müller-Krumbhaar 1974b). Thus the behaviour of the ‘geometric’ Ising clusters strongly reflects the approach towards this percolation transition, which has no effect on the behaviour of the Ising spin pair correlations.

Consequently, even in the Ising ferromagnet a cluster definition different from the geometric one is needed (Binder 1976) if one wishes the cluster properties to be related in a transparent way to physical properties of the Ising system, as assumed in (4.7)–(4.12). An explicit suggestion for such a cluster definition, due to Coniglio and Klein (1980) and modified by Hu (1984), is only to count such spins as part of a cluster (inside a ‘geometric’ cluster) if they are connected by an ‘active bond’; they show that choosing bonds active with probability $p_B = 1 - \exp(-2J/k_B T)$ ensures that the percolation transition coincides with the point $T=T_c$, $m=0$ at all dimensionalities. While

this cluster definition seems to be useful along the whole coexistence curve ($H = 0$, $T < T_c$), the problem of a cluster definition valid at non-zero field or $T > T_c$ is still not solved!

Finally we mention a rather different approach, where clusters are defined in the continuum limit of Ising systems in terms of randomly nested domain walls (Bruce and Wallace 1983). This approach can be worked out in a controlled fashion near the Ising lower critical dimension, $d = 1$, and one can show that the cluster size distribution takes a scaled form near T_c , similar—but not identical—to the suggestion (4.12). The reason for this discrepancy is not understood.

Although the first principles theory of droplets and cluster models is thus still in bad shape, the concept nevertheless is very useful in a heuristic way, if one uses it at low enough temperatures. For example, figure 20(a) shows the droplet distribution in a two-dimensional Ising model (Binder and Müller-Krumbhaar 1974) at $J/k_B T = 0.46$; it happens to agree nicely with the Fisher (1967) model, (4.10), but this is somewhat accidental—for $d = 3$ this model does not fit (Müller-Krumbhaar and Stoll

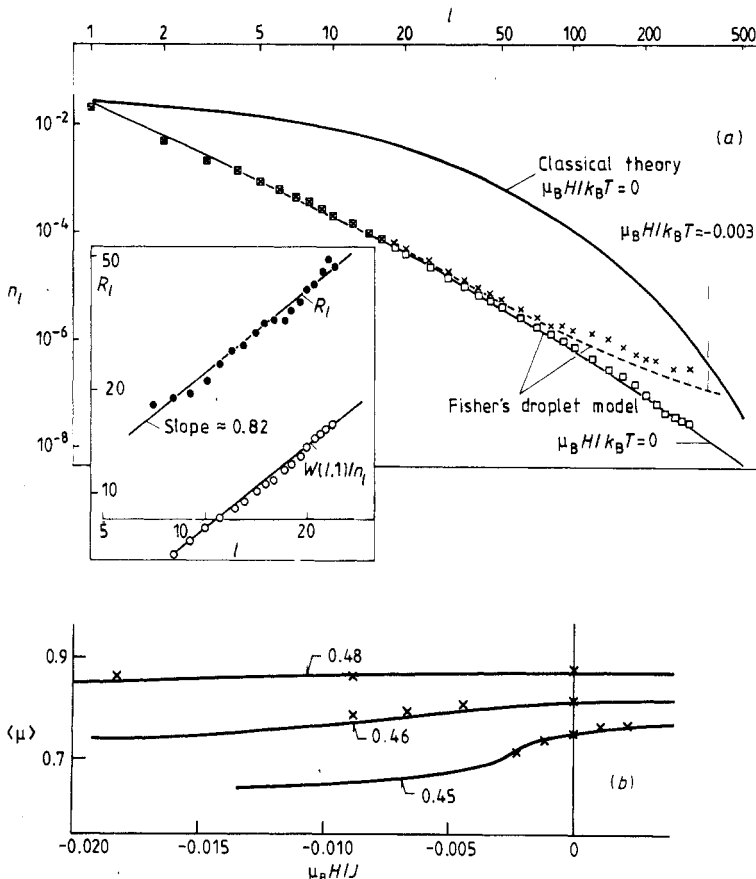


Figure 20. (a) Droplet concentration n_l against l for the square nearest-neighbour Ising lattice at $J/k_B T = 0.46$ (points) at two fields, compared with Fisher's droplet model and classical nucleation theory. The inset shows the cluster reaction rate R_l and the reaction rate due to monomers only (denoted as $W(l, 1)/n_l$). (b) Magnetisation of stable and metastable states plotted against field. The full curves are predictions based on (4.13). The parameter of the curves is $J/k_B T$ (from Binder and Müller-Krumbhaar 1974).

1976, Marro and Toral 1983). In this case, (4.10) can now be used to treat nucleation (§ 5.1) and predict the properties of metastable states. In the framework of the droplet model, this is done by using a modified form of (4.9), which will be justified later:

$$m = 1 - 2 \sum_{l=1}^{l^*} \ln l. \quad (4.13)$$

Here the ‘critical cluster size’ l^* is defined from the maximum of ΔF_l , $\partial(\Delta F_l)/\partial l|_{l^*} = 0$ (see § 5.1). Figure 20(b) shows that the resulting prediction for the metastable continuations of m are in reasonable accord with observations from computer simulations.

4.3. ‘Essential’ singularity at a first-order phase transition

While isotropic magnets exhibit a divergent susceptibility $\chi = (\partial m / \partial H)_T$ for $H \rightarrow 0^+$ at all temperatures below T_c , as discussed in § 2.2, it has been proven rigorously for the Ising model that all derivatives of the free energy F at the coexistence curve (i.e. for $H \rightarrow 0^+$) exist (Martin-Löf 1973). Nevertheless, there occurs a (very weak!) singularity at the coexistence curve, the so-called ‘essential singularity’ (Fisher 1962, 1967, Andreev 1964, Langer 1967, Binder 1976, Günther *et al* 1980). This implies that expanding F for $H=0$ in a power series in H one obtains a series, the radius of convergence of which is zero, i.e.

$$\lim_{k \rightarrow \infty} \left((k+1) \frac{(\partial^k F / \partial H^k)_T}{(\partial^{k+1} F / \partial H^{k+1})_T} \right)_{H \rightarrow 0^+} = 0. \quad (4.14)$$

This singularity was first suggested by Fisher (1962, 1967) using his droplet model, (4.9) and (4.10). As discussed in § 4.2, we feel that (4.10) is not meaningful for $V_l \gg \xi^d$, where one has the classical droplet model (4.7) instead of (4.10). Thus the treatment presented here (Binder 1976) is close in spirit to that of Andreev (1964).

Let us assume we have performed a coarse graining over cells of size $L \gg \xi$ (cf (2.21) and (2.22)). The total free energy of the system is then \mathcal{H}_{cg} plus a correction due to fluctuations of linear dimensions exceeding L . There are two kinds of such fluctuations. First we have ‘homophase fluctuations’ where the local order parameter $\phi(x)$ deviates from m by $\pm \delta\phi$. For $L \gg \xi$, $\delta\phi/m \rightarrow 0$; in addition, $P(\delta\phi)$ is essentially a Gaussian distribution (Binder 1981b). These fluctuations will not produce any singular behaviour as $H \rightarrow 0$. So the important fluctuations are the ‘heterophase’ fluctuations, i.e. droplets. Since only droplets with radii $V_l^{1/d} > L \gg \xi$ can occur, all smaller-scale fluctuations being integrated out, it makes sense to use $F = \mathcal{H}_{cg} - k_B T \sum_{V_l \geq L^d} n_l$, in analogy to (4.11), and choose (4.7) in $n_l = n_0 \exp(-\Delta F_l/k_B T)$, i.e.

$$F(T, H) = \mathcal{H}_{cg}(T, H) - n_0 \int_{L^d}^{\infty} dV \exp\left(-\frac{2mH}{k_B T} V\right) \exp(-bV^{1-1/d}) \quad (4.15)$$

where the sum has been transformed into an integral and $b = S_d V_d^{1/d-1} (f_{int}/k_B T)$.

Now with $h \equiv -2mH/k_B T$ one finds

$$\frac{\partial^k F}{\partial h^k} = \frac{\partial^k \mathcal{H}_{cg}}{\partial h^k} - n_0 \int_{L^d}^{\infty} dV V^k \exp(-bV^{1-1/d}). \quad (4.16)$$

Since for $k \rightarrow \infty$ the lower limit of the integration may be replaced by zero with negligible error, and the term $\partial^k \mathcal{H}_{\text{cg}} / \partial h^k$ may be neglected against the integral which is proportional to $\Gamma([1/(d-1)](k-1-1/d)-1)$, one finds

$$\lim_{k \rightarrow \infty} \left((k+1) \frac{\partial^k F / \partial h^k}{\partial^{k+1} F / \partial h^{k+1}} \right) \propto \lim_{k \rightarrow \infty} k^{-1/(d-1)} = 0. \quad (4.17)$$

The result (4.17) remains valid irrespective of any logarithmic correction terms as in (4.10) or (4.12) (see Binder 1976).

An alternative calculation, due to Langer (1967) and Günther *et al* (1980), starts from the field theoretic Hamiltonian (2.3) and (2.23) and evaluates the contribution to the free energy due to 'droplet' or 'instanton' solutions (Lowe and Wallace 1980) of the non-linear analogue of (2.5):

$$\frac{\delta \mathcal{F} / k_B T}{\delta \phi(x)} = r\phi + u\phi^3 - \frac{H}{k_B T} - \frac{1}{d} R^2 \nabla^2 \phi(x) = 0. \quad (4.18)$$

For $H < 0$, (4.18) admits a spherically symmetric solution with non-uniform ϕ such that $\phi \approx -\phi_0 (= (-r/u)^{1/2}$, cf (2.4)) for radii $\rho < \rho^*$ and $\phi \approx \phi_0$ for radii $\rho > \rho^*$, the critical droplet radius (cf figure 21) being given by

$$\rho^* = R \left(\frac{2u}{d} \right)^{1/2} \frac{\phi_0^2}{H/k_B T}. \quad (4.19)$$

This droplet solution prevents a real analytic continuation of F from positive H to negative H , because F has a cut singularity along the negative H axis when analytically continued in the complex plane. The discontinuity across the cut, or equivalently the

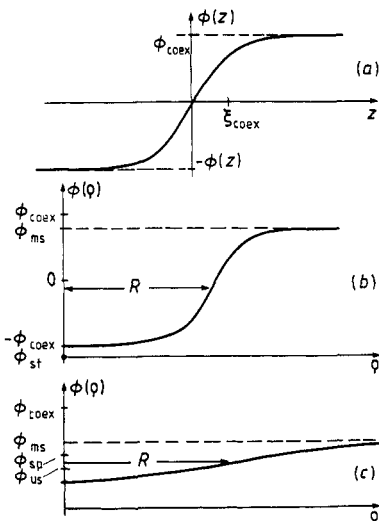


Figure 21. (a) Order parameter profile $\phi(x)$ across an interface between two coexisting bulk phases, the interface being oriented perpendicular to the z direction, and the radial order parameter profile for a marginally stable droplet (b) near the coexistence curve and (c) near the spinodal curve. In (a) and (b) the 'intrinsic' thickness of the interface is of the order of the correlation length at coexistence, ξ_{coex} , while in (c) it is of the same order as ρ^* (from Binder 1984b).

imaginary part of F , arises from the existence of the critical droplet, (4.19), and is given by (Günther *et al* 1980)

$$\text{Im } F(H, \arg H = \pi) = -B|H|^a \exp[-A|H|^{-(d-1)}(1 + O(H^2))] \quad (4.20)$$

where the exponent $a = -7/3$ for $d = 3$ and $a = (3-d)d/2$ for $1 < d < 5$, $d \neq 3$. The correction term $|H|^a$ includes fluctuations of the droplet surface (namely capillary wave excitations). A and B in (4.20) are non-universal constants. Langer (1967, 1969) shows in the framework of a Fokker-Planck description for the dynamics of the metastable state that $\text{Im } F$ controls the lifetime of the metastable state: the nucleation rate is simply proportional to $\text{Im } F$. In the Fokker-Planck description, one constructs the flow over the saddle point in the multidimensional configuration space; this saddle point, separating the metastable minimum from the stable one, is also due to a configuration containing a critical droplet. Since $\text{Im } F$ is also related to the probability that a critical droplet occurs, it is not surprising that $\text{Im } F$ and the nucleation rate can be related in the limit $H \rightarrow 0^-$.

Lowe and Wallace (1980) use (4.20) in the Cauchy integral formula with the contour enveloping the cut

$$F(H) = \frac{1}{\pi} \int_{-\infty}^0 \text{Im } F(\arg H' = \pi) \frac{dH'}{H' - H}. \quad (4.21)$$

Discarding the contour at infinity, they obtain the expansion coefficients F_k of the series $F = \sum_k H^k F_k$ and show that indeed $F_k \propto \Gamma((k-a)/(d-1))$, consistent with the leading behaviour resulting from (4.16). Lowe and Wallace show further that systematic low-temperature series expansions (Baker and Kim 1980) yield numerical evidence in favour of their results for F_k . This evidence has been strengthened by Harris (1984). Also position space renormalisation group arguments (Klein *et al* 1976) lead to the conclusion that there exists an ‘essential’ singularity at the Ising model coexistence curve ($H = 0$, $T < T_c$).

On the other hand, it must be emphasised that the existence of this singularity has not yet been established rigorously. In fact, if one postulates fully ramified droplets (surface area proportional to their volume), one gets a real continuation of F ending in a spinodal singularity (Domb 1976, Klein 1981). Also droplet-droplet interactions might shift the ‘essential’ singularity off the axis $H = 0$ into the metastable region (Domb 1976). We feel that these criticisms are not valid, and an ‘essential’ singularity due to compact droplet-like excitations does exist at all first-order transitions (in cases where there is no stronger singularity, as, for example, would happen in isotropic magnets). But clearly more work on this problem would be desirable. An important step towards a rigorous proof of the essential singularity in Ising models has been taken by Isakov (1984). He shows that

$$\lim_{h \rightarrow 0} \frac{1}{k!} \frac{\partial^k F}{\partial h^k} = (k!)^{1/(d-1)} \left[2(d-1) \left(\frac{2J}{k_B T} + C\xi \right) \right]^{-kd/(d-1)} \quad (4.22)$$

where $k > (2J/k_B T)^d$, C is a constant depending only on dimension, and $|\xi| \leq 1$ for sufficiently low T . A metastable state in his treatment is defined through an expansion at $h = 0$, $A = \sum A_k h^k$, which is asymptotic: the expansion has to be cut off at the minimum of the sequence $A_k h^k$. The last term of this series can be taken as a measure of the uncertainty ϵ with which a metastable state can be defined,

$$\epsilon = A_{k_{\min}} h^{k_{\min}} = \exp \left[-2^d \left(\frac{2J}{k_B T} + C\xi \right)^d \left(\frac{d-1}{h} \right)^{d-1} \right]. \quad (4.23)$$

Interestingly, the same result is found from the droplet model description (4.13), taking as the uncertainty the contribution of precisely the critical size itself (Isakov 1984).

4.4. On the significance of the ‘spinodal curve’ and related limits of metastability

In this section we return to the mean-field description of metastability, and recall that already in § 2.1 we have found a critical divergence at the ‘limit of metastability’. For example, in the thermally driven first-order transition of figures 1(b) and 2(b) we find $\chi_T \propto (T - T_0)^{-1}$, while in the transition driven by the field (figure 3(b)) we find $\chi_T \propto (H_c - H)^{-1/2} \propto (\phi - \phi_s)^{-1}$. In the following we consider mainly the singular behaviour at the ‘spinodal curve’ $\phi_s(T)$, but remember that other mean-field limits of metastability have similar properties.

From (2.6) we find, putting $\bar{\phi} = \phi - \phi_s + \phi_s = \phi - \phi_s + (-r/3u)^{1/2}$, that $\xi = (R/\sqrt{d})[3u(\phi - \phi_s)(\phi + \phi_s)]^{-1/2}$, this divergence of the correlation length implies that the spinodal curve just behaves as a line of critical points (Binder and Müller-Krumbhaar 1974, Compagner 1974, Saito 1978). In renormalisation group treatments of mean-field systems ($R \rightarrow \infty$), this line is described by a ‘spinodal fixed point’ (Gunton and Yalabik 1978, Dee *et al* 1981).

As discussed in § 4.1, these metastable branches are meaningful in the mean-field limit, $R \rightarrow \infty$, and so it is natural to ask to what extent mean-field theory is still accurate for large but finite R . This question can be answered, for instance, by extending the Ginzburg criterion for the critical point (2.24) and (2.28) to a metastable state close to the spinodal curve. We require (Binder 1984b)

$$\langle (\delta\phi(x))^2 \rangle_{T,L} \ll (\phi - \phi_s)^2 \quad (4.24)$$

and using (2.25)–(2.27) with $L = \xi \approx [R/(6du\phi_s)^{1/2}](\phi - \phi_s)^{-1/2}$ yields

$$1 \ll R^2 \xi^{d-2} (\phi - \phi_s)^2 \propto R^d \phi_s^{(2-d)/2} (\phi - \phi_s)^{(6-d)/2} \propto R^d (H_c - H)^{(6-d)/4}. \quad (4.25)$$

This condition is fulfilled if either the interaction range is very large or d exceeds $d_u = 6$. This self-consistency of the spinodal for $d > 6$, equivalent to the fact that for finite R the ‘spinodal fixed point’ is stable for $d > 6$ but unstable for $d < 6$ (Gunton and Yalabik 1978), is not yet understood.

The result $d_u = 6$ for the ‘spinodal fixed point’ can also be simply understood by the fact that the associate Ginzburg–Landau field theory has a Ψ^3 term in the variable $\Psi = \phi - \phi_s$. But the problem is the physical meaning of this spinodal singularity which might exist for $d > 6$: the lifetime of metastable states is finite everywhere in between coexistence curve and spinodal, but will diverge to infinity when the spinodal is approached!

As will be shown in § 5.4, the condition that the lifetime of the metastable state is very large is also given by (4.25). Therefore the practical limit of metastability is reached when (4.25) is taken as an equality. Hence the maximum value which χ_T can reach is $\chi_T^{\max} \propto R^{2d/(6-d)} \propto R^2 (d=3)$. Figure 22 shows Monte Carlo evidence for the approach towards mean-field behaviour, as obtained for Ising models with equal interaction strength between z neighbours, with z between 6 and 348 (Heermann *et al* 1982).

Thus for R finite a stability limit where χ_T actually diverges is not accessible. It is possible, of course, to define a hypothetical stability limit by extrapolation (see figure 19), but, this ‘pseudospinodal’ lacks any deeper physical significance—in its immediate vicinity the states are gradually relaxing towards equilibrium, and this

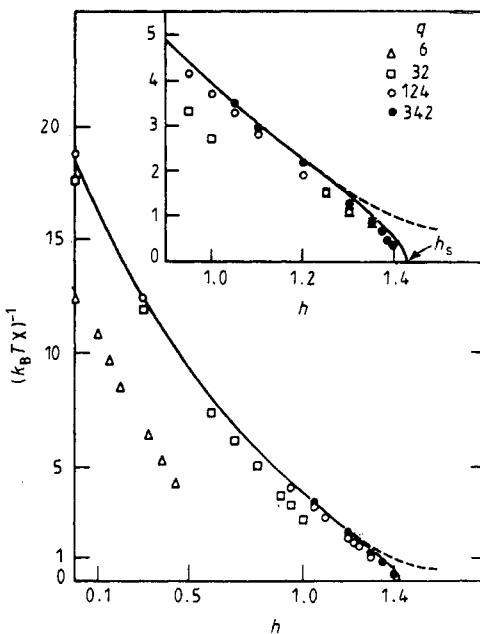


Figure 22. Inverse susceptibility of Ising ferromagnets plotted against $h = -H/k_B T$ at $T/T_c^{\text{MF}} = \frac{4}{3}$ for various ranges of the exchange interaction: each spin interacts with equal strength with q neighbours. The full curve is the molecular field approximation, the broken curve a fit to (4.13) (from Heermann *et al* 1982).

relaxation has no features associated with any singular character of this ‘pseudospinodal’. Actually, the transition from the decay of metastable states (via nucleation) to the decay of unstable states (via long-wavelength instabilities such as spinodal decomposition) is completely gradual (see § 5.4). In addition, this extrapolation is not really unique and hence the pseudospinodal H^* in figure 19 is not well defined. (Choosing in the law $\chi_T \propto (H^* - H)^{-x}$ an exponent x different from $x = \frac{1}{2}$ would also be consistent with the data, but with a different H^* .)

An alternative definition of a spinodal curve $\phi_s(T)$ is given in terms of the coarse-grained free energy $f_{\text{cg}}(\phi)$ (see (4.2)) via its inflection point $(\partial^2 f_{\text{cg}}(\phi)/\partial\phi^2)|_{\phi=\phi_s}=0$. Again, the answer obtained in this fashion is not unique either—rather ϕ_s depends distinctly on the cell size L used in the coarse graining. This point is illustrated in figure 23, where an approximate Monte Carlo calculation of ϕ_s is presented (Kaski *et al* 1984). This calculation is approximate, since it is assumed that the order parameter ϕ in a block of linear dimension L (which is a subsystem of a large system) is given by $P_L(\phi) \propto \exp(-L^d f_{\text{cg}}(\phi)/k_B T)$. By sampling $P_L(\phi)$ one can obtain $f_{\text{cg}}(\phi)$ from this assumption. Figure 23 shows that the relative distance $1 - \phi_s/\phi_{\max}$ of the spinodal from the coexistence curve (the latter here is measured as the position ϕ_{\max} where $P_L(\phi)$ is maximal) agrees with the mean-field value ($1 - 1/\sqrt{3} \approx 0.41$) only for $L/\xi \ll 1$; in the opposite limit, $L/\xi \gg 1$, this relative distance tends to zero. A similar behaviour in fact is also expected for the actual $f_{\text{cg}}(\phi)$, which is not easily accessible by such Monte Carlo methods.

Obviously a definition of a stability limit in terms of kinetics is a more sensible approach: we call a state metastable as long as it has not decayed during some given (large) time, the precise value of which is arbitrary. For the ‘cloud point’ of gas-liquid

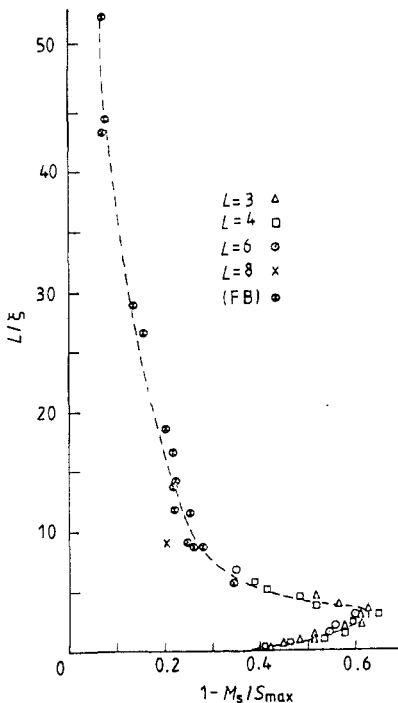


Figure 23. Monte Carlo results for the cell size dependence of the relative distance of the 'spinodal' from the coexistence curve, as deduced from cell distribution functions of the three-dimensional nearest-neighbour Ising model in the critical region. By scaling L with the correlation length, all temperatures superimpose on one 'scaling function' (from Kaski *et al* 1984).

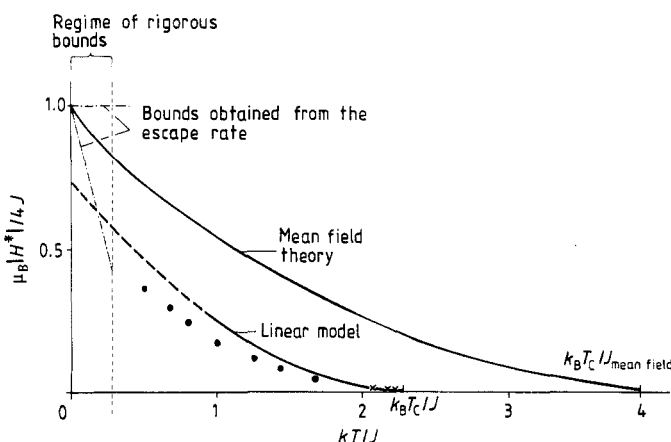


Figure 24. Stability limit of metastable states in the two-dimensional nearest-neighbour square Ising lattice. Full curves are due to the MFA and the Schofield (1969) 'linear model' equation of state. Chain lines represent bounds estimated by Capocaccia *et al* (1974) for $T \rightarrow 0$. Crosses and full circles denote Monte Carlo results due to Binder and Müller-Krumbhaar (1974) and Binder (1976) respectively (from Binder 1976).

nucleation this time may be 1 s or 1 h; in Monte Carlo simulations of the Ising square lattice (figures 19 and 24) this time may be $10^2 \tau_\mu$ or $10^3 \tau_\mu$, τ_μ being the order parameter relaxation time in equilibrium. Of course, the precise choice of this time affects the location of this kinetic stability limit somewhat: the larger is the time chosen, the closer the stability limit moves towards the coexistence curve. In practice, however, this variation may be rather small. We emphasise that such a kinetic limit of metastability (close to this limit nucleation starts to become very easy) agrees with the spinodal curve only for $R \rightarrow \infty$, as discussed further in § 5.4; for example, in figure 19 the kinetic stability limit occurs at $H_c/k_B T \approx -0.09$, while the ‘pseudospinodal’ occurs at about $H^*/k_B T \approx -0.11$.

A similar behaviour is expected for stability limits in other systems as well. For example, the famous ‘Kirkwood instability’ (Kirkwood 1951) of fluids can be viewed as the mean-field spinodal of the supercooled liquid at the liquid–solid transition. This instability is not physically meaningful for systems with short-range forces in finite dimensions (Kunkin and Frisch 1969), but can be justified in the long-range case (Grewe and Klein 1977a,b, Klein and Brown 1981) or in the infinite-dimensionality limit as has recently been suggested for hard sphere fluids (Frisch *et al* 1985, Klein and Frisch 1986).

5. Dynamics of first-order phase transitions

The dynamics of first-order phase transitions has been a field of great activity, and it recently has been reviewed extensively elsewhere (Gunton *et al* 1983, Binder 1984c, Binder and Heermann 1985, Furukawa 1986). Hence this section does not at all aim at completeness, but is rather a tutorial introduction to the main concepts about the subject.

The initial stages of such a phase transformation are treated in §§ 5.1 and 5.3, and the role that the spinodal curve plays for dynamics is elucidated in § 5.4. Some aspects of the late stages of the transformation are discussed in §§ 5.2 and 5.5.

5.1. Decay of metastable states via nucleation

The neglect of fluctuations in mean-field theory yields metastable states of infinite lifetime. Now it has been known for a long time (e.g. Becker and Döring 1935) that the important fluctuations which lead to a decay of the metastable state are ‘droplets’ or ‘heterophase fluctuations’ (see § 4.2). We now consider the dynamics of such droplets. In a gas, a fluid droplet may grow or shrink by condensation or evaporation of single atoms; then the number $n_l(t)$ of droplets containing l atoms (an ‘ l cluster’) in the unit volume at time t can be described by a rate equation for these processes:

$$\frac{dn_l(t)}{dt} = G_{l-1}n_{l-1}(t) - G_l n_l(t) + S_{l+1}n_{l+1}(t) - S_l n_l(t) \quad (l \geq 2) \quad (5.1a)$$

$$\frac{dn_1(t)}{dt} = -G_1 n_1(t) + S_2 n_2(t) \quad (l = 1) \quad (5.1b)$$

where G_l and S_l are the rates for growth and shrinking of an l cluster. These rates are assumed not to depend explicitly on time—thus any depletion of monomers is neglected in (5.1a). In the spirit of § 4.2, such clusters occur already in thermal equilibrium in the one-phase region and at the coexistence curve. It is natural to

assume that a detailed balance condition holds between any growth process and the inverse shrinking process, i.e.

$$G_l n_l^{\text{eq}} = S_{l+1} n_{l+1}^{\text{eq}} \equiv W(l, 1). \quad (5.2)$$

Thus the rates G_l and S_l in (5.1) can be eliminated in favour of one rate factor (denoted here as $W(l, 1)$) and the equilibrium cluster concentration $n_l^{\text{eq}} \equiv n_0 \exp(-\Delta F_l / k_B T)$, which again is expressed by the cluster formation free energy ΔF_l (see (4.7) or (4.10), for instance). This yields in (5.1a)

$$\begin{aligned} dn_l(t)/dt &= W(l-1, 1) \left(\frac{n_{l-1}(t)}{n_{l-1}^{\text{eq}}} - \frac{n_l(t)}{n_l^{\text{eq}}} \right) \\ &\quad + W(l, 1) \left(\frac{n_{l+1}(t)}{n_{l+1}^{\text{eq}}} - \frac{n_l(t)}{n_l^{\text{eq}}} \right) \quad (l \geq 2). \end{aligned} \quad (5.3)$$

We now transform this rate equation into a differential equation by expanding

$$\frac{n_{l\pm 1}(t)}{n_{l\pm 1}^{\text{eq}}} = \frac{n_l(t)}{n_l^{\text{eq}}} \pm \frac{\partial}{\partial l} \left(\frac{n_l(t)}{n_l^{\text{eq}}} \right) + \frac{1}{2} \frac{\partial^2}{\partial l^2} \left(\frac{n_l(t)}{n_l^{\text{eq}}} \right) \quad (5.4a)$$

$$W(l-1, 1) = W(l, 1) - \partial W(l, 1) / \partial l \quad (5.4b)$$

and find

$$\frac{\partial n_l(t)}{\partial t} = \frac{\partial}{\partial l} \left[W(l, 1) \frac{\partial}{\partial l} \left(\frac{n_l(t)}{n_l^{\text{eq}}} \right) \right] \equiv - \frac{\partial}{\partial l} J_l. \quad (5.5)$$

Here we have defined a ‘cluster current’ J_l to emphasise the fact that (5.5) has the structure of a continuity equation in cluster size space $\{l\}$. If we generalise (5.1) such that we allow growth and shrinking not only by evaporation/condensation of monomers but also by (small) clusters of size l' , we still find an equation similar to (5.5), namely (Binder and Müller-Krumbhaar 1974, Binder and Stauffer 1976, Binder 1977)

$$\frac{\partial n_l(t)}{\partial t} = \frac{\partial}{\partial l} \left[n_l^{\text{eq}} R_l \frac{\partial}{\partial l} \left(\frac{n_l(t)}{n_l^{\text{eq}}} \right) \right] = \frac{\partial}{\partial l} \left[R_l \frac{\partial}{\partial l} n_l(t) - \frac{\partial}{\partial l} \left(\frac{\Delta F_l}{k_B T} \right) R_l n_l(t) \right] \quad (5.6)$$

where we have defined a cluster reaction rate R_l in terms of rates $W(l, l')$ describing reactions $l, l' \rightleftharpoons l + l'$:

$$R_l = \frac{1}{n_l^{\text{eq}}} \sum_{l'} l'^2 W(l, l'). \quad (5.7)$$

From (5.6) it is seen that the current J_l in cluster size space consists of two terms: a ‘diffusive term’ $-R_l \partial n_l(t) / \partial l$ and a ‘drift term’ $[\partial(\Delta F_l / k_B T) / \partial l] R_l n_l(t)$. It is now assumed that (5.6) holds not only in equilibrium but can be carried over to metastable states, where one assumes that ΔF_l is still given by (4.7) or (4.10), for instance. Since now the bulk free energy of the droplet is negative, we encounter a free energy barrier ΔF^* which occurs for $l = l^*$, the maximum of ΔF (see figure 25). While a general solution of (5.6), which can be viewed as a description of Brownian motion in cluster size space $\{l\}$, usually cannot be found, it is clear that the critical cluster size l^* plays a special role. For $l < l^*$ the drift acts against the diffusion; so if a large cluster forms, it is rather likely that it disintegrates again. For $l > l^*$ the drift acts in the same direction as the diffusion; hence such supercritical clusters will grow steadily.

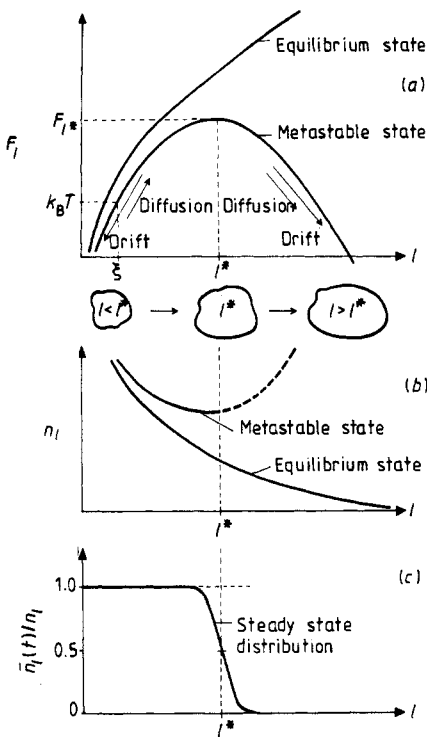


Figure 25. (a) Formation energy of a cluster as a function of cluster size (l) and the associated mechanism of cluster growth over the critical size l^* . (b) Cluster concentration n_l for metastable and equilibrium states. (c) Non-equilibrium cluster distribution in a steady state nucleation process (schematic) (from Binder 1975b).

As the system is being brought to a metastable state, one first encounters a transient period where the cluster concentrations $n_l(t)$ for $l \leq l^*$ grow until they nearly saturate at their 'equilibrium' values. After this 'time lag'—which is discussed in Kashchiev (1969), Binder and Stauffer (1976), Gitterman and Rabin (1984), Rabin and Gitterman (1984) and Trinkaus and Yoo (1987)—the nucleation current at the maximum, J_{l^*} , has nearly reached a steady state value J . We obtain this so-called *nucleation rate* J from (5.6) by imposing the following boundary conditions: instead of (5.1b) we require $\lim_{l \rightarrow 0} n_l(t)/n_l^{\text{eq}} = 1$; also we imagine that large droplets formed are removed from the system, and hence $\lim_{l \rightarrow \infty} n_l(t)/n_l^{\text{eq}} = 0$. From (5.6) it then is easy to obtain the steady state cluster concentration n_l^{ss} , since we must have $\partial n_l^{\text{ss}}/\partial t = 0$, i.e. $J_l = J$ independent of l , and thus

$$J = n_l^{\text{eq}} R_l \frac{d}{dl} \left(\frac{n_l^{\text{ss}}}{n_l^{\text{eq}}} \right) \quad \frac{n_l^{\text{ss}}}{n_l^{\text{eq}}} = J \int_l^\infty \frac{dl'}{R_l n_l^{\text{eq}}} \quad J = \left(\int_0^\infty \frac{dl}{R_l n_l^{\text{eq}}} \right)^{-1} \quad (5.8)$$

where we have used the boundary conditions at $l \rightarrow 0$ and $l \rightarrow \infty$. In cases where l^* is very large, one can approximate (5.8) by performing a quadratic expansion of ΔF_l at l^* , $\Delta F_l \approx \Delta F_{l^*} - \frac{1}{2} g k_B T (l - l^*)^2$, and hence

$$J \approx R_{l^*} n_0 \exp \left(-\frac{\Delta F_{l^*}}{k_B T} \right) \left(\frac{g}{2\pi} \right)^{1/2} \quad \frac{n_l^{\text{ss}}}{n_l^{\text{eq}}} = \frac{1}{2} \left[1 - \text{erf} \left(\frac{l - l^*}{(g/2)^{1/2}} \right) \right]. \quad (5.9)$$

Thus it is seen that $n_i^{\text{ss}}/n_i^{\text{eq}}$ changes from unity to zero in a relatively small region around l^* (figure 25). This behaviour was also the reason for choosing l^* as a cut-off size in the cluster size distribution describing a metastable state (see (4.13)).

Now this simplest version of nucleation theory (Becker and Döring 1935, Zettlemoyer 1969) has been generalised in various ways. One obvious approach is the generalisation to several cluster coordinates; i.e. we have a multidimensional space $\{l\}$ (Binder and Stauffer 1976; see also Binder 1980b). This may be useful for including fluctuations in cluster shape (in addition to the size l we may keep the surface area excess s over the minimal possible area as a second coordinate, etc) or to treat problems where droplets are formed from two constituents: nucleation of a fluid mixture droplet from the gas (Stauffer 1976), nucleation of voids filled with He gas in irradiated metals (Trinkaus 1983), etc. If we still work in the steady state approximation, the problem is formally equivalent to Maxwell's equations for steady state currents in the cluster size space $\{l\}$:

$$\nabla \times \mathbf{E}(l) = 0 \quad \nabla \cdot \mathbf{j}(l) = 0. \quad (5.10)$$

Here the 'field' is expressed in terms of a 'potential' ϕ

$$\mathbf{E}(l) = -\nabla \phi \quad \phi = -n^{\text{ss}}(l)/n^{\text{eq}}(l) \quad (5.11)$$

and we maintain the boundary condition at the origin that steady state cluster concentration $n^{\text{ss}}(l)$ and equilibrium concentration $n^{\text{eq}}(l)$ are equal, and hence $\phi(l \rightarrow 0) = -1$. For very large clusters, $|l| \rightarrow \infty$, we have again $n^{\text{ss}}(l)/n^{\text{eq}}(l) = 0$; thus the steady state current is maintained by a potential difference. Just as in the electrical analogy of a battery supplying electrons to maintain an electric current, here thermal fluctuations supply small clusters (in this continuum description at $l=0$) which are fed into the nucleation process and maintain the steady state nucleation current. The nucleation rate J , i.e. the number of large clusters formed per unit volume and unit time, then is the total current at large distances from the 'source' at the origin, $J = \oint \mathbf{j}(l) \cdot d\mathbf{l}$.

As in the electrical analogy, the current density $\mathbf{j}(l)$ is related to $\mathbf{E}(l)$ via the 'conductivity tensor' $\sigma(l)$:

$$\mathbf{j}(l) = \sigma(l) \cdot \mathbf{E}(l) \equiv n^{\text{eq}}(l) \mathbf{R}(l) \cdot \mathbf{E}(l) \quad (5.12)$$

with $\mathbf{R}(l)$ a tensor of cluster reaction rates describing purely kinetic factors. But unlike the one-dimensional case (5.6), which was solved formally by (5.8) in the steady state case, no such general solution exists for (5.10)–(5.12). Since we expect a saddle point geometry for $\Delta F(l)$ (see figure 26), we resort to an expansion around the saddle point:

$$\Delta F(l)/k_B T = \Delta F(l^*)/k_B T + (l - l^*) \cdot \mathbf{G} \cdot (l - l^*) + \dots \quad (5.13)$$

where the matrix \mathbf{G} has one negative eigenvalue, $-g$, and otherwise positive ones. Introducing the effective cross sectional area A^* of the saddle point region, one finds (Binder and Stauffer 1976)

$$J \propto \exp(-\Delta F(l^*)/k_B T) \sqrt{g(A^* \cdot \mathbf{R}(l^*) \cdot A^*)/|A^*|}. \quad (5.14)$$

This result closely resembles (5.9); only the pre-exponential factor now is different. We emphasise, however, that there are cases of practical interest where this saddle point approximation fails. If there is a strong enough disparity between the rate factors included in $\mathbf{R}(l)$, the main flux of clusters does not occur in the direction towards the saddle point, l^* , and then it does not pass the saddle point region but passes offset from the saddle point over the ridge (Stauffer 1976). Such phenomena are likely to occur in solids, where huge activation barriers may occur in the rate factors, and strong

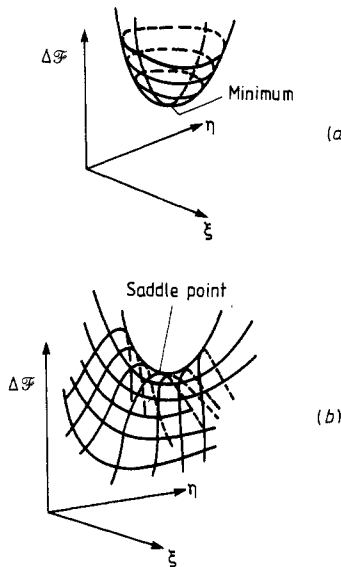


Figure 26. Free energy functional ΔF schematically displayed as a function of two phase space coordinates, η and ξ : (a) shows a minimum (corresponding to a stable or metastable homogeneous phase), while (b) exhibits a saddle point configuration, representing a metastable phase plus one droplet (here ξ and η may actually represent coordinates of the droplet) (from Binder 1984b).

disparity between different rates can be expected. Indeed, this effect is predicted to occur in the example of void nucleation in irradiated metals, mentioned above (Trinkaus 1983).

So far our discussion of nucleation has been based on a description of droplet growth and shrinking in terms of rate equations, similar to chemical kinetics. We now turn to a rather different approach, the mean-field theory of nucleation as formulated first by Cahn and Hilliard (1959). Here one does not attempt to treat the problem of the droplet size distribution developing with time, but rather focuses on the description of the free energy barrier (figures 25 and 26). This barrier is due to a droplet which just has the critical size, and sits on the background of a (uniform) metastable state. The fact that the critical droplet corresponds to an extremum of the free energy functional, namely a saddle point, suggests that one can find the free energy barrier by the usual procedure of extremising the free energy functional (see (4.18)); but rather than for a uniform solution (where $\nabla^2\phi(x)=0$) corresponding to a stable state or a metastable state without a droplet, we now look for a spherically symmetric solution (figures 21(b) and (c)) which corresponds to a metastable state containing one critical droplet at the origin. When one solves (4.18) for $\phi(\rho)$ subject to the boundary condition $\phi(\rho \rightarrow \infty) = \phi_{ms}$, one can insert this solution into the free energy functional F itself and can obtain the energy barrier ΔF^* as the free energy difference between the non-uniform solution and the uniform one (where $\phi(\rho) = \phi_{ms}$ for all ρ). This is essentially the same method as used for obtaining the interface free energy f_{int} associated with the flat planar interface between coexisting phases (figure 21(a)): there one looks for a solution non-uniform only in the z direction, perpendicular to the interface, with the boundary conditions $\phi(z \rightarrow -\infty) = \phi_1^{coex}$ and $\phi(z \rightarrow \infty) = \phi_2^{coex}$, and obtains f_{int} as the excess free energy contribution putting the profile $\phi(z)$ into the functional (2.3).

In the limit where $\phi_{\text{ms}} \rightarrow \phi_1^{\text{coex}}$ this mean-field approach agrees precisely with the conventional nucleation theory as sketched above, where one uses the classical formula (4.7) for the droplet free energy. One obtains a free energy barrier

$$\Delta F^* = \left(\frac{S_d}{d}\right)^d \left(\frac{d-1}{V_d}\right)^{d-1} \frac{f_{\text{int}}^d \chi_{\text{coex}}^{d-1}}{(\phi_2^{\text{coex}} - \phi_1^{\text{coex}})^{2(d-1)}} \left(\frac{\phi_{\text{ms}} - \phi_1^{\text{coex}}}{\phi_2^{\text{coex}} - \phi_1^{\text{coex}}}\right)^{-(d-1)} \quad (5.15)$$

where we have used ρ^* ($(\partial \Delta F(\rho)/\partial \rho = 0$ for $\rho = \rho^*$) from (4.7) and eliminated H in favour of $\phi_{\text{ms}} = \phi_1^{\text{coex}} + \chi_{\text{coex}} H$, disregarding terms of order H^2 . Obviously, the free energy barrier as given by (5.15) diverges for $\phi_{\text{ms}} \rightarrow \phi_1^{\text{coex}}$. On the other hand, if one moves deep into the metastable regime, (5.15) would predict that the barrier decreases gradually; classical nucleation theory does not contain any hint of a spinodal singularity.

Mean-field theory of nucleation, on the other hand, does yield a singular behaviour when one moves towards the spinodal (Cahn and Hilliard 1959, Klein and Unger 1983). Although the critical radius ρ^* first decreases as predicted by the classical theory, near ϕ_s it starts to increase again since the correlation length ξ diverges as $\phi \rightarrow \phi_s$ (see § 4.4) and ρ^* cannot be less than ξ . At the same time, the order parameter difference from the interior to the exterior of the droplet becomes very small (figure 21(c)); the physical interpretation of such a ‘diffuse’ droplet is that it is not a compact drop as described in (4.7) but rather a ramified cluster (Heermann and Klein 1983a,b, Klein and Unger 1983). In the mean-field critical region of a system with large but finite interaction range R , one obtains then for the free energy barrier near the spinodal (Binder 1984b)

$$\frac{\Delta F^*}{k_B T_c} \propto R^d \left(1 - \frac{T}{T_c}\right)^{(4-d)/2} \left(\frac{\phi_{\text{ms}} - \phi_s}{\phi_2^{\text{coex}} - \phi_1^{\text{coex}}}\right)^{(6-d)/2} \quad (5.16a)$$

while near the coexistence curve (5.15) yields

$$\frac{\Delta F^*}{k_B T_c} \propto R^d \left(1 - \frac{T}{T_c}\right)^{(4-d)/2} \left(\frac{\phi_{\text{ms}} - \phi_1^{\text{coex}}}{\phi_2^{\text{coex}} - \phi_1^{\text{coex}}}\right)^{-(d-1)}. \quad (5.16b)$$

It is seen that for $d < 6$ ΔF^* vanishes as one approaches the spinodal; but for large R one may nevertheless come close to the spinodal, since the scale for the nucleation barrier throughout the whole metastable region is set by the (large) factor $R^d (1 - T/T_c)^{(4-d)/2}$. One may expect that (5.16a) is meaningful as long as one requires $\Delta F^*/k_B T_c \gg 1$ —and one finds that this condition is exactly the same as (4.25)!

One may substantiate this suggestion that (5.16a) is valid if one stays inside a region for which the Ginzburg criterion renders the considered metastable state ϕ_{ms} self-consistent, by extending the Ginzburg criterion to the mean-field theory of nucleation itself. Just as for the stable and metastable minima of the free energy functional (figure 26(a)), the saddle point occurs in a high-dimensional configurational space representing the effect of fluctuations (figure 26(b)). The Cahn–Hilliard theory of nucleation assumes that a single non-uniform spherically symmetric state which extremises (2.3) also dominates the functional integral (2.23) when we look for non-uniform states near the metastable minimum. It is now clear that a necessary self-consistency condition requires that the mean-square amplitude of fluctuations of $\phi(\mathbf{x})$ along the radial profile $\phi(\rho)$ obtained from the extremisation must be smaller than the square of the difference between $\phi(\rho = 0)$ and $\phi(\rho \rightarrow \infty)$ described by the profile itself:

$$\langle (\delta\phi(\mathbf{x}))^2 \rangle_T \ll (\phi(\rho = 0) - \phi(\rho \rightarrow \infty))^2. \quad (5.17)$$

Since $\phi(\rho = 0) - \phi(\rho \rightarrow \infty) \propto \phi_s - \phi_{\text{ms}}$, (5.17) is equivalent to (4.24) and (4.25). Note

that (5.17) considers only the effect of ‘bulk fluctuations’ on the interface profile. In addition to these bulk fluctuations there are also typical long-wavelength fluctuations associated with distortions of the local interface position away from its equilibrium position. These capillary waves, which for $d \leq 3$ lead to a complete delocalisation of flat interfaces (Buff *et al* 1965, Widom 1972), represent fluctuations of the droplet shape around its average (hyper) spherical shape. Although these fluctuations have a pronounced effect on the droplet free energy, in that they yield a logarithmic correction to the classical barrier (5.16b) (see Langer 1967, Günther *et al* 1980), they are not considered here as they do not alter our conclusions on the validity of mean-field theory.

The advantage of this mean-field theory of nucleation is that it can be worked out for any phase transition for which an explicit mean-field theory exists, and quantities such as f_{int} —needed in the conventional nucleation theory based on (4.7)—are obtained within the same formalism. As an example, we mention work based on the mean-field theory of the fluid–solid transition (Ramakrishnan and Yussouf 1977, 1979, Yussouf 1981, Ramakrishnan 1982): interfacial free energies and nucleation barriers were obtained essentially along the lines of the Cahn–Hilliard approach as sketched here (Haymet and Oxtoby 1981, Oxtoby and Haymet 1982, Harrowell and Oxtoby 1984, Grant and Gunton 1985). Of course, this work is still open to question as the anisotropy of the interfacial tension of solids is not considered.

Another problem of the mean-field approach is that it yields only the free energy barrier directly, while there are clearly other factors entering the nucleation rate, as pointed out in the framework of the conventional theory of nucleation (see (5.9) and (5.14)). There must be *kinetic prefactors* as well as counterparts of the ‘Zeldovitch factor’ (Zeldovitch 1943) \sqrt{g} controlling the width of the saddle point region and hence the time a critical cluster can spend there before it substantially grows. Langer and Turski (1973) have addressed this problem by formulating a hydrodynamic theory of nucleation for the gas–liquid transition into which the mean-field result for the nucleation free energy barrier enters as an input. This approach avoids the confusion that has arisen in the earlier nucleation literature concerning correction factors due to droplet rotational and translational degrees of freedom—see Zettlemoyer (1969) and Abraham (1974) for discussions of this problem. For the solid–fluid transition, the hydrodynamic approach has recently been formulated by Grant and Gunton (1985). We are not exposing these elegant but complicated theories here—partly because of lack of space, partly because the predictive power of *any* nucleation theory is still rather uncertain. Even for the nearest-neighbour Ising model, it is not yet clear at which value of $\Delta F^*/k_B T$ significant deviations from the classical result, (5.16b), set in or in which direction they go (Stauffer *et al* 1982, Furukawa and Binder 1982) (see figure 27). While there is no doubt that the classical theory holds for $\Delta F^*/k_B T \rightarrow \infty$, significant deviations are possible—though not yet proven without doubt—for barriers in the range $20 \leq \Delta F^*/k_B T \leq 60$, which is the range of experimental interest. Further work is needed to clarify the situation and obtain the scaling function \tilde{J} for the nucleation rate in the critical region, as defined by Binder and Stauffer (1976) and Binder (1980b):

$$J = (1 - T/T_c)^{\nu(d+z)} \tilde{J}[\delta\phi/(\phi_2^{\text{coex}} - \phi_1^{\text{coex}})] \quad (5.18)$$

where ν is the correlation length exponent, z the dynamic exponent and \tilde{J} a (non-universal) amplitude factor. Lack of knowledge of this function still hampers the theoretical interpretation (Binder and Stauffer 1976, Langer and Schwartz 1980) of nucleation experiments in the critical region.

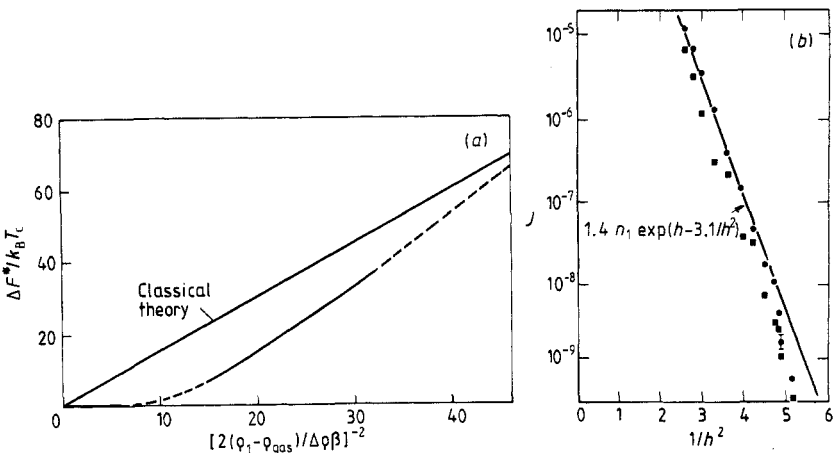


Figure 27. (a) Nucleation barrier $\Delta F^*/k_B T_c$ plotted against the variable $[2(\phi_{ms} - \phi_1^{coex})/\beta(\phi_2^{coex} - \phi_1^{coex})]^{-2}$, as obtained from Monte Carlo simulations of lattice gas models in the critical region (Furukawa and Binder 1982). The straight line represents (5.15). Note that two-scale factor universality (Stauffer *et al* 1972) implies that this plot should also apply for real gas-fluid systems and binary mixtures near their critical point. (b) Nucleation rate J observed in a nearest-neighbour Ising magnet at $T/T_c = 0.59$ in Monte Carlo simulations of a lattice of size 168^3 . Both J (circles) and the concentration n_1* of clusters of critical size (squares) are plotted logarithmically against h^{-2} where $h = -2H/k_B T$. The full line is an expression consistent with classical nucleation theory (from Stauffer *et al* 1982).

5.2. Later stages of droplet growth: coagulation, the Lifshitz-Slyozov mechanism and phenomenological structure factor scaling

Nucleation is only the first step by which the decay of a metastable state begins. As nucleated droplets grow, they take a larger and larger volume fraction of the system. This fact gives rise to several effects.

- (i) In the space taken by the droplets, no further nucleation and growth events can take place; further nucleation events can take place only in the parts of the system which have not yet been transformed.
- (ii) If the order parameter is conserved, as it is for the condensation of supercooled gas which occurs at constant overall density (or for the unmixing of supercooled binary mixtures (AB) at constant overall concentration c_B), the growth of the droplets of the high-density phase (or B-rich phase) requires transport of mass (or B atoms) from the low-density (or A-rich) phase to the droplets. Thereby the supersaturation of the metastable phase must decrease, and thus further nucleation in the phase which has not yet transformed becomes more difficult and finally impossible—the final equilibrium is a two-phase mixture of macroscopic regions of saturated gas (or A-rich phase) coexisting with liquid (or B-rich phase) at the other branch of the coexistence curve. In systems with no conservation laws—for example, when one considers the phase transition of an anisotropic magnet below T_c driven by the field—the final equilibrium is a one-phase state again, and no effect analogous to the decrease of supersaturation in regions not yet transformed occurs.

These examples already illustrate one important distinction: the qualitative aspects of nucleation phenomena are rather universal—and different dynamic properties of various systems, as exemplified in conservation laws, for instance, enter only via

different kinetic prefactors R^* in the nucleation rate, (5.9). In the later stages, however, different laws governing the dynamic evolution of the various systems do show up very distinctly, and there is much less universality.

(iii) As droplets grow, it may occur that neighbouring droplets coalesce. This 'coagulation' mechanism may get greatly enhanced if the droplets move around ('cluster diffusion and coagulation' mechanism, as discussed for phase separation by Binder and Stauffer (1974), Binder (1977) and Binder and Kalos (1980)). Even in solid alloys, some motion of clusters takes place: due to random evaporation and condensation of atoms at the surface of the clusters, the cluster centre of gravity performs a random diffusive motion. Of course, the cluster diffusion constant decreases quickly with increasing cluster size. In fluid mixtures, on the other hand, Brownian motion according to the Stokes-Einstein formula yields a cluster diffusion constant which decreases only with the inverse of the cluster radius. In fluids where both phases percolate, yet another mechanism occurs: mass may flow from the weak links of the random percolating networks to the stronger ones, and thereby the network coarsens (Siggia 1979).

(iv) A particularly interesting mechanism occurs when the order parameter is conserved and the cluster mobility is small, as happens in the late stages of phase separation in solid mixtures. Then the supersaturation is so small that no further nucleation events occur, and coarsening of the structure proceeds via a competition mechanism proposed by Lifshitz and Slyozov (1961). There one considers the random evaporation and condensation of atoms from and to the clusters; these events maintain diffusion fields between the clusters with gradients such that the largest clusters will most likely gain atoms and the smallest will lose atoms, until they are finally dissolved again. This process leads to a power law for the growth of the average linear dimension $L(t)$ with time, namely $L(t) \propto t^{1/3}$, independent of the dimensionality $d \geq 2$. Also the other mechanisms mentioned above lead to power laws, as discussed by Binder and Heermann (1985) and Furukawa (1986), though the interplay of the various mechanisms is not yet fully understood. An interesting consequence of these power laws is a scaling behaviour predicted for both droplet size distribution $n_l(t)$ and structure factor $S(\mathbf{k}, t) \equiv \langle \phi(\mathbf{k}, t) \phi(-\mathbf{k}, t) \rangle - \langle |\phi(\mathbf{k})| \rangle^2$ (see, e.g., Binder 1977, Binder *et al* 1978):

$$n_l(t) = (\bar{L}(t))^2 \tilde{n}(l/\bar{L}(t)) \quad (l \rightarrow \infty, t \rightarrow \infty) \quad (5.19)$$

$$S(\mathbf{k}, t) = (L(t))^d \tilde{S}(kL(t)) \quad (k \rightarrow 0, t \rightarrow \infty). \quad (5.20)$$

Here $\bar{L}(t) \propto t^{dx}$ is the mean cluster size and $\tilde{n}(z)$ and $\tilde{S}(z')$ are scaling functions. Quantitatively reliable theoretical predictions for these scaling functions are also a challenge for further theoretical work.

We shall not go into the mathematical details of the various mechanisms which may lead to (5.19) and (5.20) here, since many points are still under discussion. We note only that this scaling property is superficially similar to scaling assumptions near critical points—cf, for example, (4.12). But in the present case there is only one non-trivial exponent, x ; the second exponent in the prefactor multiplying the scaling function follows from simple normalisation sum rules. While approaching a critical point, a system reaches a structure which is self-similar on all length scales, ruled by some fractal dimensionality d_f ; no such fractal dimensionality can be identified in the present problem. This fact again is evident for the Lifshitz-Slyozov theory, for which $\tilde{n}(z)$ can be explicitly calculated for $\phi_1 \rightarrow \phi_1^{\text{cex}}$, and one finds that $\tilde{n}(z \geq z_{\max}) = 0$, $\tilde{n}(z \rightarrow 0) \rightarrow 0$ and a smooth maximum occurs in between (figure 28). In contrast, (4.12) reflects nicely the fractal structure of the cluster size distribution at criticality ($H = 0$, $1 - T/T_c = 0$) due to its power law decay.

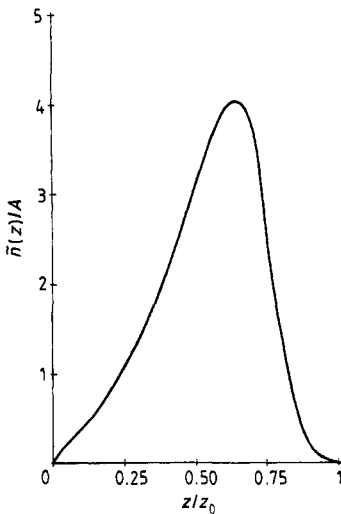


Figure 28. Scaling function $\tilde{n}(z)$ plotted against z/z_{\max} (z_{\max} is denoted as z_0 in the figure), calculated in the spirit of the theory of Lifshitz and Slyozov (1961) for $d = 2$. Here A is a renormalisation constant fixed by the condition $\phi_1 - \phi_1^{\text{coex}} = \int_0^\infty dz z \tilde{n}(\zeta)$ (from Binder 1977).

5.3. Decay of unstable mixtures via spinodal decomposition

In the previous sections we have been concerned with the dynamics of the transition when the initial state where the transition starts to take place is metastable. We now consider the alternative situation when the initial state is unstable: then no nucleation barrier needs to be overcome in the phase transformation. Rather the instability of the initial state shows up in the spontaneous growth of long-wavelength fluctuations (figure 29(a)).

For many transitions this decay of unstable initial states proceeds so quickly that it is impossible to observe it under well defined conditions: the system never can be

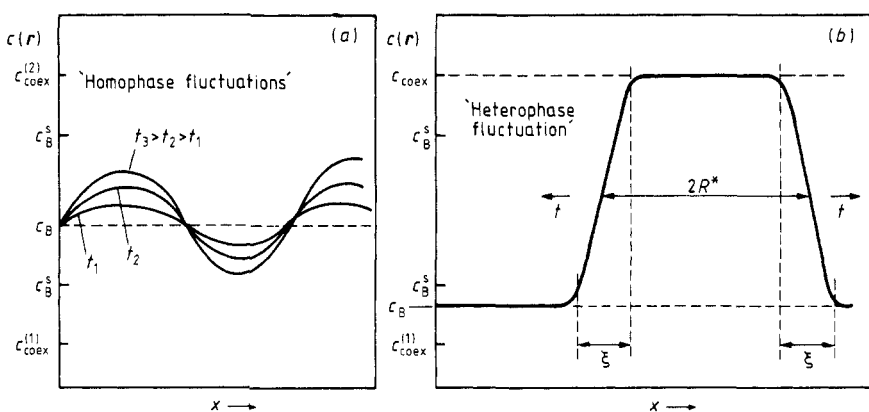


Figure 29. Unstable fluctuations in the two-phase regime of a binary mixture AB at a concentration c_B (a) in the unstable regime inside the spinodal curve c_B^s and (b) in the metastable regime in between the spinodal curve c_B^s and the coexistence curve $c_{\text{coex}}^{(1)}$. The local concentration $c(r)$ where $r = (x, y, z)$, is schematically plotted against the spatial coordinate x at some time t after the quench. The diameter of a critical droplet is denoted as $2R^*$, and correlation length of concentration fluctuations as ξ (from Binder 1981c).

brought to an unstable state instantaneously, but only at a finite ‘quenching rate’. Then often most of this decay occurs already during the quench. (Figure 30 indicates typical quenching experiments schematically.)

An interest in the initial stages of the decay of unstable states hence exists only if the dynamics of the system considered is sufficiently slow. This happens for binary mixtures, when one brings (e.g. by sudden temperature changes) the system from a state in the one-phase region, where it is homogeneous to deep inside the two-phase region. The resulting spontaneous growth of long-wavelength concentration fluctuations is known as ‘spinodal decomposition’ of the mixture (Cahn and Hilliard 1958, Cahn 1961, 1968). Here we describe the theory of spinodal decomposition only in its simplest form—more thorough recent reviews can be found in Gunton *et al* (1983) and Binder (1984c).

In the binary mixture the order parameter $\phi(\mathbf{x}, t)$ is a local concentration variable and satisfies a continuity equation

$$\partial\phi(\mathbf{x}, t)/\partial t + \nabla \cdot \mathbf{j}(\mathbf{x}, t) = 0 \quad (5.21)$$

where \mathbf{j} is a concentration current. Equation (5.21) expresses the fact that the average concentration (obtained by integrating $\phi(\mathbf{x}, t)$ over the total volume) is conserved. The current \mathbf{j} is now assumed to be proportional to the gradient of the local chemical potential difference $\mu(\mathbf{x}, t)$:

$$\mathbf{j}(\mathbf{x}, t) = -M\nabla\mu(\mathbf{x}, t) \quad (5.22)$$

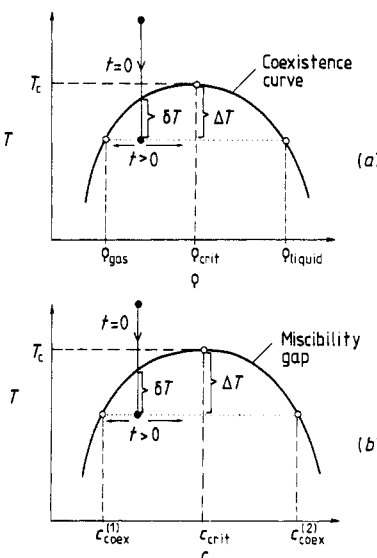


Figure 30. Schematic description of quenching experiments where the system at time $t=0$ is rapidly cooled from an initial temperature in the one-phase region to a final temperature in the two-phase region (a) for a gas-fluid system at constant density ρ and (b) for a binary (fluid or solid) mixture AB at constant concentration. As time elapses, the system starts to separate in a two-phase mixture of two distinct phases: a mixture of saturated gas and saturated liquid (at final densities $\rho_{\text{gas}}, \rho_{\text{liquid}}$) in case (a)), a mixture of A-rich and B-rich coexisting (fluid or solid) solutions (at final concentrations $c_{\text{coex}}^{(1)}, c_{\text{coex}}^{(2)}$) in case (b)). In the following the order parameter ($\rho - \rho_{\text{crit}}$ or $c - c_{\text{crit}}$ respectively) is denoted again by ϕ , so ρ_{gas} or $c_{\text{coex}}^{(1)}$ are denoted as ϕ_1^{coex} , ρ_{liquid} or $c_{\text{coex}}^{(2)}$ as ϕ_2^{coex} , etc (from Binder 1980b).

with M a mobility. Here $\mu(\mathbf{x}, t)$ is obtained by generalising the thermodynamic relation $\mu = (\partial G(T, \phi)/\partial\phi)_T$, where $G = F - \mu\phi$ is the Gibbs potential per atom, to functional derivatives (in the notation of § 2, μ is just the ordering field H) to obtain (cf (4.18) and (4.2))

$$\frac{\mu(\mathbf{x}, t)}{k_B T} = \left(\frac{\partial f_{cg}(\phi)}{\partial\phi} \right)_T - \frac{1}{d} R^2 \nabla^2 \phi(\mathbf{x}, t). \quad (5.23)$$

Then (5.21)–(5.23) yield the Cahn–Hilliard equation (Cahn and Hilliard 1958, Cahn 1961, 1968)

$$\frac{\partial\phi(\mathbf{x}, t)}{\partial t} = k_B T M \nabla^2 \left[\left(\frac{\partial f_{cg}(\phi)}{\partial\phi} \right)_T - \frac{1}{d} R^2 \nabla^2 \phi(\mathbf{x}, t) \right]. \quad (5.24)$$

Since $\partial f_{cg}(\phi)/\partial\phi$ is highly non-linear (cf figure 16), (5.24) is not analytically soluble. The standard assumption (Cahn 1968) now is that in the initial stages of unmixing $\phi(\mathbf{x}, t)$ everywhere in the system is close to its average value $\bar{\phi}$. Then it makes sense to linearise (5.24) in the variable $\delta\phi(\mathbf{x}, t) = \phi(\mathbf{x}, t) - \bar{\phi}$:

$$\frac{\partial\delta\phi(\mathbf{x}, t)}{\partial t} = k_B T M \nabla^2 \left[\left(\frac{\partial^2 f_{cg}(\phi)}{\partial\phi^2} \right)_T \Big|_{\phi=\bar{\phi}} - \frac{1}{d} R^2 \nabla^2 \right] \delta\phi(\mathbf{x}, t). \quad (5.25)$$

Introducing Fourier transforms

$$\delta\phi_k(t) \equiv \int d^d \exp(i\mathbf{k} \cdot \mathbf{x}) \delta\phi(\mathbf{x}, t) \quad (5.26)$$

one readily finds

$$\delta\phi_k(t) = \delta\phi_k(0) \exp(\omega(\mathbf{k})t) \quad (5.27)$$

where the ‘amplification factor’ $\omega(\mathbf{k})$ follows from (5.25)–(5.27) as

$$\omega(\mathbf{k}) \equiv -k_B T M k^2 \left(\frac{\partial^2 f_{cg}(\phi)}{\partial\phi^2} \right)_T \Big|_{\phi=\bar{\phi}}. \quad (5.28)$$

The quantity of interest for scattering experiments is the equal-time structure factor, defined as

$$S(\mathbf{k}, t) \equiv \langle \delta\phi_{-\mathbf{k}}(t) \delta\phi_{\mathbf{k}}(t) \rangle = \langle \delta\phi_{-\mathbf{k}}(0) \delta\phi_{\mathbf{k}}(0) \rangle_T \exp(2\omega(\mathbf{k})t). \quad (5.29)$$

Here the prefactor is simply the static structure factor of the initial state (at temperature T_0) before the quench:

$$\langle \delta\phi_{-\mathbf{k}}(0) \delta\phi_{\mathbf{k}}(0) \rangle_T = \langle \delta\phi_{-\mathbf{k}} \delta\phi_{\mathbf{k}} \rangle_{T_0} = S_{T_0}(\mathbf{k}). \quad (5.30)$$

Thus (5.29) implies that fluctuations with wavevector \mathbf{k} contained in the initial state grow exponentially with the time t after the quench (which is assumed to occur instantaneously from T_0 to T at $t=0$) if $\omega(\mathbf{k}) > 0$, they decay if $\omega(\mathbf{k}) < 0$, while $S(\mathbf{k}, t)$ is independent of time for the ‘critical wavevector’ \mathbf{k}_c for which $\omega(\mathbf{k}_c) = 0$. From (5.28) we see that the amplification factor is positive for long wavelength $\lambda = 2\pi/k$, namely for

$$0 < k < k_c = 2\pi/\lambda_c = [-(\partial^2 f_{cg}(\phi)/\partial\phi^2)_T |_{\phi=\bar{\phi}} d/R^2]^{1/2}. \quad (5.31)$$

Thus fluctuations with wavelengths $\lambda > \lambda_c$ should increase exponentially fast with time,

the fastest growth occurring for $k = k_{\max} = k_c/2$, until non-linear terms limit the growth. Of course, an unlimited growth of concentration differences in the case of figure 29(a) would not make any sense. It also is obvious that by this linearisation approximation we have lost the information on non-linear unstable fluctuations, the ‘heterophase fluctuations’ or droplets of figure 29(b). In the regime in between the coexistence curve and the spinodal, where $(\partial^2 f_{cg}(\phi)/\partial\phi^2)_T > 0$, the present linearised theory predicts that all ‘homophase fluctuations’ decay, another expression of the notion that the state is ‘metastable’, while inside the spinodal it is ‘unstable’.

A convincing experimental test of this theory is not straightforward for several reasons.

(i) The parameters M , $(\partial^2 f_{cg}(\phi)/\partial\phi^2)_T|_{\phi=\bar{\phi}}$ and R are usually not known independently; if they are used as adjustable fitting parameters, a full test of the theory is no longer performed.

(ii) The actual quench never leads instantaneously from one state to another, as assumed in figure 30, but at a finite quench rate. This leads to significant deviations of the structure factor $S(k, t)$ from its behaviour for instantaneous quenches, as model calculations show (Carmesin *et al* 1986).

(iii) In systems where the diffusion proceeds relatively fast, one can investigate intermediate and late stages of phase separation only, while early stages are hardly accessible.

In view of these problems, the usefulness of the linearised Cahn–Hilliard theory for experiments has been a matter of long discussion in literature (Gunton *et al* 1983, Binder 1984c, Haasen *et al* 1984). A very convincing test, however, is possible by computer simulations of Ising models where none of the problems (i)–(iii) occur. For the nearest-neighbour Ising model, the linearised theory of spinodal decomposition is found to be qualitatively wrong (Bortz *et al* 1974, Marro *et al* 1975, Sur *et al* 1977) (see figure 31). There is neither a time-independent intersection point k_c of the structure factor $S(k, t)$ at different times nor a time-independent position of maximum growth, k_m , nor is there a regime of initial times where $S(k, t)$ grows according to an exponential. Rather $k_m(t) \rightarrow 0$ as $t \rightarrow \infty$, reflecting a ‘coarsening’ of the structures which are built up, and this behaviour sets in already during the initial stages of phase separation. The initial growth of $S(k, t)$ at fixed k is even slower than linear with time. On the other hand, if one considers Ising models with a large but finite range of the forces (Heermann 1984a), one finds much better agreement with the linearised theory of spinodal decomposition. There is an initial regime of exponential growth clearly visible (figure 32(a)), and the resulting growth rate agrees with the theory quantitatively (which is easily worked out in the MFA without adjustable parameters being present (figure 32(b)). Thus we find, as in our discussion of metastability (§ 4.1) and nucleation (§ 5.1), that it matters whether or not a system behaves mean-field-like.

We shall return to a discussion of the validity of the linearised theory for systems with a large but finite range of the forces in § 5.4, and here merely emphasise that, for systems with a very short range of interaction, the linearised theory is completely invalid, since non-linear effects are important from the start. The full non-linear equation (5.24), which also has to be supplemented with a random force term (Cook 1970) to account for thermal fluctuations at the final temperature T of the quench, has been studied by various authors (e.g. Cahn 1966, Langer 1971, 1973, Langer and Baron 1973, Binder 1974). A fairly successful approximation was finally developed by Langer *et al* (1975)—for extensions see also Kawasaki and Ohta (1978a,b), Binder *et al* 1978, Billotet and Binder (1979), and Horner and Jüngling (1979): this theory

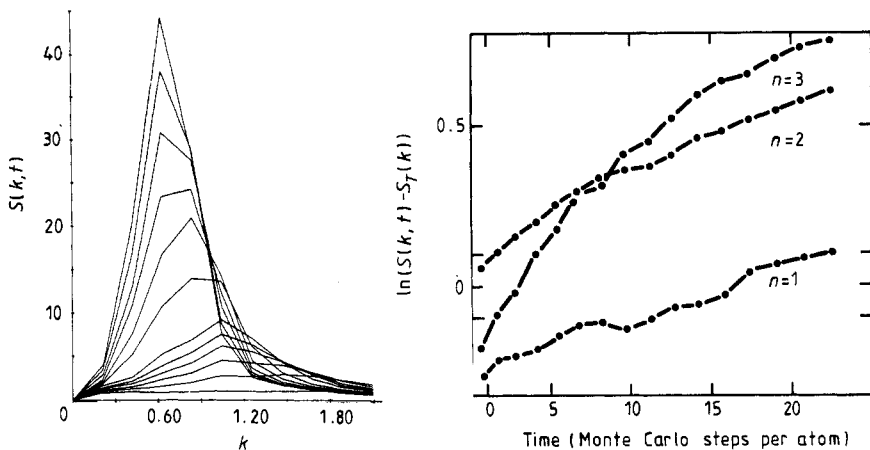


Figure 31. (a) Spherically averaged structure factor of a three-dimensional simple cubic Ising system with nearest-neighbour ferromagnetic exchange plotted against wavenumber k for various times. The system is quenched from a random spin configuration (corresponding to $T_0 \rightarrow \infty$) to $T = 0.6 T_c$, and evolves there according to a spin exchange dynamics (spin up corresponds to atomic species A, spin down to B, and the concentration has its critical value $c = \frac{1}{2}$). Time is measured in units of attempted Monte Carlo steps per atom; the lattice spacing is unity. Due to the periodic boundary condition for the $30 \times 30 \times 30$ lattice k is defined only for discrete values $k_n = 2\pi n/30$, $n = 1, 2, \dots$; these discrete values of $S(k_n, t)$ are connected by straight lines to guide the eye. (b) Similar data, but plotted as the logarithm of the structure factor against time for $n = 1, 2, 3$ for $c = 0.2$ (from Marro *et al* 1975).

yields predictions for $S(k, t)$ in fair agreement with the computer simulations at early times, at least for the quenches at critical concentration. However, we shall not expose this theory here as it also has its drawbacks (Binder *et al* 1978, Billotet and Binder 1979): it yields neither a reasonable description for the gradual crossover from non-linear spinodal decomposition to nucleation and growth, as one moves in concentration towards the coexistence curve, nor a good description of the scaled structure factor (5.20) at the later stages of the quench. In contrast, extending nucleation theory to a ‘cluster dynamics’ approach which takes the conservation of concentration (or density) (5.21) properly into account, both the gradual transition from nucleation to spinodal decomposition and the scaling (5.20) emerge in a natural way (Binder and Stauffer 1974, Binder 1977, Mirold and Binder 1977, Binder *et al* 1978). However, this approach shares all the disadvantages of the conventional theory of nucleation, as discussed in §§ 4.2 and 5.1: the ‘clusters’ are somewhat ill defined, and many unknown phenomenological parameters are involved. Although one can estimate the scaling function \tilde{S} in (5.20) with plausible assumptions (Rikvold and Gunton 1982), a quantitatively reliable theory for predicting both $L(t)$ and \tilde{S} in (5.20) is still not at hand. (This problem can only be solved easily in the (unrealistic) spherical model limit n -vector Hamiltonian with $n \rightarrow \infty$; see Tomita (1978) and Mazenko and Zannetti (1984).) In this author’s opinion, the relatively most reliable theoretical predictions for $L(t)$ and \tilde{S} in binary mixtures are due to Monte Carlo computer simulations (Marro *et al* 1979, Lebowitz *et al* 1982, Fratzl *et al* 1983). We shall not continue this subject here, as some aspects are still rather controversial, but rather refer to recent other reviews (Gunton *et al* 1983, Binder and Heermann 1985, Furukawa 1986) for more detailed discussions and further references, as well as for a discussion of corresponding experiments.

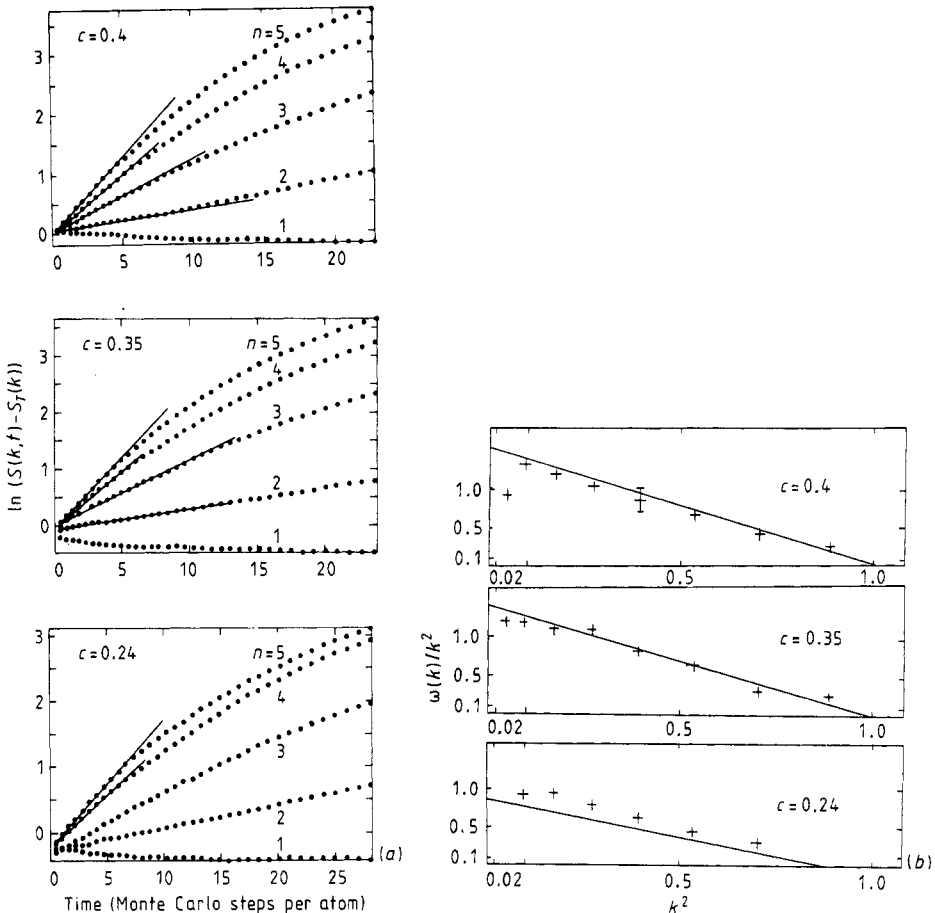


Figure 32. (a) Logarithm of spherically averaged structure factors of a 60^3 simple cubic Ising lattice, where each spin interacts with $q=124$ neighbours with equal interaction strength J , quenched from infinite temperature to $T=\frac{4}{9}T_c^{\text{MF}}=\frac{4}{9}qJ/k_B$. Three concentrations are shown, as indicated in the figure, and the five smallest wavevectors $k_n=2\pi n/60$. Straight lines for short times indicate exponential growth and thus yield $\omega(k)$. (b) Plot of $\omega(k)/k^2$ against k^2 , as extracted from data such as shown in (a). Crosses are the Monte Carlo results; straight lines are the predictions of the linearised theory (from Heermann 1984a).

A general point, however, is not controversial and deserves to be emphasised. Whether or not there is a rather gradual or a rather sharp distinction between the decay mechanisms during the initial stages of phase separation (nucleation against spinodal decomposition), this distinction plays no role at late stages: there we always expect (5.20) to hold, and \tilde{S} gradually changes with volume fraction $\delta\phi/(\phi_2^{\text{coex}} - \phi_1^{\text{coex}})$ of the minority phase as one moves away from the coexistence curve towards the centre of the miscibility gap in figure 30. While the morphology of the phase-separated structure changes—an assembly of well separated growing droplets near ϕ_1^{coex} (see Binder and Stauffer 1976) and an interconnected ‘percolating’ structure in the centre of the miscibility gap—the percolation transition separating these regimes (Binder 1980c, Heermann 1984b) hardly affects $S(k, t)$ and has nothing to do with the spinodal curve.

5.4. The spinodal curve revisited

In the previous section we have seen that the simple Cahn (1961, 1968) linearised theory of spinodal decomposition is completely invalid for systems with short-range interactions, but holds approximately for systems with a large but finite range of interaction. This again raises the question on the significance of the spinodal curve, which in the theory sketched in (5.21)–(5.31) shows up by the fact that the range of unstable wavenumbers ($0 < k < k_c$) shrinks to zero when the spinodal is approached, since there $\lambda_c \rightarrow \infty$. Using a free energy function $f_{\text{cg}}(\phi)$ consistent with the phase diagrams of figure 30, we have

$$\lambda_c \propto R(1 - T/T_c)^{-1/2}(1 - \phi/\phi_s)^{-1/2}. \quad (5.32)$$

Thus λ_c diverges when $\phi \rightarrow \phi_s$ in a fashion completely analogous to that of the correlation length ξ when one approaches the spinodal from the metastable side (see § 4.4). This observation already suggests that we again apply the Ginzburg criterion to check also the validity of the linear theory of spinodal decomposition. Similar to (4.24), we now must require

$$\langle (\delta\phi(x, t))^2 \rangle_{T,L} \ll (\phi - \phi_s)^2. \quad (5.33)$$

We may estimate $\langle (\delta\phi(x, t))^2 \rangle_{T,L}$ as

$$\langle (\delta\phi(x, t))^2 \rangle_{T,L} \approx \langle (\delta\phi(x, 0))^2 \rangle_{T,L} \exp(2\omega(k_{\max})t) \quad (5.34)$$

and estimate $\langle (\delta\phi(x, 0))^2 \rangle_{T,L} = \langle (\delta\phi(x))^2 \rangle_{T_0,L}$ as in (4.24) and (4.25), but using now $L = \lambda_c$ as the maximum permissible choice of a coarse-graining cell size. This yields

$$R^{-2}\lambda_c^{2-d} \exp(2\omega(k_{\max})t) \ll (\phi - \phi_s)^2 \quad (5.35)$$

and using also (5.32) we find

$$\exp(2\omega(k_{\max})t) \ll R^d(1 - T/T_c)^{(4-d)/2}(1 - \phi/\phi_s)^{(6-d)/2}. \quad (5.36)$$

Thus the time range over which the linearised theory is valid increases only slowly with increasing R , namely logarithmically, $t \propto \ln R$. After this time non-linear effects come into play already, which limit the exponential growth, (5.29). Of course, in order to have an initial regime where the linearised theory is valid, the right-hand side of the inequality (5.36) must exceed unity: this is exactly the same condition as formulated already in our discussion of metastability, (4.25), and the mean-field theory of nucleation, (5.16a)!

In the centre of the miscibility gap, on the other hand, $\phi - \phi_s$ is of the same order as the order parameter ϕ_{coex} , and λ_c of the same order as ξ_{coex} : then (5.35) yields

$$\exp(2\omega(k_{\max})t) \ll \phi_{\text{coex}}^2 R^2 \xi_{\text{coex}}^{d-2}. \quad (5.37)$$

In the mean-field critical region, which occurs for $1 \ll R^d(1 - T/T_c)^{(4-d)/2}$,

$$\exp(2\omega(k_{\max})t) \ll R^d(1 - T/T_c)^{(4-d)/2}. \quad (5.38)$$

On the other hand, for a system with short-range forces we would find in its critical region, from (2.25), that

$$\langle (\phi(x))^2 \rangle_{T,L=\xi_{\text{coex}}} \propto \xi_{\text{coex}}^{\gamma/\nu-d} \quad \phi_{\text{coex}} \propto \xi_{\text{coex}}^{-\beta/\nu}$$

and hence

$$\exp(2\omega(k_{\max})t) \ll \xi_{\text{coex}}^{d-(\gamma+2\beta)/\nu}. \quad (5.39)$$

Since the hyperscaling relation implies $d\nu = \gamma + 2\beta$, the right-hand side of (5.39) is unity, and hence the linearised theory of spinodal decomposition is then never self-consistent. This conclusion is corroborated by approximate theories of non-linear effects in spinodal decomposition, such as the theory of Langer *et al* (1975). These non-linear effects are controlled in strength by a parameter $1/f_0$ given by

$$f_0 \propto (1 - T/T_c)^{-d\nu+2\beta+\gamma} \xi_0^d B^2/\Gamma \quad (5.40)$$

where ξ_0 , B and Γ are the critical amplitudes of correlation length, order parameter and susceptibility. This parameter f_0 is essentially the same as that which appears on the right-hand side of the Ginzburg criterion. In fact, two-scale factor universality (Stauffer *et al* 1972) implies that f_0 is a universal constant. On the other hand, in the mean-field critical region $f_0 \propto R^d (1 - T/T_c)^{(4-d)/2} \gg 1$, and hence non-linear effects are initially small, as demonstrated by explicit calculation (Carmesin *et al* 1986). Unfortunately, this Langer-Baron-Miller theory does not become exact even in first order in f_0^{-1} , and a more systematic theory is very complicated (Grant *et al* 1985).

Figure 33 summarises our statements on the validity of the spinodal line and the mean-field theories of nucleation and spinodal decomposition. We emphasise that both the linearised theory of spinodal decomposition (exponential amplification of fluctuations, with time-independent k_{\max} and k_c) and the concept of 'spinodal' nucleation (Klein and Unger 1983, Heermann and Klein 1983a,b), i.e. nucleation of ramified droplets which first compactify and then grow, are concepts which hold in a mean-field critical region only. One expects to find such a behaviour in polymer mixtures (Binder 1983, 1984c). In most other systems, however, we expect a behaviour

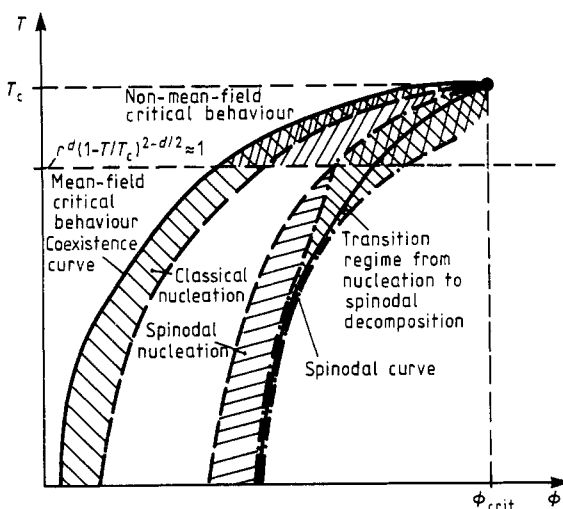


Figure 33. Various regions in the temperature-order parameter plane near T_c . Due to the symmetry around the critical point, only one half of the phase diagram is shown. Full curves are the coexistence and spinodal curves. The regime inside the two chain curves around the spinodal curve is the regime where a gradual transition from nucleation to spinodal decomposition occurs. The regime between the coexistence curve and the left of the two broken curves is described by classical nucleation theory. In this regime, a further smooth crossover occurs at $R^d (1 - T/T_c)^{(4-d)/2}$ from mean-field-like critical behaviour to non-mean-field-like behaviour. The regime between the right broken curve and the left chain curve is the regime of 'spinodal nucleation' via ramified clusters. It exists only in the regime of mean-field critical behaviour. (from Binder 1984c).

as sketched in figure 34(b). Close to the coexistence curve, we have high nucleation barriers and classical nucleation theory applies. Moving deeper into the two-phase region, however, the barriers are no longer much larger than $k_B T$. Then nucleation is relatively easy; many nuclei are formed and grow simultaneously in the system, leading to a quick decay of the metastable state. The situation is not fundamentally different from a description in terms of a wavepacket of growing unstable modes, strongly coupled by non-linear effects. Thus there is a wide regime of undercooling (or supersaturation or order parameter difference $\phi - \phi_{\text{coex}}$) where a completely gradual transition from nucleation to spinodal decomposition occurs. We think that essentially the same picture applies for other first-order phase transition too: $\phi - \phi_{\text{coex}}$ in figure 34 simply has to be replaced by the appropriate parameter driving the considered transition. Usually, however, the phase transition proceeds very quickly when ΔF^* is no longer large; and then the regime of long-wavelength instabilities cannot be reached in practice, although it exists in principle.

5.5. The completion time

In this section we briefly discuss the concept of the ‘completion time’ τ_c (e.g. Binder and Stauffer 1976, Langer and Schwartz 1980, Goldburg 1981, Avrami 1939), i.e. the time it takes in a quenching experiment (figure 30) for the reaction (condensation or unmixing) to go halfway to completion.

Consider, for simplicity, the growth of supercritical liquid droplets out of a metastable gas phase. At a droplet of radius r , we will have a net current $j_r = D(\rho - \rho_{\text{gas}})/r$ where D is the diffusion coefficient. Experimentally, the temperature is varied by T at constant density ρ (see figure 30). Expanding $\rho = \rho_{\text{gas}} - \delta T(d\rho_{\text{gas}}/dT)$ and using $\rho_{\text{liquid}} - \rho_{\text{gas}} \propto (1 - T/T_c)^{\beta}$ gives $j_r = (D/r)(\rho_{\text{liquid}} - \rho_{\text{gas}})[\beta\delta T/2(T_c - T)]$. Due to the current impinging on the droplet, the droplet radius increases as (in three dimensions)

$$4\pi r^2 j_r = (\rho_{\text{liquid}} - \rho)4\pi r^2 dr/dt. \quad (5.41)$$

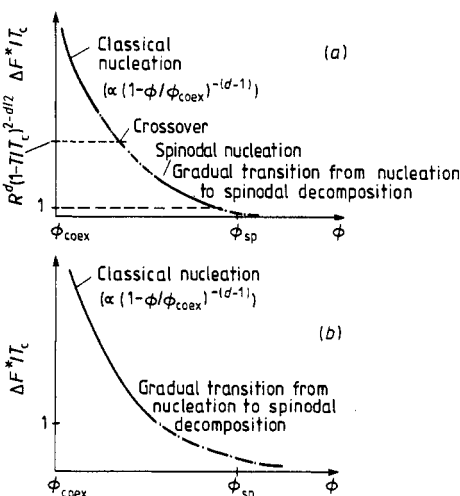


Figure 34. Schematic plots of the free energy barrier for (a) the mean-field critical region, i.e. $R^d(1 - T/T_c)^{(4-d)/2} \gg 1$ and (b) the non-mean-field critical region, i.e. $R^d(1 - T/T_c)^{(4-d)/2} \ll 1$, lower part. Note that due to large prefactors to the nucleation rate, the constant of order unity, where the gradual transition from nucleation to spinodal decomposition occurs, is about 10^4 rather than 10^0 (from Binder 1984c).

Putting $\rho \approx \rho_{\text{gas}}$ in this relation and using the expression for j_r , (5.41) is readily integrated as

$$(r(t-t'))^2 = r^{*2} + \beta \frac{\delta T}{T_c - T} D(t-t') \quad (5.42)$$

where we have assumed that the droplet was nucleated (at critical size r^*) at time t' .

Through the combined effect of nucleation with a rate $J(t)$ and growth, the fraction $\delta\rho(t)/(\rho_{\text{liquid}} - \rho_{\text{gas}})$ will be transformed according to the law

$$\delta\rho(t) = \int_0^t dt' J(t') \frac{4\pi}{3} (\rho_{\text{liquid}} - \rho_{\text{gas}}) (r(t-t'))^3. \quad (5.43)$$

A time dependence of $J(t)$ is expected because of the decrease in supersaturation and because of time lag effects (Binder and Stauffer 1976). A simple explicit estimate is only obtained, however, if the time dependence of $J(t)$ is neglected. We now consider the completion time in the critical region, using for $J(t)$ the steady state expression (5.18), neglecting r^* in (5.42), and using $D = \hat{D} (1 - T/T_c)^\nu$, $z = d = 3$:

$$\begin{aligned} \frac{\delta\rho(t)}{\rho_{\text{liquid}} - \rho_{\text{gas}}} &= \left(\frac{\beta \delta T}{T_c - T} D \right)^{3/2} \frac{8\pi}{15} J t^{5/2} \\ &= \frac{8\pi}{15} \left(\frac{\beta \delta T}{T_c - T} \right)^{3/2} \hat{D}^{3/2} \left(1 - \frac{T}{T_c} \right)^{15\nu/2} \tilde{J} \tilde{J} \left(\frac{\delta T}{T_c - T} \right) t^{5/2}. \end{aligned} \quad (5.44)$$

Here we have changed the argument $\delta\phi/(\phi_2^{\text{coex}} - \phi_1^{\text{coex}})$ of the scaling function \tilde{J} to $\delta T/(T_c - T)$, which is convenient if we wish to compare the theory with experimental data. The completion time τ_c results from (5.44) by putting $\delta\rho(t)/(\rho_{\text{liquid}} - \rho_{\text{gas}}) = \frac{1}{2}$ (another fraction of order unity would lead to an unimportant change of the prefactor only). Thus

$$\tau_c = \left(1 - \frac{T}{T_c} \right)^{3\nu} \left[\frac{16\pi}{15} \left(\beta \hat{D} \frac{\delta T}{T_c - T} \right)^{3/2} \tilde{J} \tilde{J} \left(\frac{\delta T}{T_c - T} \right) \right]^{2/5} = \left(1 - \frac{T}{T_c} \right)^{3\nu} \tilde{\tau}_c \left(\frac{\delta T}{T_c - T} \right). \quad (5.45)$$

This result shows that dynamic scaling (Hohenberg and Halperin 1977) also holds far from equilibrium; while the explicit expression for the scaling function τ_c certainly is rather approximate, we believe that the scaling structure $\tau_c = (1 - T/T_c)^{3\nu} \tilde{\tau}_c [\delta T/(T_c - T)]$ holds general for liquid-gas condensation and phase separation of fluid binary mixtures, not only in the regime where the phase separation starts by nucleation, but also in the regime where it starts by spinodal decomposition. For solid binary mixtures, we have instead $\tau_c = (1 - T/T_c)^{\gamma+2\nu} \tilde{\tau}_c' [\delta T/(T_c - T)]$, γ being the ‘susceptibility’ exponent. Figure 35 shows the supercooling $\delta T/(T_c - T)$ for which $\tau_c = 1$ s as a function of $1 - T/T_c$ for various gas-liquid systems and fluid binary mixtures (Goldburg 1981). Although the data are somewhat rough, they indicate that the dynamic scaling behaviour (5.45) probably is valid, though the scaling function $\tilde{\tau}_c$ proposed by Binder and Stauffer (1976) certainly is not quantitatively accurate. Langer and Schwartz (1980) took the time dependence of $J(t)$ due to the decrease of supersaturation into account, by combining the coarsening theory of Lifshitz and Slyozov (1961) and nucleation. Their scaling function yields a much steeper rise of $\delta T/(T_c - T)$ as $T_c - T \rightarrow 0$ in figure 35. The quantitative explanation of the nucleation experiments shown in figure 35 is thus still under discussion. Gitterman and Rabin (1984) and Rabin and Gitterman (1984) rather suggest that critical slowing down of the time lag yields the important time dependence of $J(t)$ needed for a proper interpretation of

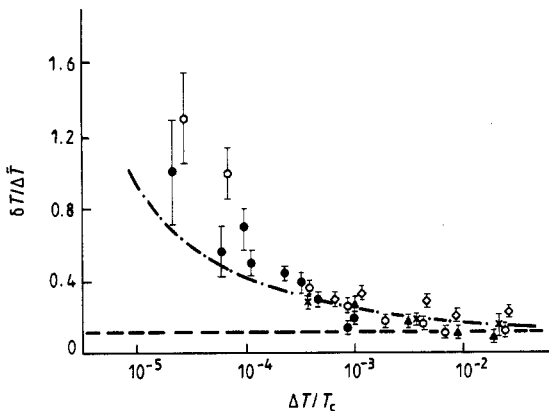


Figure 35. Reduced supercooling $\delta T/\Delta \tilde{T} = \delta T/|T_c - T - \delta T|$ plotted against the relative distance from the critical point, $\Delta T/T_c = |T_c - T|/T_c$, for binary mixtures $C_7F_{14}-C_7H_{14}$ (open diamonds, from Heady and Cahn (1973)), 2.6 lutidine-water (full and open circles, from Schwartz *et al* (1980)) and simple fluids, ^3He (crosses, from Dahl and Moldover (1971)) and CO_2 (triangles, from Huang *et al* (1975)). The horizontal broken line is the Becker-Döring theory, with parameters relevant to CO_2 . The chain curve is the theoretical result of Binder and Stauffer (1976), calculated for a completion time $\tau_c = 1$ s (after Goldburg 1981).

the experiments. Their conclusion, however, seems at variance with direct measurements of J in isobutyric acid/water mixtures performed with a new two-step quench technique (Siebert and Knobler 1984). Alternative theories were also proposed by McGraw and Reiss (1979) and Furukawa (1983). Thus more work seems necessary to understand nucleation and spinodal decomposition near critical points completely. We also note in passing that behaviour similar to figure 35 is also seen in phase separation experiments near the tricritical point of ^3He - ^4He mixtures (Alpern *et al* 1982, Sinha and Hoffer 1983, Hoffer and Sinha 1986).

The Langer-Schwartz (1980) approach of a combined numerical treatment of nucleation, droplet growth and droplet coarsening has been extended by Kampmann and Wagner (1984) to solid alloys off the critical region, and reasonable agreement with their own experiments could be obtained (Kampmann and Wagner 1984, 1986). Other recent measurements of completion times in solid alloys are found in a pioneering paper by Simon *et al* (1984), where also the anisotropy of the scaling function \tilde{S} in (5.20) was demonstrated. Finally we draw attention to recent elegant work on nucleation under time-dependent supersaturation conditions (Trinkaus and Yoo 1987).

6. Concluding remarks

The purpose of this brief final section is twofold: (i) to provide a summary of the main concepts described in this review and (ii) to draw attention to topics which also would fall under the heading ‘theory of first-order phase transitions’ but have not been covered because of lack of space and expertise.

This review has emphasised a phenomenological description of phase transitions within the framework of statistical mechanics. No first principles description of condensed matter systems was intended; for example, we have not discussed phase

transitions between various solid phases at $T = 0$ K driven, e.g., by pressure: for this problem, reliable calculations of electronic properties (band structures, ground state energies, etc) are required rather than statistical mechanics. Also, finite temperature transitions which require an essentially quantum mechanical treatment are left aside as well.

Thus our description has been centred around the Landau description of phase transitions and related mean-field-type theories of a slightly more microscopic character. We have not intended to present exhaustive classifications of various phase transitions which can occur in Landau theory—doing this just for two-dimensional orderings would fill a separate review (see e.g. Ipatova and Kitaev 1985, Schick 1981); rather we tried to give the general spirit of the approach, describe the type of results that can be obtained, and discuss their validity, particularly with respect to the neglect of statistical fluctuations. For the latter purpose, we have given short descriptions of the renormalisation group approach to phase transitions, mainly in its position space version. We have emphasised the question to what extent the theory is able to predict correctly the order of a phase transition and to compute accurately the phase diagram. We have seen that neither of these problems is fully solved: for example, comparing renormalisation group predictions on fluctuation-induced first-order transitions with experiment, one apparently encounters both successes and failures. Further work, both theoretical and experimental, seems necessary to resolve such discrepancies. Similarly, phase diagram calculations beyond the mean-field or self-consistent phonon level are possible mainly for simple lattice models with discrete degrees of freedom. The specific examples which have been discussed show that an accurate treatment of statistical fluctuations is essential also for the statistical mechanics of first-order transitions, if a description on a quantitatively reliable level is desired.

At this point it must be emphasised that this review is intended to give an introduction for a broad audience, rather than address the experts in the field; so we have aimed neither at completeness nor at rigour. Thus problems which are mainly of interest in mathematical physics but not in practical applications to real systems have been left out. For example, we have not discussed ‘anomalous first-order transitions’ (Fisher and Milton 1987), where jumps occur in isotherms in an intensive rather than extensive variable (e.g. a jump in a pressure isotherm occurring at constant density). These occur in various somewhat pathological models with effectively long-range interparticle interactions (Fisher 1972, Milton and Fisher 1983, Israel 1975, 1979). Similarly, the reader interested in the more rigorous aspects of the theory of metastability should consult the review by Penrose and Lebowitz (1979) and the references contained therein.

In our discussion of metastability, nucleation and transition kinetics we again have emphasised the general concepts, in particular the mean-field theories of nucleation and spinodal decomposition, the significance of the spinodal curve, etc. Topics of current research, such as theories of coarsening, kinetics of domain growth and structure factor scaling, non-linear theories of spinodal decomposition, etc, are treated only rather briefly. In addition, not much attention is given to the application of these concepts to particular physical systems, which is outside the scope of this review. (For a recent discussion of nucleation and growth of thin films at surfaces see Venables *et al* (1984) for instance.) Thus our discussion has focused on the general ideas about the initial stages of the dynamics of first-order transitions. We have seen that even this problem is not yet fully understood—in particular, a quantitative theory describing the gradual crossover from nucleation to long-wavelength instabilities (such as spinodal decomposition in mixtures) is still lacking.

A field with much recent activity is the problem of ‘surface effects’. If a first-order transition from an ordered to a disordered state occurs, one may see a gradual decrease of order near the surface, such that the local order parameter vanishes continuously at the surface though it disappears discontinuously in the bulk. For reviews on the ‘surface-induced disordering’ see Lipowsky (1984, 1987). On the other hand, one may also have phase transitions at the surface when there is no transition in the bulk. In the wetting transitions of gas–fluid systems, on a wall of a container one may observe a transition from a ‘non-wet’ state (the wall is exposed to the gas phase, with no fluid adsorbed at the wall) to a ‘wet’ state (with a thick fluid layer adsorbed at the wall). This wetting transition typically is first-order but may also become second-order. Related phenomena occur in binary mixtures too. We refer to Sullivan and Telo da Gama (1985), de Gennes (1985) and Dietrich (1987) for recent reviews on this subject.

Finally we emphasise that important recent progress has been made in the theoretical description of first-order transitions for particular systems which also has been somewhat outside the scope of this review. An example are the order parameter theories of the solid–fluid transition (Ramakrishnan and Yussouf 1977, 1979, Yussouf 1981, Ramakrishnan 1982), where using data on the liquid phase one can make reasonable predictions for the transition towards the solid phases and their properties.

References

- Abraham F F 1974 *Homogeneous Nucleation Theory* (New York: Academic)
 —— 1982 *Rep. Prog. Phys.* **45** 1113
 —— 1983 *Phys. Rev. Lett.* **50** 978
 —— 1984 *Phys. Rev. B* **29** 2606
- Abraham F F and Barker J A 1975 *J. Chem. Phys.* **63** 2266
- Aharony A 1976 *Phase Transitions and Critical Phenomena* vol 6, ed C Domb and M S Green (New York: Academic) p 357
- Aharony A and Bruce A 1979 *Phys. Rev. Lett.* **42** 462
- Aizu K 1970 *Phys. Rev. B* **2** 754
- Alder B J and Hoover W G 1968 *Physics of Simple Liquids* ed H N V Temperley, J S Rowlinson and G S Rushbrooke (Amsterdam: North-Holland) ch 4
- Alexander S 1975 *Phys. Lett.* **54A** 353
- Allesandrini A, Cracknell A P and Przystawa J A 1976 *Commun. Phys.* **1** 51
- Alpern P, Benda Th and Leiderer P 1982 *Phys. Rev. Lett.* **49** 1267
- Als-Nielsen J, Birgeneau R J, Kaplan M, Litster J D and Safinya C R 1977 *Phys. Rev. Lett.* **39** 1668
- Andreev A F 1964 *Sov. Phys.-JETP* **18** 1415
- Aslanyan T A and Levanyuk A P 1977 *Sov. Phys.-Solid State* **19** 812
 —— 1978 *Sov. Phys.-Solid State* **20** 66
- Avrami M 1939 *J. Chem. Phys.* **7** 1103
- Bak P and Domany E 1979 *Phys. Rev. B* **20** 2818
- Bak P, Krinsky S and Mukamel D 1976 *Phys. Rev. Lett.* **36** 52
- Bak P and Mukamel D 1979 *Phys. Rev. B* **19** 1604
- Bak P, Mukamel D, Villain J and Wentowska K 1979 *Phys. Rev. B* **19** 1610
- Baker G A Jr and Kim D 1980 *J. Phys. A: Math. Gen.* **13** L103
- Bakker A F, Bruin C and Hilhorst H J 1984 *Phys. Rev. Lett.* **52** 449
- Barber M N 1983 *Phase Transitions and Critical Phenomena* vol 8, ed C Domb and J L Lebowitz (New York: Academic) p 145
- Barber M N and Fisher M E 1972 *Phys. Rev. Lett.* **28** 1516
- Baxter R J 1973 *J. Phys. C: Solid State Phys.* **6** L445
- Bean C P and Rodbell D S 1962 *Phys. Rev.* **126** 104
- Becker R and Döring W 1935 *Ann. Phys., Lpz* **24** 719
- Berker A N and Andelman D 1982 *J. Appl. Phys.* **53** 7923

- Berker A N, Ostlund S and Putnam F A 1978 *Phys. Rev. B* **17** 3650
 Billotet C and Binder K 1979 *Z. Phys. B* **32** 195
 Binder K 1973 *Phys. Rev. B* **8** 3423
 —— 1974 *Z. Phys.* **267** 213
 —— 1975a *J. Chem. Phys.* **63** 2265
 —— 1975b *Fluctuations, Instabilities and Phase Transitions* ed T Riste (New York: Plenum) p 53
 —— 1976 *Ann. Phys., NY* **98** 390
 —— 1977 *Phys. Rev. B* **15** 4425
 —— (ed) 1979 *Monte Carlo Methods in Statistical Physics* (Berlin: Springer)
 —— 1980a *Phys. Rev. Lett.* **45** 811
 —— 1980b *J. Physique* **41** C4–51
 —— 1980c *Solid State Commun.* **34** 191
 —— 1981a *Z. Phys. B* **43** 119
 —— 1981b *Z. Phys. B* **45** 61
 —— 1981c *Stochastic Nonlinear Systems in Physics, Chemistry and Biology* ed L Arnold and R Lefever (Berlin: Springer) p 62
 —— 1983 *J. Chem. Phys.* **79** 6387
 —— (ed) 1984a *Applications of the Monte Carlo Method in Statistical Physics* (Berlin: Springer)
 —— 1984b *Phys. Rev. A* **29** 341
 —— 1984c *Condensed Matter Research using Neutrons* ed S W Lovesey and R Scherm (New York: Plenum) p 1
 —— 1985 *J. Comput. Phys.* **59** 1
 —— 1986 *Festkörperprobleme—Advances in Solid State Physics* vol XXVI, ed P Grosse (Braunschweig: Vieweg) p 133
 —— 1987 *Ferroelectrics* in press
 Binder K, Billotet C and Mirol P 1978 *Z. Phys. B* **30** 183
 Binder K and Heermann D W 1985 *Scaling Phenomena in Disordered Systems* ed R Pynn and A Skjeltorp (New York: Plenum) p 207
 Binder K and Kalos M H 1980 *J. Stat. Phys.* **22** 363
 Binder K, Kinzel W and Selke W 1983 *J. Magn. Magnet. Mater.* **31–34** 1445
 Binder K and Landau D P 1984 *Phys. Rev. B* **30** 1477
 Binder K, Lebowitz J L, Phani M K and Kalos M H 1981 *Acta Metall.* **29** 1655
 Binder K and Müller-Krumbhaar H 1974 *Phys. Rev. B* **9** 2328
 Binder K and Stauffer D 1974 *Phys. Rev. Lett.* **33** 1006
 —— 1976 *Adv. Phys.* **25** 343
 Binder K, Stauffer D and Müller-Krumbhaar H 1975 *Phys. Rev. B* **12** 256
 Blankschtein D and Aharony A 1981 *Phys. Rev. Lett.* **47** 439
 —— 1983 *Phys. Rev. B* **28** 3386
 Blankschtein D and Mukamel D 1981 *Phys. Rev. B* **25** 6939
 Bloch D and Mauri R 1973 *Phys. Rev. B* **7** 4883
 Bloch D, Vettier C and Burlet P 1980 *Phys. Lett.* **75A** 301
 Blöte H W and Swendsen R H 1979 *Phys. Rev. Lett.* **43** 799
 Blume M 1966 *Phys. Rev.* **141** 517
 Born M and Huang K 1954 *Dynamical Theory of Crystal Lattices* (Oxford: Oxford University Press)
 Bortz A B, Kalos M H, Lebowitz J L and Zendejas M A 1974 *Phys. Rev. B* **10** 535
 Boyer L L 1980 *Phys. Rev. Lett.* **45** 1858
 —— 1981a *Phys. Rev. Lett.* **46** 1172
 —— 1981b *Ferroelectrics* **35** 83
 Boyer L L and Hardy J R 1981 *Phys. Rev. B* **24** 2577
 Brazovskii S A 1975 *Sov. Phys.-JETP* **41** 85
 Brazovskii S A and Dzyaloshinskii I E 1975 *JETP Lett.* **21** 164
 Brazovskii S A, Dzyaloshinskii I E and Kukharenkov B G 1976 *Sov. Phys.-JETP* **43** 1178
 Brézin E and Wallace D J 1973 *Phys. Rev. B* **7** 1967
 Brout R 1965 *Phase Transitions* (New York: Benjamin)
 Bruce A D and Cowley R A 1981 *Structural Phase Transitions* (London: Taylor and Francis)
 Bruce A D and Wallace D J 1983 *J. Phys. A: Math. Gen.* **16** 1721
 Bucher E, Maita J P, Hull G W Jr, Longinotti L D, Lüthi B and Wang P S 1976 *Z. Phys. B* **25** 41
 Buff F P, Lovett R A and Stillinger F H Jr 1965 *Phys. Rev. Lett.* **15** 621
 Burkhardt T W 1980 *Z. Phys. B* **39** 159
 Burkhardt T W, Knops H J F and den Nijs M P M 1976 *J. Phys. A: Math. Gen.* **9** L179

- Burkhardt T W and van Leeuwen J M J (ed) 1982 *Real-Space Renormalization* (Berlin: Springer)
- Buzaré J Y, Fayet J C, Berlinger W and Müller K A 1979 *Phys. Rev. Lett.* **42** 465
- Cahn J W 1961 *Acta Metall.* **9** 795
- 1966 *Acta Metall.* **14** 1685
- 1968 *Trans. Metall. Soc. AIME* **242** 166
- Cahn J W and Hilliard J E 1958 *J. Chem. Phys.* **28** 258
- 1959 *J. Chem. Phys.* **31** 688
- Capocaccia D, Cassandro M and Olivieri E 1974 *Commun. Math. Phys.* **39** 185
- Cardy J L and Nightingale M P 1983 *Phys. Rev. B* **27** 4256
- Carmesin H-O, Heermann D W and Binder K 1986 *Z. Phys. B* **65** 89
- Challa M S S, Landau D P and Binder K 1986 *Phys. Rev. B* **34** 1841
- Chu B, Schoenes F J and Fisher M E 1969 *Phys. Rev.* **185** 219
- Compagner A 1974 *Physica* **72** 115
- Coniglio A and Klein W 1980 *J. Phys. A: Math. Gen.* **13** 2775
- Cook H E 1970 *Acta Metall.* **18** 297
- Cowley R A 1976 *Phys. Rev. B* **13** 4877
- Dahl D and Moldover M R 1971 *Phys. Rev. Lett.* **27** 1421
- Danielian A 1964 *Phys. Rev.* **133** A1344
- Dasgupta C 1977 *Phys. Rev. B* **15** 3460
- Dee G, Gunton J D and Kawasaki K 1981 *J. Stat. Phys.* **24** 87
- de Fontaine D 1979 *Solid State Physics* vol 34, ed H Ehrenreich, F Seitz and D Turnbull (New York: Academic) p 73
- de Gennes P G 1985 *Rev. Mod. Phys.* **57** 827
- De Jongh L J and Miedema A R 1974 *Adv. Phys.* **23** 1
- den Nijs M P M 1979 *Physica* **95A** 444
- de Raedt B, Binder K and Michel K H 1981 *J. Chem. Phys.* **75** 2977
- Dickman R and Schieve W C 1982 *Physica* **112A** 51
- Diep H T, Ghazali A, Berge B and Lallemand P 1986 *Europhys. Lett.* **2** 603
- Dietrich S 1987 *Phase Transitions and Critical Phenomena* vol 11, ed C Domb and J L Lebowitz (New York: Academic)
- Domany E, Mukamel D and Fisher M E 1977 *Phys. Rev. B* **15** 5432
- Domany E, Shnidman Y and Mukamel D 1982 *J. Phys. C: Solid State Phys.* **15** L495
- Domb C 1976 *J. Phys. A: Math. Gen.* **9** 283
- Dünweg B and Binder K 1987 *Preprint*
- Elschner S, Knorr K and Loidl A 1985 *Z. Phys. B* **61** 209
- Feder J and Pytte E 1968 *Phys. Rev.* **168** 640
- Finel A and Ducastelle F 1986 *Europhys. Lett.* **1** 135
- Fisher M E 1962 *IUPAP Conf. on Statistical Mechanics, Boston* 1962 unpublished
- 1967 *Physics* **3** 255
- 1971 *Critical Phenomena* ed M S Green (New York: Academic) p 1
- 1972 *Commun. Math. Phys.* **26** 6
- 1974 *Rev. Mod. Phys.* **46** 597
- Fisher M E and Berker A N 1982 *Phys. Rev. B* **26** 2507
- Fisher M E and Milton G W 1987 to be published
- Fisher M E and Privman E 1985 *Phys. Rev. B* **32** 447
- Folk R, Iro H and Schwabl H 1976 *Z. Phys. B* **25** 69
- Fratzl P, Lebowitz J L, Marro J and Kalos M H 1983 *Acta Metall.* **31** 1849
- Frazer B C, Shirane G and Cox D E 1965 *Phys. Rev.* **140** A1448
- Frisch H L, Rivier N and Wyler D 1985 *Phys. Rev. Lett.* **54** 2061
- Furukawa H 1983 *Phys. Rev. A* **28** 1729
- 1986 *Adv. Phys.* **34** 703
- Furukawa H and Binder K 1982 *Phys. Rev. A* **26** 556
- Gahn U 1973 *Z. Metallk.* **64** 268
- 1974 *Z. Metallk.* **65** 418
- 1982 *J. Phys. Chem. Solids* **43** 977
- 1986 *J. Phys. Chem. Solids* **47** 1153
- Galam S and Birman J L 1982 *Phys. Lett.* **93A** 83
- Ginzburg V L 1960 *Fiz. Tela* **2** 2031 (*Sov. Phys.-Solid State* **2** 1824)
- Gitterman M and Rabin Y 1984 *J. Chem. Phys.* **80** 2234
- Glauber R J 1963 *J. Math. Phys.* **4** 294

- Goldburg W I 1981 *Scattering Techniques Applied to Supramolecular and Nonequilibrium Systems* ed S H Chen, B Chu and R Nossal (New York: Plenum) p 383
- Grant M and Gunton J D 1985 *Phys. Rev. B* **32** 7299
- Grant M, San Miguel M, Vinals S and Gunton J D 1985 *Phys. Rev. B* **31** 302
- Grazhdankina N P 1969 *Sov. Phys.-Usp.* **11** 727 (*Usp. Fiz. Nauk.* **96** 291)
- Grewen N and Klein W 1977a *J. Math. Phys.* **18** 1729
- 1977b *J. Math. Phys.* **18** 1735
- Guérard D and Herold A 1975 *Carbon* **13** 337
- Guilluy M and Toledano P 1981 *Ferroelectrics* **36** 281
- Günther N J, Nicole D A and Wallace D J 1980 *J. Phys. A: Math. Gen.* **13** 1755
- Gunton J D, San Miguel M and Sahni P S 1983 *Phase Transitions and Critical Phenomena* vol 8, ed C Domb and J L Lebowitz (New York: Academic) p 267
- Gunton J D and Yalabik C 1978 *Phys. Rev. B* **18** 6199
- Guymont M 1978 *Phys. Rev. B* **18** 5385
- 1981 *Phys. Rev. B* **24** 2647
- Haasen P, Gerold V, Wagner R and Ashby M F (ed) 1984 *Decomposition of Alloys: The Early Stages* (Oxford: Pergamon)
- Halperin B I and Hohenberg P C 1969 *Phys. Rev.* **177** 952
- Halperin B I, Lubensky T C and Ma S K 1974 *Phys. Rev. Lett.* **32** 292
- Hansen M 1958 *Constitution of Binary Alloys* (New York: McGraw-Hill)
- Harris C K 1984 *J. Phys. A: Math. Gen.* **17** 1767
- Harrowell P and Oxtoby D W 1984 *J. Chem. Phys.* **80** 1639
- Haymet A D J and Oxtoby D W 1981 *J. Chem. Phys.* **74** 2559
- Heady R B and Cahn J W 1973 *J. Chem. Phys.* **58** 896
- Heermann D W 1984a *Phys. Rev. Lett.* **52** 1126
- 1984b *Z. Phys. B* **55** 309
- 1986 *An Introduction to Computer Simulation Methods in Theoretical Physics* (Berlin: Springer)
- Heermann D W, Coniglio A, Klein W and Stauffer D 1984 *J. Stat. Phys.* **36** 447
- Heermann D W and Klein W 1983a *Phys. Rev. Lett.* **50** 1962
- 1983b *Phys. Rev. B* **27** 1732
- Heermann D W, Klein W and Stauffer D 1982 *Phys. Rev. Lett.* **49** 1262
- Hilliard J E 1970 *Phase Transformations* ed H I Aronson (Metals Park, OH: American Society for Metals)
- Hockney R V and Eastwood J W 1981 *Computer Simulations Using Particles* (New York: McGraw-Hill)
- Hoffer J K and Sinha D N 1986 *Phys. Rev. A* **33** 1918
- Hohenberg P C and Halperin B I 1977 *Rev. Mod. Phys.* **49** 435
- Hornfer H and Jüngling K 1979 *Z. Phys. B* **36** 97
- Hornreich R M 1979 *Phys. Rev. B* **19** 3799
- Hu C-K 1984 *Phys. Rev. B* **29** 5103
- Huang J S, Goldburg W I and Moldover M R 1975 *Phys. Rev. Lett.* **34** 639
- Hulliger F, Natterer B and Ott H R 1978 *J. Magn. Magnet. Mater.* **8** 87
- Hulliger F and Siegrist T 1979 *Z. Phys. B* **35** 81
- Iglói F and Sólyom J 1983a *J. Phys. C: Solid State Phys.* **16** 2833
- 1983b *Phys. Rev. B* **28** 2792
- Imry Y 1980 *Phys. Rev. B* **21** 2042
- Imry Y and Wortis M 1979 *Phys. Rev. B* **19** 3580
- Ipatova I P and Kitaev Yu E 1985 *Prog. Surf. Sci.* **18** 189
- Isakov S N 1984 *Commun. Math. Phys.* **95** 427
- Ishibashi Y 1978 *Ferroelectrics* **20** 103
- 1981 *Ferroelectrics* **35** 111
- Israel R B 1975 *Commun. Math.* **43** 59
- 1979 *Convexity in the Theory of Lattice Gases* (Princeton, NY: Princeton University Press)
- Jacucci G, Perini A and Martin G 1983 *J. Phys. A: Math. Gen.* **16** 369
- Kadanoff L P 1975 *Phys. Rev. Lett.* **34** 1005
- Kampmann R and Wagner R 1984 *Decomposition of Alloys: The Early Stages* ed P Haasen, V Gerold, R Wagner and M F Ashby (Oxford: Pergamon) p 91
- 1986 *Atomic Transport and Defects in Metals by Neutron Scattering* ed C Janot, W Petry, D Richter and T Springer (Berlin: Springer) p 73
- Kashchiev D 1969 *Surf. Sci.* **14** 209
- Kaski K, Binder K and Gunton J D 1984 *Phys. Rev. B* **29** 3996
- Katsura S 1963 *Adv. Phys.* **12** 416

- Kawasaki K 1972 *Phase Transitions and Critical Phenomena* vol 2, ed C Domb and M S Green (New York: Academic) p 443
- Kawasaki K, Imaeda T and Gunton J D 1981 *Perspectives in Statistical Physics* ed H J Raveche (Amsterdam: North-Holland) p 203
- Kawasaki K and Ohta T 1978a *Prog. Theor. Phys.* **67** 147
- 1978b *Prog. Theor. Phys.* **68** 129
- Kerszberg M and Mukamel D 1979 *Phys. Rev. Lett.* **43** 293
- 1981a *Phys. Rev. B* **23** 3943
- 1981b *Phys. Rev. B* **23** 3953
- Khachaturyan A G 1973 *Phys. Status Solidi b* **60** 9
- Kihara T, Midzuno Y and Shizume T 1954 *J. Phys. Soc. Japan* **9** 681
- Kikuchi R 1951 *Phys. Rev.* **81** 998
- 1967 *J. Chem. Phys.* **47** 1664
- 1974 *J. Chem. Phys.* **60** 1071
- Kirkwood J G 1951 *Phase Transitions in Solids* ed R Smoluchowsky, J E Meyer and A Weyl (New York: Wiley) p 97
- Kleemann W, Schäfer F J and Tannhäuser D S 1980 *J. Magn. Magnet. Mater.* **15-18** 415
- Klein W 1981 *Phys. Rev. B* **24** 5254
- Klein W and Brown A C 1981 *J. Chem. Phys.* **74** 6960
- Klein W and Frisch H L 1986 *J. Chem. Phys.* **84** 2
- Klein W and Unger C 1983 *Phys. Rev. B* **28** 445
- Klein W, Wallace D J and Zia R K P 1976 *Phys. Rev. Lett.* **37** 639
- Knak-Jensen S J, Mouritsen O G, Hansen E K and Bak P 1979 *Phys. Rev. B* **19** 5886
- Knorr K, Loidl A and Kjems J K 1985 *Phys. Rev. Lett.* **55** 2445
- Knorr K, Loidl A and Vettier C 1983 *Phys. Rev. B* **27** 1769
- Kötzler J 1984 *Z. Phys. B* **55** 119
- Kötzler J and Raffius G 1980 *Z. Phys. B* **38** 139
- Kötzler J, Raffius G, Loidl A and Zeyen C M E 1979 *Z. Phys. B* **35** 125
- Kunkin W and Frisch H L 1969 *J. Chem. Phys.* **50** 1817
- Landau D P and Binder K 1978 *Phys. Rev. B* **17** 2328
- 1985 *Phys. Rev. B* **31** 5946
- Landau L D and Lifshitz E M 1958 *Statistical Physics* (Oxford: Pergamon)
- Langer J S 1967 *Ann. Phys., NY* **41** 108
- 1969 *Ann. Phys., NY* **54** 258
- 1971 *Ann. Phys., NY* **65** 53
- 1973 *Acta Metall.* **21** 1649
- 1974 *Physica* **73** 61
- Langer J S and Baron M 1973 *Ann. Phys., NY* **78** 421
- Langer J S, Baron M and Miller H D 1975 *Phys. Rev. A* **11** 1417
- Langer J S and Schwartz A J 1980 *Phys. Rev. A* **21** 948
- Langer J S and Turski J A 1973 *Phys. Rev. A* **8** 3230
- Lebowitz J L, Marro J and Kalos M H 1982 *Acta Metall.* **30** 297
- Lebowitz J L and Penrose O 1966 *J. Math. Phys.* **7** 98
- Lebowitz J L, Phani M K and Styer D F 1985 *J. Stat. Phys.* **38** 413
- Lee J K, Barker J A and Abraham F F 1973 *J. Chem. Phys.* **58** 3166
- Levy F 1969 *Phys. Kondens. Mater.* **10** 85
- Li Y Y 1949 *J. Chem. Phys.* **17** 449
- Liebmann R 1981 *Phys. Lett.* **85A** 59
- Lifshitz E M 1942 *J. Physique* **6** 61
- Lifshitz I M and Slyozov V V 1961 *J. Phys. Chem. Solids* **19** 35
- Lines M E and Jones E D 1965 *Phys. Rev.* **139** A1313
- Ling D D, Friman B and Grinstein G 1981 *Phys. Rev. B* **24** 2718
- Lipowsky R 1984 *J. Appl. Phys.* **55** 2485
- 1987 *Ferroelectrics* in press
- Lowe M J and Wallace D J 1980 *J. Phys. A: Math. Gen.* **13** L381
- Ma S-K 1976 *Modern Theory of Phase Transitions* (Reading, MA: Benjamin)
- McGraw R and Reiss H 1979 *J. Stat. Phys.* **20** 385
- McGuire T R, Gambino R J, Pickart S J and Alperin H A 1969 *J. Appl. Phys.* **40** 1009
- Mahan G D and Claro F H 1977 *Phys. Rev. B* **16** 1168
- Marro J, Bortz A B, Kalos M H and Lebowitz S L 1975 *Phys. Rev. B* **12** 2000

- Marro J, Lebowitz J L and Kalos M H 1979 *Phys. Rev. Lett.* **43** 282
 Marro J and Toral R 1983 *Physica* **122A** 563
 Martin-Löf A 1973 *Commun. Math. Phys.* **32** 75
 Marx R 1985 *Phys. Rep.* **125** 1
 Mazenko G F and Zannetti M 1984 *Phys. Rev. Lett.* **53** 2106
 Metropolis N, Rosenbluth A W, Rosenbluth M N, Teller A H and Teller E 1953 *J. Chem. Phys.* **21** 108
 Michel L 1980 *Rev. Mod. Phys.* **52** 617
 Milchev A, Heermann D W and Binder K 1986 *J. Stat. Phys.* **44** 749
 Milton G W and Fisher M E 1983 *J. Stat. Phys.* **32** 413
 Mirol P and Binder K 1977 *Acta Metall.* **25** 1435
 Mohri T, Sanchez J M and de Fontaine D 1985 *Acta Metall.* **33** 1171
 Moncton D E, Axe J D and Di Salvo F J 1977 *Phys. Rev. B* **16** 801
 Morin P and Schmitt D 1983 *Phys. Rev. B* **27** 4412
 Morita T 1972 *J. Math. Phys.* **13** 115
 Mouritsen G, Knak-Jensen S J and Bak P 1977 *Phys. Rev. Lett.* **39** 629
 Mukamel D and Hornreich R M 1980 *J. Phys. C: Solid State Phys.* **13** 161
 Mukamel D and Krinsky S 1976a *Phys. Rev. B* **13** 5065
 — 1976b *Phys. Rev. B* **13** 5078
 Mukamel D, Krinsky S and Bak P 1976 *AIP Conf. Proc.* **29** 474
 Mukamel D and Wallace D J 1979 *J. Phys. C: Solid State Phys.* **12** L851
 Müller-Krumbhaar H 1974a *Phys. Lett.* **48A** 459
 — 1974b *Phys. Lett.* **50A** 27
 Müller-Krumbhaar H and Stoll E 1976 *J. Chem. Phys.* **65** 4294
 Nattermann T 1976 *J. Phys. C: Solid State Phys.* **9** 3337
 Nattermann T and Trimper S 1975 *J. Phys. A: Math. Gen.* **8** 2000
 Nauenberg M and Cambier J L 1986 *Fractals in Physics* ed L Pietronero and E Tosatti (Amsterdam: North-Holland) p 421
 Nelson D R 1976 *Phys. Rev. B* **13** 2222
 Nelson D R and Halperin B I 1979 *Phys. Rev. B* **19** 2457
 Nereson N and Arnold G 1971 *J. Appl. Phys.* **42** 1625
 Newman C M and Schulman L S 1980 *J. Stat. Phys.* **23** 131
 Niemeijer T and van Leeuwen J M J 1976 *Phase Transitions and Critical Phenomena* vol 6, ed C Domb and M S Green (New York: Academic) p 425
 Nienhuis B, Berker A N, Riedel E K and Schick M 1979 *Phys. Rev. Lett.* **43** 737
 Nienhuis B and Nauenberg M 1975 *Phys. Rev. Lett.* **35** 477
 Nienhuis B, Riedel E K and Schick M 1980a *J. Phys. A: Math. Gen.* **13** L31
 — 1980b *J. Phys. A: Math. Gen.* **13** L189
 Nightingale M P 1976 *Physica* **83A** 561
 — 1982 *J. Appl. Phys.* **53** 7927
 Onsager L 1944 *Phys. Rev.* **65** 117
 Ott H R, Kjems J K and Hulliger F 1979 *Phys. Rev. Lett.* **42** 1378
 Oxtoby D W and Haymet A D J 1982 *J. Chem. Phys.* **76** 6262
 Parrinello M and Rahman A 1980 *Phys. Rev. Lett.* **45** 1196
 Parrinello M, Rahman A and Vashishta P 1983 *Phys. Rev. Lett.* **50** 1073
 Patashinskii A Z and Pokrovskii V I 1979 *Fluctuation Theory of Phase Transitions* (Oxford: Pergamon)
 Pearce P A and Baxter R J 1981 *Phys. Rev. B* **24** 5295
 Penrose O and Lebowitz J L 1971 *J. Stat. Phys.* **3** 211
 — 1979 *Studies in Statistical Mechanics VII* ed J L Lebowitz and E W Montroll (Amsterdam: North-Holland) p 1
 Phani M K, Lebowitz J L and Kalos M H 1980 *Phys. Rev. B* **21** 4027
 Polgreen T L 1984 *Phys. Rev. B* **29** 1468
 Potts R B 1952 *Proc. Camb. Phil. Soc.* **48** 106
 Privman V and Fisher M E 1983 *J. Stat. Phys.* **33** 385
 Privman V and Schulman L S 1982 *J. Stat. Phys.* **29** 205
 Rabin Y and Gitterman M 1984 *Phys. Rev. A* **29** 1496
 Rahman A 1964 *Phys. Rev.* **136** A405
 Ramakrishnan T V 1982 *Phys. Rev. Lett.* **48** 541
 Ramakrishnan T V and Yussouf M 1977 *Solid State Commun.* **21** 389
 — 1979 *Phys. Rev. B* **19** 2775
 Rikvold P A and Gunton J D 1982 *Phys. Rev. Lett.* **49** 286

- Rikvold P A, Kaski K, Gunton J D and Yalabik M C 1984 *Phys. Rev. B* **29** 6285
 Rikvold P A, Kinzel W, Gunton J D and Kaski K 1983 *Phys. Rev. B* **28** 2686
 Roth W L 1958 *Phys. Rev.* **110** 1333
 Rottmann C and Wortis M 1984 *Phys. Rep.* **103** 59
 Rudnick J 1978 *Phys. Rev. B* **18** 1406
 Safinya C R 1977 *Phys. Rev. Lett.* **39** 1668
 Saito Y 1978 *Prog. Theor. Phys.* **59** 375
 Sanchez J M and de Fontaine D 1980 *Phys. Rev. B* **21** 216
 —— 1982 *Phys. Rev. B* **25** 1759
 Sanchez J M, de Fontaine D and Teitler W 1982 *Phys. Rev. B* **26** 1465
 Sangster M J L and Dixon M 1976 *Adv. Phys.* **25** 247
 Schäfer L and Horner H 1978 *Z. Phys. B* **29** 251
 Schick M 1981 *Prog. Surf. Sci.* **11** 245
 Schofield P 1969 *Phys. Rev. Lett.* **22** 606
 Schwartz A J, Krishnamurthy S and Goldburg W I 1980 *Phys. Rev. A* **21** 1331
 Shockley W 1938 *J. Chem. Phys.* **6** 130
 Siebert E D and Knobler C M 1984 *Phys. Rev. Lett.* **52** 1133
 Siggia E 1979 *Phys. Rev. A* **20** 595
 Simon J R, Guyot P and Ghilarducci de Salva A 1984 *Phil. Mag. A* **49** 151
 Sinha D N and Hoffer J K 1983 *Phys. Rev. Lett.* **50** 515
 Smart J S 1966 *Effective Field Theories of Magnetism* (New York: Saunders)
 Sólyom J and Pfeuty P 1981 *Phys. Rev. B* **24** 218
 Stanley H E 1971 *An Introduction to Phase Transitions and Critical Phenomena* (Oxford: Oxford University Press)
 Stauffer D 1976 *J. Aerosol. Sci.* **7** 319
 —— 1979 *Phys. Rep.* **54** 1
 Stauffer D, Coniglio A and Heermann D W 1982 *Phys. Rev. Lett.* **49** 1299
 Stauffer D, Ferer M and Wortis M 1972 *Phys. Rev. Lett.* **29** 345
 Stoll E, Binder K and Schneider T 1972 *Phys. Rev. B* **6** 2777
 Straley J P and Fisher M E 1973 *J. Phys. A: Math., Nucl. Gen.* **6** 1310
 Sullivan D E and Telo da Gama M M 1985 *Fluid Interfacial Phenomena* ed C A Croxton (New York: Wiley) p 45
 Sur A, Lebowitz J L, Marro J and Kalos M H 1977 *Phys. Rev. B* **15** 3014
 Swift J 1976 *Phys. Rev. A* **14** 2274
 Swift J and Hohenberg P C 1977 *Phys. Rev. A* **15** 319
 Toledano J-C 1981 *Ferroelectrics* **35** 31
 Toledano P and Pascoli G 1980 *Ferroelectrics* **25** 427
 Tolman R C 1949 *J. Chem. Phys.* **17** 333
 Tomita H 1978 *Prog. Theor. Phys.* **59** 1116
 Toulouse G 1977 *Commun. Phys.* **2** 115
 Trinkaus H 1983 *Phys. Rev. B* **27** 7372
 Trinkaus H and Yoo M H 1987 to be published
 Vaks V G, Larkin A I and Pikin S A 1967 *Zh. Eksp. Teor. Fiz.* **53** 281 (*Sov. Phys.-JETP* **26** 188)
 Venables J A, Spiller G D T and Hanbrücken M 1984 *Rep. Prog. Phys.* **47** 399
 Vettier C, Alberts H L and Bloch D 1973 *Phys. Rev. Lett.* **31** 1414
 Wegner F J 1967 *Z. Phys.* **206** 465
 Widom B 1972 *Phase Transitions and Critical Phenomena* vol 2, ed C Domb and M S Green (New York: Academic) p 79
 Wilson K G and Kogut J 1974 *Phys. Rep.* **12** 75
 Wortis M 1985 *Fundamental Problems in Statistical Mechanics VI* ed E G D Cohen (Amsterdam: North-Holland) p 87
 Wu F Y 1982 *Rev. Mod. Phys.* **54** 235
 Yussouf M 1981 *Phys. Rev. B* **23** 5871
 Zeldovitch Ya B 1943 *Acta Physiochim. (USSR)* **18** 1
 Zettlemoyer A C (ed) 1969 *Nucleation* (New York: Dekker)